PHYLOGEOGRAPHIC RESOLUTION OF *Botrylloides affinis leachii* (SAVIGNY, 1816) FROM THE NORTH-EASTERN MEDITERRANEAN SEA

A THESIS SUBMITTED TO
THE INSTITUTE OF MARINE SCIENCES
OF
MIDDLE EAST TECHNICAL UNIVERSITY

BY

BERİVAN TEMİZ

IN PARTIAL FULFILLMENT OF THE REQUIREMENTS
FOR
THE DEGREE OF MASTER OF SCIENCE
IN
MARINE BIOLOGY & FISHERIES

AUGUST 2019

Approval of the thesis:

PHYLOGEOGRAPHIC RESOLUTION OF *Botrylloides affinis leachii* (SAVIGNY, 1816) FROM THE NORTH-EASTERN MEDITERRANEAN SEA

Submitted by **BERİVAN TEMİZ** in partial fulfilment of the requirements for the degree of **Master of Science in Marine Biology & Fisheries, Middle East Technical University- Institute of Marine Sciences** by,

Assoc. Prof. Dr. Barış Salihoğlu
Director, **Graduate School of Marine Sciences, METU** _____

Prof. Dr. Zahit Uysal
Head of Department, **Graduate School of Marine Sciences, METU** _____

Examining Committee Members:

Assoc. Prof. Dr. Arzu Karahan
Supervisor, **Graduate School of Marine Sciences, METU** _____

Assist. Prof. Dr. Ebru Derici Eker
Faculty of Pharmacy, Mersin University _____

Assist. Prof. Dr. Korhan Özkan
Graduate School of Marine Sciences, METU _____

Date: 29.08.2019

I hereby declare that all information in this document has been obtained and presented in accordance with academic rules and ethical conduct. I also declare that, as required by these rules and conduct, I have fully cited and referenced all material and results that are not original to this work.

Berivan Temiz
Signature:

ABSTRACT

PHYLOGEOGRAPHIC RESOLUTION OF *Botrylloides affinis leachii* (SAVIGNY, 1816) FROM THE NORTH-EASTERN MEDITERRANEAN

Temiz, Berivan
Master of Science, Marine Biology & Fisheries
Supervisor: Assoc. Prof. Dr. Arzu Karahan
August 2019, 119 pages

Sea squirts (Tunicates) are the closest invertebrate relatives of the chordates. *Botryllus* and *Botrylloides* are the two genera of botryllid ascidians (Family Styelidae; sub family Botryllinae) which is the only chordate group having the ability of whole-body regeneration. In this study, we targeted to do phylogeographic analysis of *Botrylloides affinis leachii* from the North-eastern Mediterranean Sea using mitochondrial and nuclear DNA markers (Cytochrome oxidase I (COI), Histon-3 (H3), Adenine Nucleotide Transporter/ADP-ATP Translocase (ANT), 18S rRNA and 28S rRNA). To elucidate population dynamics, spatial and temporal analyses were conducted separately by scaling with the molecular analyses. From west to the east in total 214 samples were collected from 8 spatial stations: 1) Kemer (Antalya) 2) Side (Antalya) 3) Alanya (Antalya) 4) Tersane (Antalya) 5) Tisan (Mersin) 6) Kızkalesi (Mersin) 7) Mezitli (Mersin) and 8) Konacık (Iskenderun). For the temporal analyses, Kızkalesi time series station was monitored for a year (between the November 2017 and October 2018). In order to increase resolution of the network analysis and phylogeographic trees, present study sequences were compared with the sequences that mined from the GenBank. Furthermore, living individuals were investigated under the light and stereo microscopes to monitor their life cycles. High taxonomic assignment was recorded for the North-Eastern Mediterranean *botryllid* samples via COI, H3 and 28S markers. In total 4 and 14 haplotypes were observed for the COI and H3 genes respectively. Intraspecific distance of H3 gene was recorded higher than the COI gene. On the other hand, whereas 60 mutation step differences were recorded the between present the study and Israel *B. leachii* samples for COI gene, it was 5 for the nuclear DNA marker (H3). Based on the negative Tajima's D values on both COI and H3 gene regions it can be said that the North-eastern Mediterranean populations of Turkey are under the negative selection. However, 18S rRNA marker created confusion during the BLAST analyses and ANT was found to have greater sequential diversification compared to other markers. Phenotypic variation was not differentiated with the current study's molecular markers.

Keywords: Ascidian, Phylogeography, North-eastern Mediterranean, DNA barcoding, H3, ANT

ÖZ

KUZEY-DOĞU AKDENİZ'DEN *Botrylloides affinis leachii*'nin FİLOCOĞRAFİK ÇÖZÜMLENMESİ

Temiz, Berivan
Yüksek Lisans, Deniz Biyolojisi & Balıkçılık
Tez Danışmanı: Doç. Dr. Arzu Karahan
Ağustos 2019, 119 sayfa

Deniz tulumluları (Tunicata) omurgalıların en yakın omurgasız akrabasıdır. *Botryllus* ve *Botrylloides*, tüm vücut onarımı yapabilen tek omurgalı grubu olan iki botrillid cinsidir. Bu çalışmada, mitokondriyal ve nükleer DNA belirteçleri (Cytochrome oxidase I (COI), Histon-3 (H3), Adenine Nucleotide Transporter/ADP-ATP Translocase (ANT), 18S rRNA and 28S rRNA) kullanılarak *Botrylloides affinis leachii'*nin Kuzey-doğu Akdeniz'deki filocoğrafik çözünürlüğünün belirlenmesi hedeflenmiştir. Popülasyon dinamiklerini net bir şekilde açığa çıkarmak için, moleküler analizlerle ölçeklendirmek üzere ayrı ayrı bölgesel ve zamansal analizler gerçekleştirilmiştir. Batıdan doğuya 8 mekânsal istasyondan: 1) Kemer (Antalya) 2) Side (Antalya) 3) Alanya (Antalya) 4) Tersane (Antalya) 5) Tisan (Mersin) 6) Kızkalesi (Mersin) 7) Mezitli (Mersin) ve 8) Konacık (İskenderun) olmak üzere, toplamda 214 örnek toplanmıştır. Mevsimsel analizler için, Kızkalesi zaman serisi istasyonu bir sene boyunca takip edilmiştir (Kasım 2017- Ekim 2018). Mevcut çalışma dizileri, veri tabanlarından çekilen moleküler dizilerle karşılaştırılarak, filocoğrafik analizler tamamlanmıştır. Ayrıca, canlı *B. aff. leachii* bireylerinin yaşam döngüleri ışık ve stereo mikroskobu altında incelenmiştir. Moleküler analizler sonucunda COI, H3 ve 28S genlerinin Kuzey-doğu Akdeniz *B. aff. leachii* popülasyonlarının tür tayini için iyi çözünürlük sağladığı görülmüştür. COI ve H3 genleri için toplamda sırasıyla 4 ve 14 haplotip kaydedilmiştir. H3 genindeki tür içi çözünürlük COI genine göre daha yüksek bulunmuştur. Diğer yandan, çalışmadaki örnekler ve İsrail'in *B. leachii* örneklerinin COI genleri arasında 60 mutasyon farkı bulunurken, H3 nükleer genleri arasında 5 mutasyon fark bulunmuştur. Türkiye'nin Doğu Akdeniz kıyılarında yaşayan *B. aff. leachii* popülasyonlarının COI ve H3 genlerindeki negatif Tajiima D değerleri baz alındığında, bu genlerin negatif seleksiyon altında oldukları bulunmuştur. Bunun aksine, 18S rRNA belirtecinin BLAST analizlerinde karışıklık yaratabileceği görülürken, en yüksek sekans çeşitliliğine ANT geninde rastlanmıştır. Organizmalarda kaydedilen fenotipik varyasyon, kullanılan moleküler belirteçlerin hiçbiriyle çözülememiştir.

Anahtar Kelimeler: Ascidian, Filocoğrafya, Kuzeydoğu Akdeniz, DNA barkotlama, H3, ANT

To Arzu Karahan

ACKNOWLEDGMENTS

I want to express my biggest and very first thankfulness to my advisor Assoc. Prof. Dr. Arzu Karahan. Her endless thrill, curiosity, passion and kindness towards science, nature and all living creatures taught me so much more than any book. I always felt so lucky to have such an amazing advisor that has a unique and genuine perspective. Her guidance, support and teachings on every aspect empowered me in a way that I can feel the change on me compared to the day I arrived here. I will always be grateful for the time I had with her.

I want to thank to my thesis committee to Assist. Prof. Dr. Ebru Derici Eker and Assist. Prof. Dr. Korhan Özkan for their valuable criticism and comments. I am thankful for their time and help.

I am deeply thankful to Assist. Prof. Dr. Koray Özhan for helping me when I needed. He was always very supportive and kind. I am very thankful to him for sharing his time, advices and academic motivation.

I want to thank to Dr. Ünsal Karhan for sharing his knowledge, time and kind friendship. Through sharing his academic collection and connections, he helped me a lot and I am very thankful for his support and motivation.

I want to thank to my lab-mates Esra Öztürk and Fatıma Nur Oğul for their support and collaboration. I want to thank to Kenan Murat Karahan, Begüm Tohumcu and Merve Kurt for helping us during the samplings. I want to thank to microplastic lab, especially to Mehmet Özalp & Ertan Keş for their kind help. I want to thank to Emel Kocaman for her support and friendship. I also thank to İsmail Akçay for him being helpful and sharing his time and knowledge. I want to thank to METU-IMS.

I want to thank my family especially to my sister Hasret Temiz and all my friends for their support and motivation.

This project was supported by Middle East Tech. Uni. Scientific Research Project (Project no: AP- YÖP-701-2018-2666) -'Identification of North-eastern Mediterranean Botryllid ascidians via molecular tools', DEKOSIM – METU-IMS and COST Action Project (Stem cells of marine/aquatic invertebrates)- CA16203 - Stem cells of marine/aquatic invertebrates: from basic research to innovative applications.

TABLE OF CONTENTS

ABSTRACT v

ÖZ vi

ACKNOWLEDGMENTS viii

TABLE OF CONTENTS ix

LIST OF TABLES xi

LIST OF FIGURES xii

LIST OF ABBREVIATIONS xiii

LIST OF SYMBOLS xiv

1. INTRODUCTION 1

1.1. General Information on Tunicates 1

1.2. Taxonomy of Botryllid Ascidians 4

1.3. Taxonomy of *Botrylloides leachii* 4

1.4. Life Cycles 6

1.4.1. Allorecognition 7

1.5. Whole-body regeneration 8

1.6. Hibernation 9

1.7. Distribution 10

1.8. DNA Barcoding 11

1.9. Phylogeography 13

2. AIM OF THIS STUDY 13

3. MATERIALS & METHODS 14

3.1. Sample Collection & Study Area 14

3.1.1. Spatial Sampling 14

3.1.2. Time Series Sampling……....15
3.2. Morphological Identification of Specimens…….16
3.3. DNA Extraction & Polymerase Chain Reaction……..16
3.3.1. Primers……...18
3.4. Bioinformatics……..18
3.4.1. Sequencing, alignment, editing and bioinformatics analyses……....18
3.3.1. Barcoding of Life Database (BOLD) submission…….19
4. RESULTS……19
4.1. Morphology & Life cycles……...19
4.1.1. Morphological Records on the Zooid and Colonial bases……19
4.1.2. Morphological diversity……20
4.2. Asexual Reproduction – Blastogenic Cycle / Palleal Budding……....21
4.3. Hibernation……...24
4.4. Life spans of the living colonies……25
4.5. Molecular Results……27
4.5.1. Spatial Results……...27
4.5.1.1. Mitochondrial COI Gene Analyses…….27
4.5.1.1.1. Distance Analysis……..27
4.5.1.1.2. Network Analysis……..28
4.5.1.1.3. Bayesian Phylogeographic Analyses……29
4.5.1.1.4. Spatial Populations Parameters ……31
4.5.1.2. Nuclear H3 Gene Analyses……....33
4.5.1.2.1. Distance Analysis……..33
4.5.1.2.2. Network Analysis……..34
4.5.1.2.3. Bayesian Phylogeographic Analyses…….35
4.5.1.2.4. Spatial population analyses……...37

4.5.1.3. Nuclear ANT Gene Analyses……...39

4.5.1.3.1. BLAST Analyses……..39

4.5.1.3.2. Distance Analysis…….40

4.5.1.3.3. Bayesian Tree ……..……..40

4.5.2. Temporal Results……...42

4.5.2.1. Mitochondrial COI Gene Analyses……..42

4.5.2.1.1. Temporal Population Parameters……..42

4.5.3. Additional Nuclear Gene (18S & 28S) analyses……...44

5. DISCUSSION……..45

6. CONCLUSION……....50

REFERENCES……51

APPENDICES

A. Blastogenic Cycles

B. Sampled Specimens

LIST OF TABLES

Table 1. Taxonomy of *Botrylloides leachii* (Savigny, 1816)……4

Table 2. Details of sampling stations. ……...15

Table 3. Additional samples from the Kızkalesi station.…….....15

Table 4. Kızkalesi time series station…….....16

Table 5. PCR programs for COI, H3, ANT, 28S rRNA and 18S rRNA genes……...17

Table 6. Primers of the present study……..18

Table 7. The life span of the *B. aff. leachii* colonies those were cultured in IMS-METU aquaculture room…….....25

Table 8. Mean distance of between populations are given in the lower triangle, upper triangle shows the standard deviations.……..28

Table 9. Spatial populations parameters based on the COI locus of the North-eastern Mediterranean populations. ……..…….....31

Table 10. Gene flow (Nm) parameters for spatial stations (Nei, 1973)…….33

Table 11. Pairwise genetic differentiation (F_{st}) within spatial populations. The method is applied for 10.000 permutations (Hudson, Slatkin & Maddison, 1992). 33

Table 12. Intraspecific mean distance between the present study populations (except Tersane) are shown in the lower triangle, upper triangle reflects the standard deviations.……34

Table 13. Spatial population parameters based on the H3 gene of the North-eastern Mediterranean populations …….....37

Table 14. Gene flow (Nm) estimation based on H3 gene (Nei, 1973…….39

Table 15. Pairwise genetic differentiation (Fst) for H3 gene. 10.000 permutations were used (Hudson, Slatkin & Maddison, 1992……39

Table 16. Intraspecific mean distance between present study samples based on ANT gene are shown in the lower triangle.……..40

Table 17. Kızkalesi time series population parameters……42

Table 18. Gene flow (Nm) approximations for temporal stations (Nei, 1973)……43

Table 19. Pairwise genetic differentiation (Fst) within the temporal populations from Kızkalesi time series station. The method is applied for 10.000 permutations (Hudson, Slatkin & Maddison, 1992)……...44

LIST OF FIGURES

Figure 1. Maximum likelihood tree based on genomic data of 33,800 aligned amino acid positions proved the categorization of tunicates in the Olfactores which is a clade within the Chordata including the Tunicata (Urochordata) and the Craniata (Vertebrata) (Delsuc et al., 2006)…….1

Figure 2. Tunicate figures of three primary classes. Clockwise from top left: A solitary ascidian, *Ciona savignyi*. An appendicularian, *Oikopleura dioica*. Three thaliaceans: *Pyrosoma atlanticum*; *Dolioletta gegenbauri*; and a solitary salp, *Cyclosalpa affinis* (Holland, 2016)…….2

Figure 3. A lateral capture of a solitary Ascidian larva, *Ciona intestinalis*. The sensory vesicle belonging to the central nervous system, the adhesive papillae and the notochord in the middle of the tail are demonstrated. (Sasakura et al., 2016).....3

Figure 4. A) The ventral view of *B. leachii*, endostyle is lining thoroughly, ovary and testis are located below. B) Dorsal view, the larvae in the incubatory pouches is clear (Brunetti, 2009)…….....5

Figure 5. A dorsal view of *B. leachii* colony. Ladder-like arrangement of zooids is observed. Ampullae can be seen at the external border of the colony lining side by side towards the end of tunic (Blanchoud et al., 2018a). …….....5

Figure 6. Blastogenesis of *B. leachii*. The budding cycle of a mature zooid which grows buds in the first stages and further budlets are generated. In the takeover phase the mature zooid is reabsorbed and recycled in the vascular system (Blanchoud et al., 2018a).....……..6

Figure 7. Three fusion/rejection responses are illustrated in botryllid ascidians: A) Complete fusion B) Resorption C) Separation (Saito et al., 1994). .....…….7

Figure 8. Whole-body regeneration phenomenon of *B. leachii* is illustrated by Blanchoud et al., (2018a). A) The colony is seen to be including zooids. B) The zooids are taken out and vessels left only. C) The colony is observed grow new zooids from the vascular system. .....…….8

Figure 9. Torpor morphology of *B. leachii* is seen where the carpet-like view was shaped by ampullae without any zooids (Hyams et al., 2017). .....…….9

Figure 10. Worldwide distribution of *B. leachii* is demonstrated with diamonds; closely confused sister species *B. nigrum* is stated with circles (Reem et al., 2017)……10

Figure 11. Time series temperature, salinity and oxygen concentration of Mersin Harbour for the first *B. leachii* record period (Pınar, 1976)…….....11

Figure 12. Sampling stations ……14

Figure 13. An orange *B. aff. leachii* morph. A) General morphology and structure of the colony. B) Zooid morphology from the dorsal side. C) Inside the buccal siphon, 4 larger and 4 smaller tentacles are observed……19

Figure 14. An illustration of *B. leachii* colony. A colony, zooid, ampullae (vascular termini) and the buccal siphon with tentacles were depicted. …….....20

Figure 15. Illustration of *B. aff. leachii* major morph patterns ……..……21

Figure 16. Illustration blastogenic cycle of *B. aff. leachii* ……...21

Figure 17. Blastogenic cycle of *B. aff. leachii*. Cycle was monitored daily basis and images were recorded under stereo microscope……..23

Figure 18. *B. aff. leachii* on hibernation. A) A Typical *B. aff. leachii* morph from Tisan station (specimen code G8). B) Same morph was also taken from Kızkalesi station (specimen code GK13). C) G8 is recorded during hibernation. D) Hibernation morphology of GK13 is also provided. ……24

Figure 19. Median Joining Network analysis of *B. aff. leachii* based on COI locus was constructed. Circles were remarked by the haplotype name. Size differences of circles state frequency while colours reflect regions where the haplotype was taken. The region names were seen on the right of the network. Numbers represent mutation steps between the haplotypes USA samples (brown): sample clustered in H1 is *Botrylloides nigrum*, -H2 is *B. leachii*……..29

Figure 20. A) Coupled runs were resulted the posterior probabilities of the Bayesian analysis (Summary Statistic: mean = -1294; std. dev. of mean = 8.6; 95% HPD lower = -1304; 95% HPD upper = -1285; auto-correlation time (ACT) = 277.85; effective sample size (ESS) =3289) B) Bayesian phylogeographic analyses based on 519 bp partial COI sequences of haplotypes was constructed. Distance scale was supplied below the tree and the haplotypes were specified on the tree. Branches were scaled in colour with respect to the length mean. Colour range is provided. C) Bayesian consensus tree with the illustration of polymorphic sites.…….....30

Figure 21. Population size changes were demonstrated based on mismatch distribution of COI gene for Kızkalesi, Mezitli, Konacık and all populations. Raggedness statistic values (r) for each analysis was supplied ($r > 0.05$). The X-axis states the number of pairwise differences while the Y-axis represents frequency. Red line indicates observed frequency for stable population size and green line shows expected frequency……32

Figure 22. Median Joining Network estimation of *B. aff. leachii* based on H3 locus was illustrated. Circles reflects the haplotype name. Size differences of circles represent frequency. Colours depicts regions where the haplotype was located. The region names were given on the right of the network. Numbers shows mutation steps between the haplotypes……...35

Figure 23. A) The posterior probabilities of the Bayesian analysis were calculated for coupled runs (Summary Statistic: mean = -722; std. dev. of mean = 0.114; 95% HPD lower = -733; % HPD upper =-713; auto-correlation time (ACT) = 425.858; effective sample size (ESS) =2113) B) Bayesian phylogeographic analyses based on 280 bp partial H3 sequences of haplotypes was modelled. Distance scale was provided below the tree and the haplotypes were stated on the tree. Branches were scaled in colour with respect to the length mean. Colour

range is given. C) Bayesian consensus tree with the illustration of polymorphic sites……..……...36

Figure 24. Population size changes were illustrated based on mismatch distribution of H3 for all populations. Raggedness statistic values (r) for each analysis was provided (r > 0.05). The X-axis shows the number of pairwise differences while the Y-axis states frequency. Red line infers observed frequency for stable population size and green line represents expected frequency……38

Figure 25. BLAST result of the present study ANT consensus sequences and database sequences (JF962229.1; Teske et al., 2011)…….. …….....40

Figure 26. The posterior probabilities of the Bayesian analysis were measured for coupled runs (Summary Statistic: mean = -3897; std. dev. of mean = 0.277; 95% HPD lower = -3912; % HPD upper =-3884; auto-correlation time (ACT) = 675.078; effective sample size (ESS) =666). B) Bayesian phylogeographic analyses based on ~300-1200 bp partial ANT sequences of *B. aff leachii* was drawn. Distance scale was provided below the tree and the haplotypes were represented on the tree. Branches were scaled in colour with respect to the length mean. Colour range is supplied C) Bayesian consensus tree based on ANT locus is supplied with the illustration of the polymorphic sites…….....41

Figure 27. Population size changes of Kızkalesi time series station based on mismatch distribution of COI. Raggedness statistic values (r) for each analysis was seen on the graph (r > 0.05). The X-axis shows the number of pairwise differences while the Y-axis states frequency. Red line shows observed frequency for stable population size and green line represents expected frequency……43

1. INTRODUCTION

1.1. General information on tunicates

Tunicata (Lamarck, 1816) are one of the three sub-phyla of Chordata phylum and encompasses approximately 3000 species, all living in marine habitats as filter feeder (Shenkar et al., 2019). The existence of tunicates dates back to the Early Cambrian (Chen et al., 2003) and the first identification was done by Lamarck (1816) based on the exoskeleton covering the organism called “tunic”.

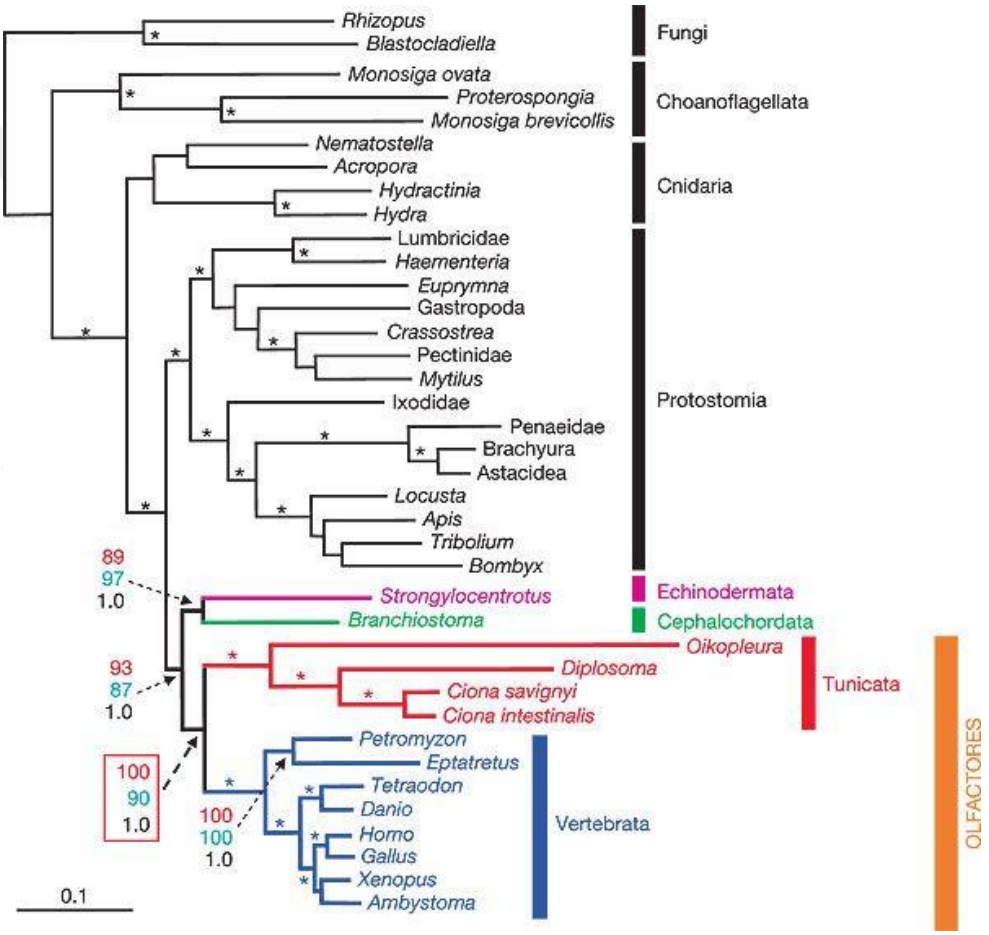


Figure 1. Maximum likelihood tree based on genomic data of 33,800 aligned amino acid positions proved the categorization of tunicates in the Olfactores which is a clade within the Chordata including the Tunicata (Urochordata) and the Craniata (Vertebrata) (Delsuc et al., 2006).

The closest living relatives of vertebrates are tunicates (Fig. 1, Delsuc et al., 2006). They have both solitary and colonial life forms and were classified in three classes; Appendicularia, Thaliacea and Ascidiacea (Figure 2).

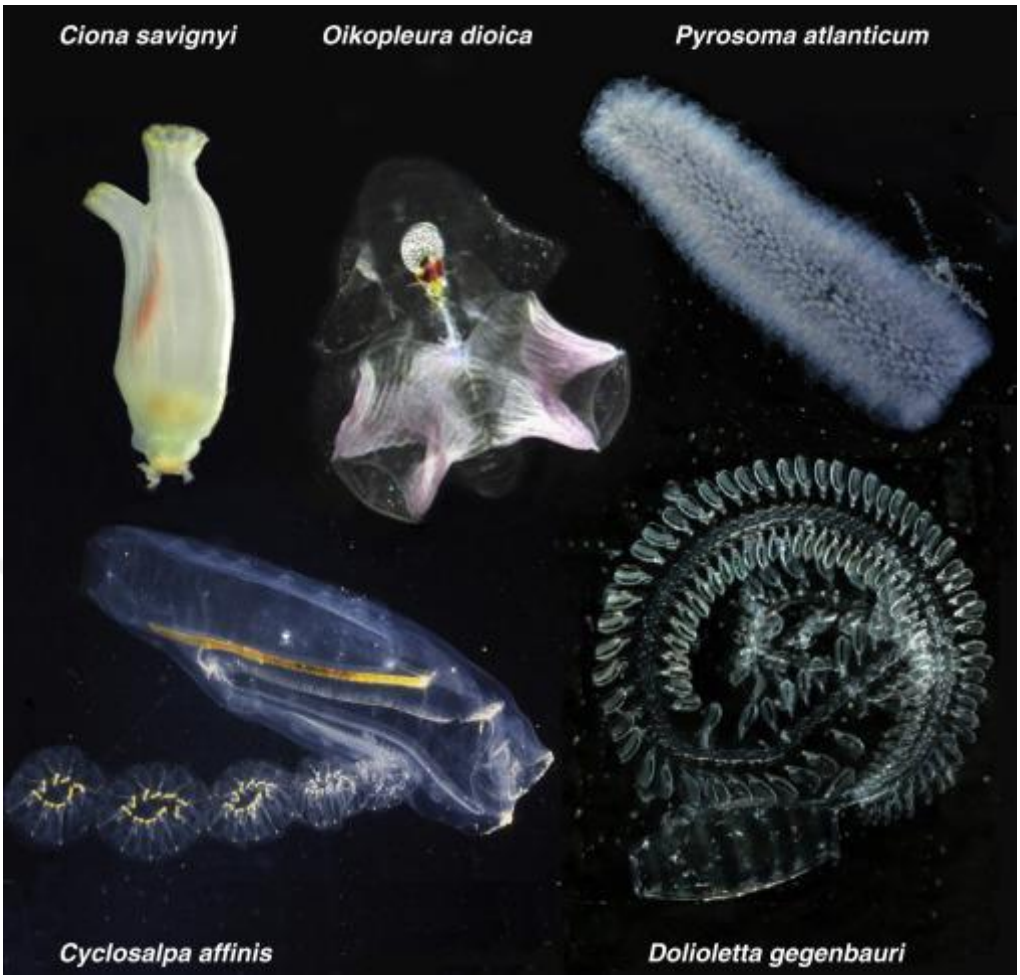


Figure 2. Tunicate figures of three primary classes. Clockwise from top left: A solitary ascidian, *Ciona savignyi*. An appendicularian, *Oikopleura dioica*. Three thaliaceans: *Pyrosoma atlanticum*; *Dolioletta gegenbauri*; and a solitary salp, *Cyclosalpa affinis* (Holland, 2016).

Appendicularia comprises pelagic tunicates identified by their adult body structure is similar to the tadpole larvae. Thaliacea contains holoplanktonic and colonial tunicates differing from other groups by their life cycles and colony aggregateness (Govindarajan et al., 2011). Ascidiacea contains sessile marine non-vertebrate chordate group (Berrill, 1950), they are characterized by morphological features of the branchial sac that is used to concentrate the particles from the environment. An Ascidiacea larva has free-living life stage before attaching to any substrate, after metamorphosis they become a sessile animal.

Reproduction types of ascidians were demonstrated varieties from the ovoviviparity to viviparity (production of living individual from eggs that hatch within the body and giving birth, Zaniolo et al., 1994). Solitary ascidians are known to spawn eggs and sperm into water where the fertilization take place (Millar, 1971), sperms of a colonial ascidians eject out from

the colony, later on these sperms enter another colony through the siphons and fertilize the egg inside of the body cavity (Kott 1985). Sexual reproduction is observed when the water temperature is warmer enough such as summer period of a temperate region, while a continuous process has been recorded in tropical waters (Millar, 1971; Turon and Becerro, 1992). Because of the transient larval stage (between 6 to 24 hours, Berrill, 1950), the new introduction of the sessile forms is thought to be happen through the transport of adult animals by attaching to ship hulls (Lambert, 2002).

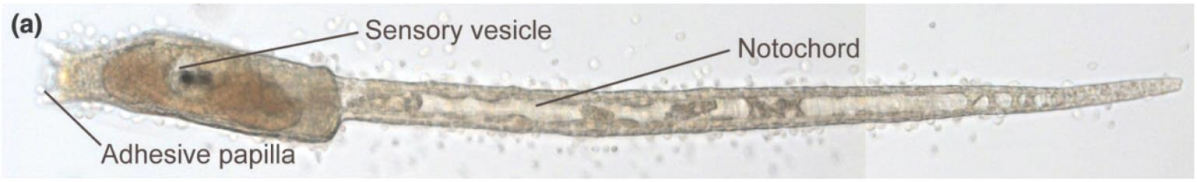


Figure 3. A lateral capture of a solitary Ascidian larva, *Ciona intestinalis.* The sensory vesicle belonging to the central nervous system, the adhesive papillae and the notochord in the middle of the tail are demonstrated. (Sasakura et al., 2016).

Metamorphosis is a common process for all ascidian larvae regardless of being solitary or compound (Berrill, 1950). Ascidian larvae possess a central nervous system on the dorsal part and a notochord located in the tail (Berrill, 1950; Sasakura et al., 2016; Fig. 3). Possessing a notochord that similar to the chordates makes their phylogenetic position highly important. Although an adult form is less similar to the chordate phenotype, the tadpole larvae closely resemble to the chordate morphology. During the larval stage, feeding from the environment is not possible, the larva has to attach a surface before consuming all body food stock. In most of the compound ascidians the initiation of metamorphosis through the organ level happens before the settlement (Cloney, 1982). At the end of the free-swimming life stage the larvae became sticky and attach to a solid substratum, then starting to differentiate by losing most of its anatomical compartments such as notochord and nerve cord through a massive apoptotic process (Glaser and Anslow, 1949; Cloney, 1982). Tail is digested in minutes or seconds (Cloney, 1982). Once the metamorphosis takes place, the feeding process is started through filtering of particles from the water column by taking into the branchial sac using the buccal siphon, the water is then squirted out via common or singular atrial siphon (Millar, 1971). Because of this feature the taxon has been named as ‘Sea squirts’.

1.2. Taxonomy of Botryllid Ascidians

Botryllid ascidians live on the hard substratum by building flat and gelatinous colonies. These species are viviparous and hermaphrodite (Mukai, 1977). *Botryllus* and *Botrylloides* are two genera of Ascidiacea and containing 32 and 19 species respectively (Shenkar et al., 2019). The first taxonomic identification was based on the anatomical features (Milne-Edwards, 1841), it was then changed with the existence of incubatory pouch - the internal space for the development of the larvae - and the position of ovary and testis (Arnback, 1923; Hartmeyer and Michaelsen, 1928). Later, the first assigned taxonomic criteria were changed and these two genera classified solely based on the incubatory pouch (Kott, 1985). But these identifications criteria were not applied universally because of not being inclusive (Mukai, 1977; Saito et al., 2001) and debates were continued (Monniot and Monniot, 1987; Saito and Okuyama, 2003). Today, *Botryllus* and *Botrylloides* are classified based on the distinctions of colonial system morphology (Milne- Edwards, 1841; Brunetti, 2009). For a long time, the species of both genera were misclassified as taxonomically, lacking of interspecific morphological differentiations and also having high intraspecific variability are some of the main reasons of this confusion (Bock et al. 2012; Reem et al., 2017).

1.3. Taxonomy of *Botrylloides leachii*

Botrylloides leachii (Savigny, 1816) is classifying in the Ascidiacea (Class), Stolidolidobranchia (Order), Styelidae (Family) and *Botrylloides* (Genus) (Table 1, Shenkar et al., 2019).

Table 1. Taxonomy of *Botrylloides leachii* (Savigny, 1816).

Kingdom	:	Animalia
Phylum	:	Chordata
Subphylum	:	Tunicata
Class	:	Ascidiacea
Order	:	Stolidobranchia
Family	:	Styelidae
Genus	:	*Botrylloides*
Species	:	*Botrylloides leachii*

The thickness of a colony is approximately 1.5 mm. The colours of living colonies might vary from the orange with yellow bands, brownish-red, brown with white bands to violet with white bands. The zooids are 1.5 to 3 mm long lining perpendicularly to the substratum; do not contain

atrial siphons but have a common atrial opening (individual siphon for defecation) and commonly 4 large and 4 small tentacles (teeth-like structures for capturing the food) are seen on the mouth side (Brunetti, 2009; Blanchoud et al., 2018a).

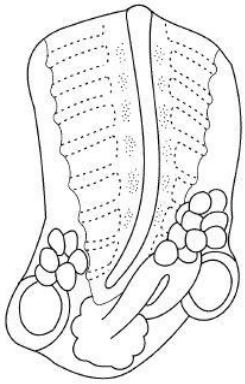
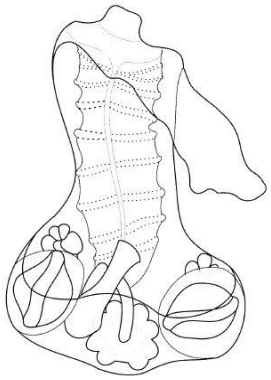
A  B 

Figure 4. A) The ventral view of *B. leachii*, endostyle is lining thoroughly, ovary and testis are located below. B) Dorsal view, the larvae in the incubatory pouches is clear (Brunetti, 2009).

Each zooid possesses a heart and open blood circulation is seen in the colony (Millar, 1953) Colony-wise interaction is sustained through the shared blood vessels. External border of the colony is confined with the ampullae also known as vascular termini. Whole colony is located within a tunic (Fig. 5).

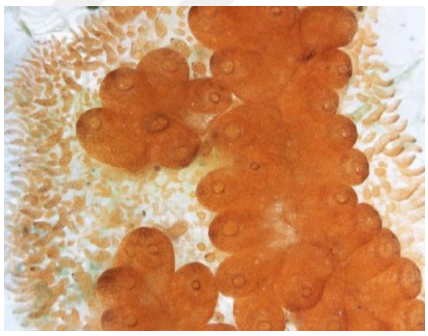


Figure 5. A dorsal view of *B. leachii* colony. Ladder-like arrangement of zooids is observed. Ampullae can be seen at the external border of the colony lining side by side towards the end of tunic (Blanchoud et al., 2018a).

1.4. Life Cycles

Ascidian have three different reproduction systems; 1) asexual reproduction also known as budding, 2) fusion of colonies a process also known as allorecognition and 3) sexual reproduction (Berrill, 1947; Millar, 1971). Only sexual reproduction is common among all ascidians, asexual reproduction and fusion are special for some subgroups. Since these species are hermaphrodite, the gonads of both sexes develop on either side of the zooid. During the

sexual reproduction, egg fertilized after ovulation and development start inside of the main colony and it continues until the larva released-out to the water (Berrill, 1947; Mukai, 1977). During the asexual reproduction the adult zooid produces primary buds from the brachial epitheliums' stem cells (Fig. 4; Millar, 1971; Mukai, 1977; Blanchoud et al., 2018a). Palleal budding is a circular process repeating every 5 to 8 days (Rinkevich et al., 1995). When the primary bud develops enough the old zooid digest with an apoptotic processes and primary bud becomes zooid (Berrill, 1947).

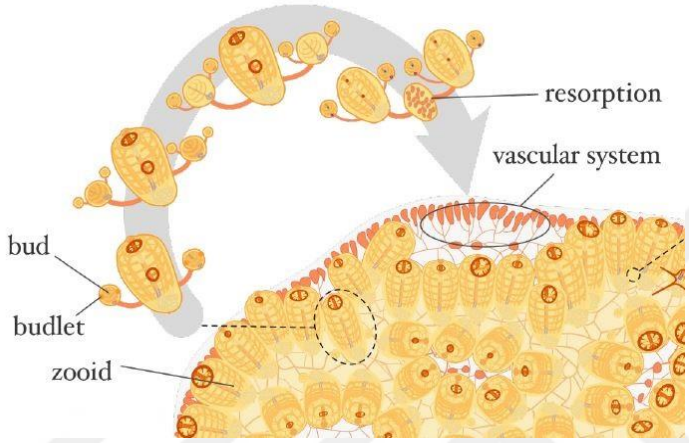


Figure 6. Blastogenesis of *B. leachii*. The budding cycle of a mature zooid which grows buds in the first stages and further budlets are generated. In the takeover phase the mature zooid is reabsorbed and recycled in the vascular system (Blanchoud et al., 2018a).

Blastogenic cycle is a weekly budding process happens through four phases (A-D) resulting in new generation of zooids also called primary and secondary buds (Berrill 1957; Mukai & Watanabe, 1976). Each cycle is terminated with phase D also known as take-over phase which the old zooids are absorbed with a massive apoptotic process (Mukai & Watanabe, 1976; Rinkevich et al., 2007). Following the take-over, emergence of budding through the stages A-C by thickening of atrial epithelium of the main zooid results in the formation of primary and secondary buds (Mukai & Watanabe, 1976). Buds stay attached until reaching full maturity (Rinkevich et al, 1995). Further, the degeneration of subsequent zooids is followed by the full maturity and detachment of new zooids (Mukai & Watanabe, 1976; Rinkevich et al, 1995).

To understand the distribution and ecology, the life cycles of *B. leachii* was investigated in the Venetian Lagoon (Italy) by Brunetti (1976). It was reported that the sexual reproduction happens between the May and July at 17-25^{o}C temperature range. The life span for most of the *B. leachii* colonies was reported as 12 months. Hibernation was seen when the temperature

decreases below the 10ºC. When the temperature comes to moderate degrees (above 10ºC) the pigmentation of the colony declines, zooid and blood circulations become visible and blastogenic cycle take places. Hibernation terminates by March for the Venetian Lagoon samples (Brunetti, 1976). As these are the first detailed records of *B. leachii*, it was further used to estimate with the other populations such as from Israel (Rinkevich et al., 1993) and found that Israeli populations reproduce through the year and the highest peak was observed during the summer period.

1.4.1. Allorecognition

Presence of a special allorecognition system was documented by Scofield et al., (1982) among compound ascidians. Allorecognition is a definition of immunologic response; when two different colonies contact with each other through their ampullae also known as vascular termini that are present at the edges of the tunic, they may end up with transplantation through vascular system or termination can happen via cytotoxic reaction (Fig 5; Rinkevich et al., 1994; Saito et al., 1994).

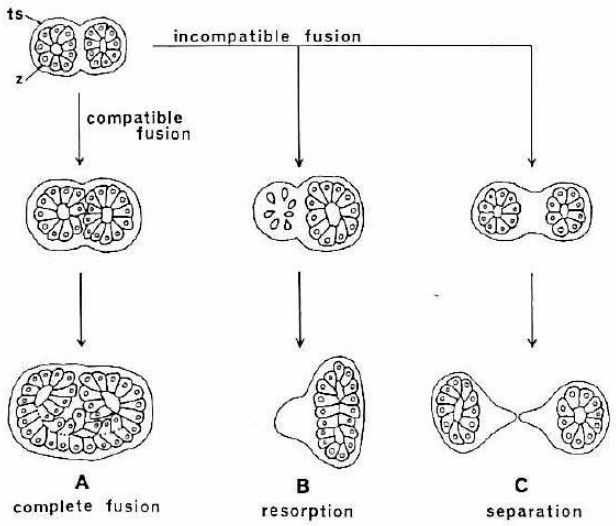


Figure 7. Three fusion/rejection responses are illustrated in botryllid ascidians: A) Complete fusion B) Resorption C) Separation (Saito et al., 1994).

The control mechanism of this process is sustained through a single but immensely polymorphic gene, is named tunicate fusibility/histocompatibility complex (Fu/HC) (Weissman et al., 1990). If both colonies contain even one common allele, the conjoining happens; if there is no common allele at least in one of the colonies, the rejection is recorded

(Rinkevich & Weissman, 1987; Rinkevich et al., 1994; Paz & Rinkevich, 2002; Saito et al., 1994; Kassmer et al., 2016). Multi-partner chimera (fusing of relative species) studies on *Botrylloides* species were investigated by Paz and Rinkevich (2002) and it was found to be common and uncorrelated with species types. It was also stated that the evolution of multi-partner chimera phenomenon is shaped under the pressure of groups rather than the individual joints (Paz and Rinkevich, 2002).

The resemblances between the vertebrate and invertebrate fusibility/histocompability mechanisms have led to the idea arose that based on 'the evolutionary origins of this gene might originate from the ascidian immune system' (Weissman et al., 1990).

1.5. Whole-Body Regeneration

Regeneration is one of the most fundamental topics among the developmental and immuno-biological studies in metazoans. The regeneration abilities of multicellular organisms are highly variable and mostly related with the organism complexity.

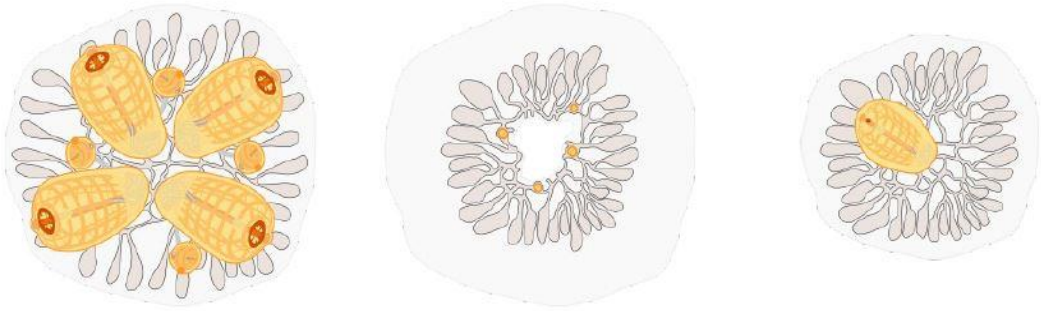


Figure 8. Whole-body regeneration phenomenon of *B. leachii* is illustrated by Blanchoud et al., (2018a). A) The colony is seen with zooids. B) The zooids are taken out and vessels left only. C) The colony is observed grow new zooids from the vascular system.

On the other hand, the whole-body regeneration (WBR) is an exceptional phenomenon. So far it has only been observed in *Botryllinae* (Urochordate) that include *B. leachii.* It was reported that *Botryllus schlosseri* can construct a whole organism from a single blood cell (Rinkevich et al., 1995). This process was referred to may originate from a couple of totipotent stem cells, those settle in the circulation system (Rinkevich et al., 1995; Zondag et al., 2016; Blanchoud et al., 2018a; Blanchoud et al., 2018b). Exceptionally, the studies on commonly studied botryllid ascidian, *Botrylloides schlosseri,* is found to proceed whole-body regeneration if only the adult zooids were absorbed and there was no zooid left during the blastogenesis (take-over

phase), yet *B. leachii* is documented to undergo WBR any stage of blastogenesis (Rinkevich et al., 2007; Kürn et al., 2011; Blanchoud et al., 2018b). For these reasons, *B. leachii* is commonly used for regeneration and development studies to compare with other taxa to gain essential knowledge with respect to evolutionary origins among to chordate and invertebrate groups (Zondag et al., 2016; Blanchoud et al., 2018a; Blanchoud et al., 2018b).

1.6. Hibernation

Hibernation also known as torpor is another distinctive characteristic of *B. leachii,* it is the only botryllid ascidian can undergo hibernation when the thermal conditions are not favourable, beside of the other unsuitable reasons that happen especially during the winter season (Bancroft, 1903; Burighel et al., 1976; Rinkevich et al., 1995; Hyams et al., 2017).



Figure 9. Torpor morphology of *B. leachii* is seen where the carpet-like view was shaped by ampullae without any zooids (Hyams et al., 2017).

When a colony is entering the hibernation, the bud development reduces and the zooids are started to be absorbed with great number of macrophages (Burighel et al., 1976; Rinkevich et al., 1995; Hyams et al., 2017). In the end, the dormant colony left with no zooid but only covered with ampullae having numerous haemocytes along with undifferentiated cells which in overall has “carpet-like” morphology and the vascular budding is observed during this stage (Burighel et al., 1976). The hibernation is terminated once the temperature increases, then the zooids formation is initiated, filtering activates start again, blood circulation and metabolism increase (Burighel et al., 1976).

1.7. Distribution

It is discussed that *B. leachii* was originated from the Mediterranean Sea, then distributed to worldwide among the intertidal zone due to the presence of highest observed haplotype diversity in that region (Fig. 9; Rinkevich et al., 1993; Shenkar et al., 2019). The range of distribution of the species extends from the Atlantic to Red Sea, from Pacific to Australia (Berrill, 1950; Dybern, 1969; Medioni, 1970; Burighel, 1976, 1979; Brunetti et al., 1980; Kott, 1985; 1986; Turon, 1988; Myers, 1990). In the Eastern Mediterranean, the first records of *B. leachii* was given by Harant in 1939. Further study confirmed the presence of *B. leachii* on the Mediterranean coasts of Israel by Peres (1958), but not with present-day annotation, given as *Metrocarpa nigrum* which is one of the synonyms species of *Botrylloides nigrum* that is often confused with *B. leachii* taxonomically. The existence of *B. leachii* was also confirmed in the Egyptian coasts and Suez Canal (Ghobashy and Abdel Messeih, 1991; Halim and Abdel Messeih 2016).

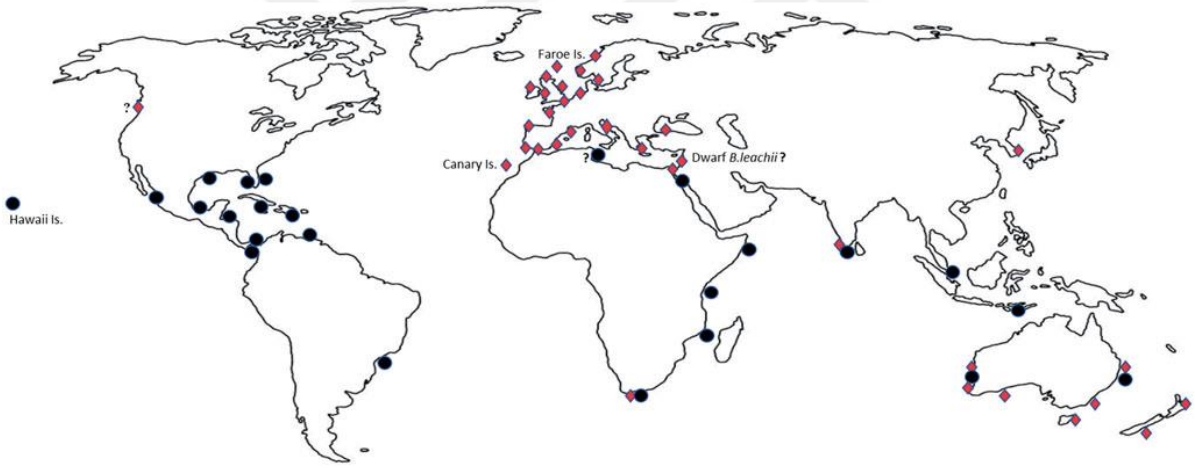


Figure 10. Worldwide distribution of *B. leachii* is demonstrated with diamonds; closely confused sister species *B. nigrum* is stated with circles (Reem et al., 2017).

The first record of *B. leachii* from the Levantine coasts of Turkey was documented in Mersin Harbour (Pınar, 1974). Between October 1968 and October 1969, previously placed neutral plaques were monitored as monthly. Physical parameters of the station were documented in Fig. 11. The water temperature during this period of time was recorded to between 16 and 27.6^{0}C. Salinity was reported to fluctuate between 31.6 and 39,4 ppt from April to July. The water of the harbour was found to be semi-polluted and decreasing oxygen concentration was recorded throughout the monitored year. The area was emphasized to be out of any current

effect. During the monitored period, *B. leachii* was observed on the plaques only between April-June period. No morphological documentation of *B. leachii* was provided within the study. In the study, no any other *B. leachii* record was given for any other Turkish coastline stations (Marmara and Aegean seas) (Pınar, 1974).

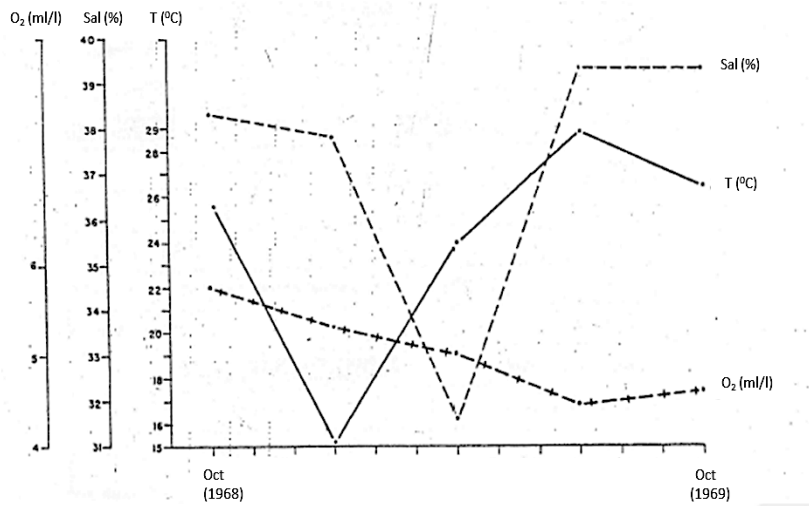


Figure 11. Time series temperature, salinity and oxygen concentration of Mersin Harbour for the first *B. leachii* record period (Pınar, 1976).

1.8. DNA Barcoding

DNA barcoding is a novel tool to identify species based on a short but conserved DNA sequence or sequences depending on the taxa (Hebert et al., 2003). Basically, it is an act of tagging the living organisms to differentiate correctly. Molecular data those are combined with morphological identification is found to supply more accurate taxa assignment, especially for the species which classical taxonomy did not discriminate well. At the beginning it was not fundamentally used for taxonomy but as supplementary, but nowadays, it is primarily used for species identification and accepted as one of the most efficient methods for biodiversity assessment without a need of a taxonomist (Bucklin et al., 2011)

DNA barcoding has an essential novelty where DNA sequence analysis is using to separate or unite the molecular data by supplying fast, proper and accurate identification (Hebert & Gregory, 2005). The barcodes especially are useful for cryptic species delineation or morphologically similar groups which are hardly differentiated solely based on the phenotype (Bucklin et al., 2011). Most commonly gene that use for the DNA barcoding in the Animalia kingdom is mitochondrial Cytochrome Oxidase Subunit I (COI) which is around 650 base pairs

long (Hebert et al. 2003). Determined threshold distance to discriminate a species divergence for COI gene is generally less than 2% in metazoans while interspecific distance can be between 10 to 25% (Hebert et al. 2003). Based on this knowledge, within some exceptions, if the distance between two metazoans sample is more than 2%, they are accepted as different species (Hebert et al., 2003). This is known as cladistic species concept, in this concept, a lineage of populations between two phylogenetic branch points is accepted as a species (Hennig, 1966).

Additionally, there are many important reasons about why COI is commonly used for this concept and recommended barcode region for most of the metazoan taxa;

1. Located in the mitochondrial genome where there are no introns
2. DNA repair mechanism is very low
3. It has great number of copies in each cell
4. Inherited by maternally
5. Each feature is represented with one gene-Haploid (Avise et al., 1987; Galtier et al., 2007; Gissi et al., 2008; Bucklin et al., 2011).

It has been known that DNA barcoding is a practical tool to catalogue the biodiversity. In the Levant, DNA barcoding studies of marine organisms highly increased, especially to evaluate invasions from the Suez Canal (Karahan et al., 2017). Monitoring biodiversity through the barcoding methods has positive effect to improve conservation policies. Acceleration of these studies in the Levantine basin to understand marine species dispersal and interactions has great impact on the combining knowledge about ecosystem dynamics and future implementations (Smith et al., 2008; Borges et al., 2012; Azzurro et al., 2015; Bariche et al., 2015; Karahan et al., 2017; Reem et al., 2017; Golestani et al., 2019). In the last decade barcoding studies in the Turkish coasts also has gained a momentum (Eryılmaz et al., 2006; Keskin & Atar, 2013; Oter et al., 2013; Bilgin et al., 2014; Seyhan & Turan, 2016; Tuney et al., 2016; Çiftçi et al., 2017; Ozbek et al., 2017; Turan et al., 2017). Most of these researches have been performed to give the first records of the species. Along with mitochondrial genes, nuclear genome is also analysed by looking for conserved but also polymorphic loci such as 18S rRNA nuclear locus (Neigel et al., 2007). In the scenarios where COI unsuccessful, other possible barcoding gene regions such as internal transcribed spacers (ITS) of nuclear rRNA genes were also used to enable adequate distinction for various marine taxa (Bucklin et al., 2011). Essentially,

comparative analyses among several barcode regions revealed that using multi-barcodes was favourable regardless of sufficiency the COI barcode alone for species identification (Neigel et al., 2007).

1.9. Phylogeography

Phylogeography is relatively recent field that investigates the geographical distribution of genealogical lineages (Avise et al., 1987). After the common use of molecular markers to understand the linkage between congeneric species, geography was also found to be connected with the evolutionary relations (Avise, 2009).

Genealogical studies show that tracing the ancestry through genome of populations could lead to untangle of phylogenies (Avise, 2009). In terrestrial environments, spatial analyses of populations are relatively easier unlike aquatic systems where the population dynamics are more turbulent and harder to estimate. When the advancement in maritime traffic and aquaculture is considering, establishments of marine organisms to new environment is inevitable (Ruiz et al., 1997). Thus, phylogeographic studies on marine environments could elucidate the dispersal of the populations. As a result, gene flow, genetic diversity, isolation patterns, barriers, bottlenecks could be enlightened (Avise et al., 2000).

There are increasing number of phylogeographic studies trying to resolve the genetic network of various tunicate species regarding with the spatial distance (Tarjuelo et al., 2004; Rius et al., 2008; Goldstien et al., 2011; Haydar et al., 2011; Lejeusne et al., 2011; Pineda et al., 2011; Sheets et al., 2016). Regardless of being solitary or compound, by these researches, it has been tried to address the questions on the dispersion, genetic variation and evolutionary origin of many tunicate species. For instance, *Botryllus schlosseri* and *Botrylloides violaceus* are ecologically similar colonial tunicates but on the other hand their dispersal vessel is different: *B. schlosseri* use ship fouling and *B. violaceus* shellfish aquaculture trade (Lejeusne et al. 2011). Further, Pineda et al. (2011) stated no phylogeographic difference in a solitary ascidian, populations, *Styela plicata*, for both COI and ANT markers. These findings support the necessity and importance of phylogeography to understand the populations' genetic backgrounds, interactions through an evolutionary and ecological perspective.

So far, there is no phylogeographical research on the *B. leachii*. However, a phylogeographical study using mitochondrial COI and nuclear ANT markers on *B. nigrum* was published by Sheets et al. in 2016. According to the study, *B. nigrum* have low genetic divergence for both

loci. But beside of this, chimeras based on mitochondrial locus were identified by emphasizing on having a novel haplotype diversity.

2. AIM OF THIS STUDY

In the present study, it was aimed to enlighten the genetic and morphological diversity of the North-eastern Mediterranean *B. aff. leachii* populations by investigation morphological features and using 5 molecular markers (COI, H3, ANT, 18S and 28S). By comparing current study sequences with other sequences those mined from GenBank, the evolutionary and phylogeographical relations were tried to estimate. Additionally, two other nuclear genes (18S rRNA & 28S rRNA) of several specimens were amplified to increase the molecular resolution. With this study, the first barcode of *B. aff. leachii* from the Levantine coasts of Turkey are acquired and used to understand the spatial variation within the North-eastern Mediterranean populations and also with several populations from other seas. To resolve temporal variation, Kızkalesi station was monitored for a year by time series sampling. Another aim of the study was to correlate morphological characteristics of *B. aff. leachii* with the molecular results. For this reason, morph variation and blastogenic cycles were monitored and analysed.

3. MATERIALS & METHODS

3.1. Sample Collection & Study Area

The North-eastern Mediterranean has been chosen as study area because of the lack of any tunicate research before. Also, the region was described as hot-spot area for species infestations (Karahan et al., 2017). The sampling stations were selected from the preliminary field trips. Most of the coastal shores of the Levantine were visited and searched for the presence of tunicates. The stations were basically determined where there were botryllid ascidians.

3.1.1. Spatial sampling

Specimens were sampled from the coastal area of Mersin (Mezitli-Kızkalesi-Tisan), Hatay (Konacık) and Antalya (Side-Kemer-Alanya-Tersane) in late September and October period (Fig. 12). The samples were collected from the stones and were removed by using a single edged razor blade from their substrate and taken to a microscope slide attaching with a sewing thread. Sample collection were done in the shore and water depth was approximately 30-50

cm. Coordinates, salinity, pH and sampling dates of the sampling area are given in Table 2. In total 137 spatial samples were collected.

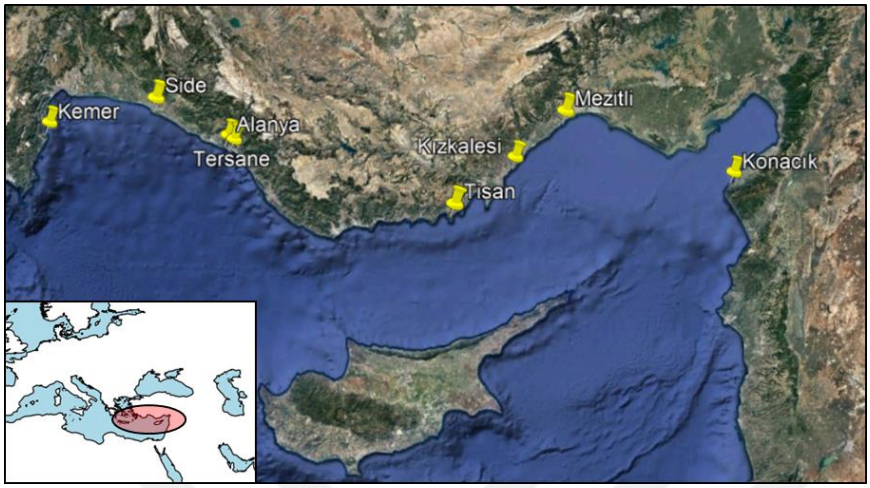


Figure 12. Sampling stations

Table 2. Details of sampling stations.

Region	Station	Date	Coordinates	Salinity (ppt)	pH	n
Mersin	Kızkalesi	03/10/18	36°27' 27.52" N/34°08' 38.17" E	39-40	~ 8	38
	Mezitli	14/10/18	36°43'58.76"N/34°31'18.53"E	39.2	8.13	14
	Tisan	03/10/18	36°09' 27.95" N/33°40' 59.90" E	40.2	8.35	14
Hatay	Konacık	26/09/18	36°21' 38.79" N/35°49' 16.90" E	40	7.9	5
Antalya	Alanya	24/10/18	36°33' 33.85" N/31°57' 07.41" E	39.8	8	23
	Side	24/10/18	36°46' 00.78" N/31°23' 07.62" E	37.5	7.8	10
	Kemer	25/10/18	36°35' 59.55" N/30°34' 30.66" E	40.1	7.9	30
	Tersane	29/10/18	36°32' 05.14" N/31°59' 53.89" E	-	-	3

n: sample number

Besides of 2018, some specimen was also collected during the previous and following field trips (Table 3).

Table 3. Additional samples from the Kızkalesi station.

Date	n
July - 2014	3
September - 2014	16
March - 2019	1
April - 2019	1

n: samples number

3.1.2. Time series sampling

To investigate the effect of climate on the population dynamics, *B. aff. leachii* specimens were collected monthly from Kızkalesi station between November 2017 and October 2018 (Table 4). The size and number of the colonies were getting to increase through June to October period (Table 4).

Table 4. Kızkalesi time series station.

Date	n
November - 2017	18
December -2017	0
January - 2018	0
February - 2018	0
March – 2018	0
April – 2018	0
May - 2018	0
June - 2018	0
July - 2018	4
August - 2018	17
September – 2018	25
October -2018	38

n: sample number

3.2. Morphological Identification of Specimens

All tunicate specimens were identified by morphological examination with respect to their zooid distribution, colour and habitat preferences. The living specimens that were taken to laboratory were examined under stereo and light microscope. Since, morphological identification of botryllid ascidians could lead in ambiguities, species identification was fundamentally performed based on molecular taxonomy.

3.3. DNA Extraction & Polymerase Chain Reaction

DNA extraction was done by following Paz et al. (2003) protocol. Each sample was placed into 1.5 ml tube then the tubes were taken to laboratory for following processes. After adding 100 µl lysis buffer (0.25 M Tris Borate pH 8.2, 0.1 M EDTA, 2% SDS, 0.1 M NaCl) samples

were homogenized by using sterile sticks, 20 µl NaClO4 (5 M), 120 µl of phenol-chloroform-isoamyl alcohol (25:24:1) were added on the homogenized samples. Then the samples were mixed for 1 min and centrifuged at 14 000 rpm [10 000 X g] for 5 minutes. Supernatant was discarded and same volume of chloroform-isoamyl alcohol (24:1) was added onto each pellet. Again, mixed for 1 min and centrifuged at 14 000 rpm [10 000 X g] for 5 minutes. Supernatant was discarded and the pellet was precipitated with 100% absolute cold ethanol that makes DNA visible at this stage. The tubes left for overnight at -20°C. Next day, the tubes were centrifuged at 14 000 rpm [10 000 X g] for 30 minutes and then washed with 70% ethanol three times. The pellets left to dry and next day dissolved in 50 µl double distilled water. The DNA samples were kept and stored at -20°C.

DNA amplification was performed following Reem et al. (2017; Deg COI F2 & Deg COI R2) to amplify mitochondrial Cytochrome Oxidase Subunit I (COI) gene region. To amplify COI and nuclear Histone 3 (H3), 18S, 28S and Adenine Nucleotide Transporter/ADP-ATP Translocase (ANT) genes, the reactions were done following respectively as Folmer et al. (1994), Reem et al. (2017) and Teske et al. (2011) (Table 5). Two PCR products were gained from some of the samples ANT's PCR (1000-1500 bp) those products were cut from the 1% agarose gel and after purification with NucleoSpin® Gel and PCR Clean-up kit were sent to Macrogen Inc. (Seoul, South Korea) for sequencing for both forward and reverse directions.

Table 5. PCR programs for COI, H3, ANT, 28S rRNA and 18S rRNA genes

PCR	Denaturation	Annealing	Extension	Final Extension	Cycle	Ref.
COI	95ºC (1 min)	45ºC (30 sec)	72ºC (1 min)	72ºC (10 min)	35	Folmer et al., 1994
H3	95ºC (1 min)	55ºC (45 sec)	72ºC (1 min)	72ºC (10 min)	35	Reem et al., 2017
ANT	95ºC (1 min)	60ºC (45 sec)	72ºC (1 min)	72ºC (10 min)	35	Teske et al., 2011
28S	95ºC (1 min)	62ºC (45 sec)	72ºC (1 min)	72ºC (10 min)	35	Reem et al., 2017
18S	95ºC (1 min)	60ºC (45 sec)	72ºC (1 min)	72ºC (10 min)	35	Reem et al., 2017

3.3.1. Primers

The primers used in the present study were given in Table 2.

Table 6. Primers of the present study

Primer Name	Primer Sequence	Product size
DEG COI F2	5-‘AMWAATCATAAAGATATTRGWAC’-3	~700 bp
DEG COI R2	5-‘ AARAARGAMGTRTTRAAATTHCGATC’-3	
H3 F1	5-‘ATGGCTCGTACCAAGCAGACVGC’-3	~300 bp
H3 R1	5-‘ATATCCTTRGGCATRATRGTGAC’-3	
STOLIDOANT-F	5-‘CAGGGTATCATTGTRTACMGAG’-3	~300-1200 bp
ANTR1	5-‘ CCAGACTGCATCATCATKCGRCGDC’-3	
28S C1	5-‘ACCCGCTGAATTTAAGCAT’-3	~640 bp
28S D2	5-‘ TCCGTGTTTCAAGACGGG’-3	
18S A	5-‘AACCTGGTTGATCCTGCCAGT’-3	~960 bp
18S B	5-‘GATCCTTCTGCAGGTTCACCTAC’-3	

3.4 Bioinformatics

3.4.1. Sequencing, alignment, editing and bioinformatics analyses

Both directions of all sequences were aligned for each gene regions separately by using DNA Baser Assembler version 5.15.0 (DNA Sequence Assembler, 2012, Heracle BioSoft, www.DnaBaser.com). The contigs were aligned again on BioEdit version 7.0.5.3 (Hall, 1999), edited and trimmed. Polymorphic sites (Np) and haplotypes (Nh), Fu and Li’s F, Fu and Li’s D and Tajima’s D tests were used to calculate the population history and regional changes with respect to test of neutrality via DNAsp version 6.10.04 (Rozas et. al., 2003). Population analyses such as gene flow, genetic differentiations and population size changes were also performed using DNAsp. Distances among haplotypes were measured by using median joining algorithm with default settings to build the network by using NETWORK version 5.0.1.1 (Bandelt et al., 1999). Bayesian analyses were conducted by using MrBayes with InvGamma model (Ronquist et al., 2012). Coupled runs were applied and the trees were constructed by using Figtree version 1.4.3 (Rambaut, 2012).

Accession numbers of the COI sequences those taken from GenBank (https://www.ncbi.nlm.nih.gov/genbank/) are KY235403.1 (*B. leachii* from California coast of USA; unpublished), MG009578.1 (*B. leachii* from Mediterranean coast of Israel; Reem et al., 2017), KF309644.1 (*B. leachii* from Mediterranean coast of Spain; López-Legentil et al., 2015), HF548553.1 (*B. leachii* from Adriatic coast of Italy; Griggio et al., 2014), KP254541.1 (*B. nigrum* from Florida coast of USA; Leray & Knowlton, 2015) and the COI out-group

sequence is AY600987.1 (*Botryllus schlosseri* from Mediterranean coast of Spain; Turon & López-Legentil, 2004).

Accession numbers of the retrieved H3 sequences from GenBank are MG009592.1 (*B. leachii* from Mediterranean coast of Israel; Reem et al., 2017) and the out-group H3 sequence MG009595.1 (*Botryllus schlosseri* from Mediterranean coast of Israel; Reem et al., 2017).

3.4.2. Barcoding of Life Database (BOLD) submission

Sequences, trace files, image files and primer information of each haplotypes were uploaded to the Barcode of Life Data System [BOLD, http://www.boldsystems.org, (Ratnasingham & Herbert, 2007). The barcodes of each haplotypes will be public after the publication and can be find within the project file "IMS-METU-Animalia".

4. RESULTS

4.1. Morphology & Life cycles

4.1.1 Morphological Records on the Zooid and Colonial bases

Colonies within a gelatinous matrix (tunic) were attached to hard substrate, typically rocks in the shallow water. The distribution of colonial zooids was arranged like ladder shape also called as "*leachii"* type. The zooids were aligned side by side in the way their dorsal lamina facing with surrounding environment while ventral side staying on the attached side" (Fig. 13).

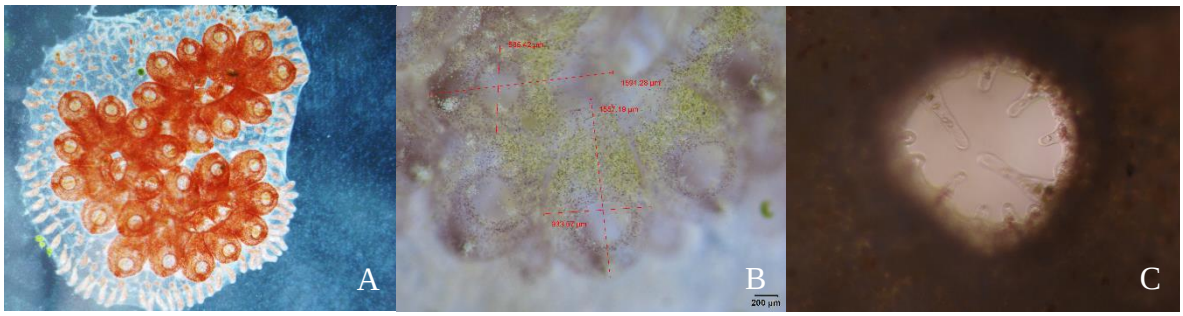


Figure 13. An orange *B. aff. leachii* morph. A) General morphology and structure of the colony. B) Zooid morphology from the dorsal side, dashed red lines respresent heigth (1557 µm) and width (933 µm) of a zooid. C) the image of the buccal siphon with 4 large and 4 small tentacles.

Different colony colour and pattern were recorded for the *B. aff. leachii* such as orange, light violet with green pigmented cells at the dorsal tongue and dark red-brownish on the sides and

orange pigmented blood cells at the dorsal lamina and around of the buccal siphon. Each animal feeding by filtering seawater through their own buccal siphon. They have 4 large and 4 small tentacles inside the buccal siphon and 8 alternative smallest protrusions observed also (Fig. 14). Pigmented blood cells were also recorded on the tentacles, especially on the two largest ones lining towards each other. Zooids do not possess atrial siphon instead they have a systemic defecation space called atrial opening. A high amount of the pigmented blood cells on both sides of the endostyle are lining from top to bottom. Without taking histological section a detailed anatomical observation on internal organs such as cardiac swelling, pyloric caecum and gut-intestine were insufficient.

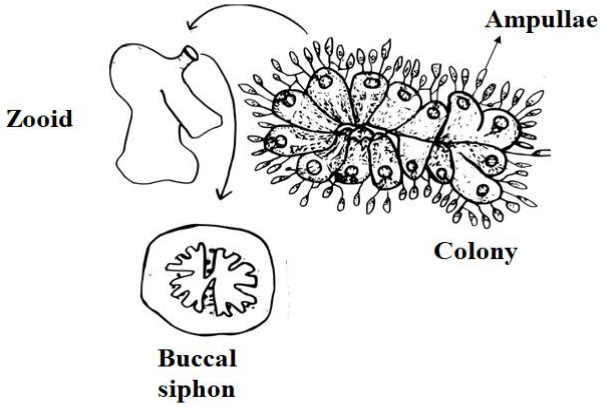


Figure 14. An illustration of *B. aff. leachii* colony. A colony, zooid, ampullae (vascular termini) and the buccal siphon with tentacles were depicted.

4.1.2. Morphological diversity

Nine different morphs were observed among the sampled colonies (Fig. 15). The recorded morphs were orange, brown, red, brown with orange stripes, brown with white stripes, brown-violet with green stripes, violet-green, cream, pinkish and blackish.



Figure 15. Illustration of *B. aff. leachii* major morph patterns

4.2. Asexual Reproduction - Blastogenic Cycle / Palleal Budding

Blastogenic cycle was occurred as the replacement of a functioning adult zooid through the development of newly formed identical primary zooid from this adult also called as parental zooid and by this process asexual reproduction also takes place. This biological process is also called as blastogenesis or palleal budding since the primary zooids are created through budding from parental zooids (Figure 16).

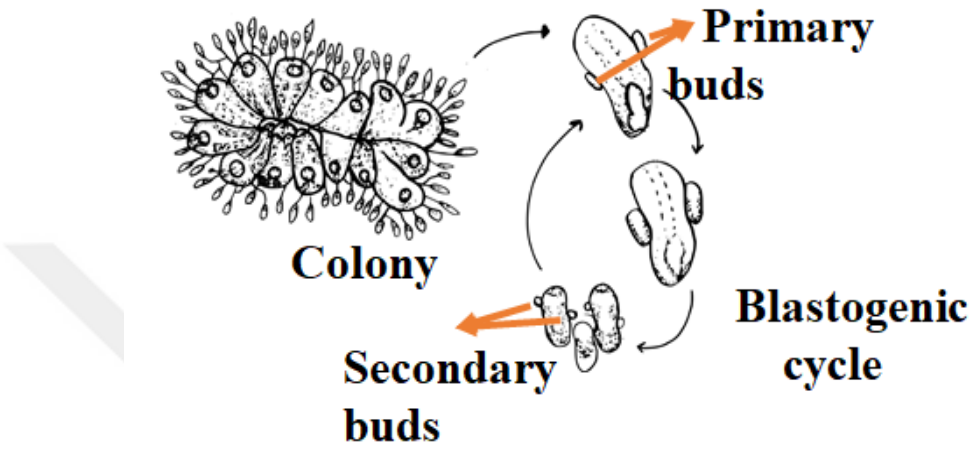


Figure 16. Illustration blastogenic cycle of *B. aff. leachii*

Blastogenic cycle of *B. aff. leachi* was examined in four stages (A, B, C, D) like *Botryllus schlosseri*. Duration of blastogenesis can vary from 4 to 7 days. These cycles were sequential unless the organism is in the hibernation (stage H) or under stress. During the first cycles of blastogenesis, generally two primary blastozooids formed by budding from parental zooid as growing attached through the metamorphosis. During stage B, the flow in the cardiac swellings of the primary buds were observed. In C stage, the formation of secondary blastozooids was seen attached to primary zooids. In the last stage, also known as takeover phase, oral siphon of the parental zooids was closed and started to be reabsorbed while the identical fully mature primary zooids takeover their place. Blastogenic cycle of one morph was given in the Figure 17 and all the other monitoring records are supplied in the Appendix A.

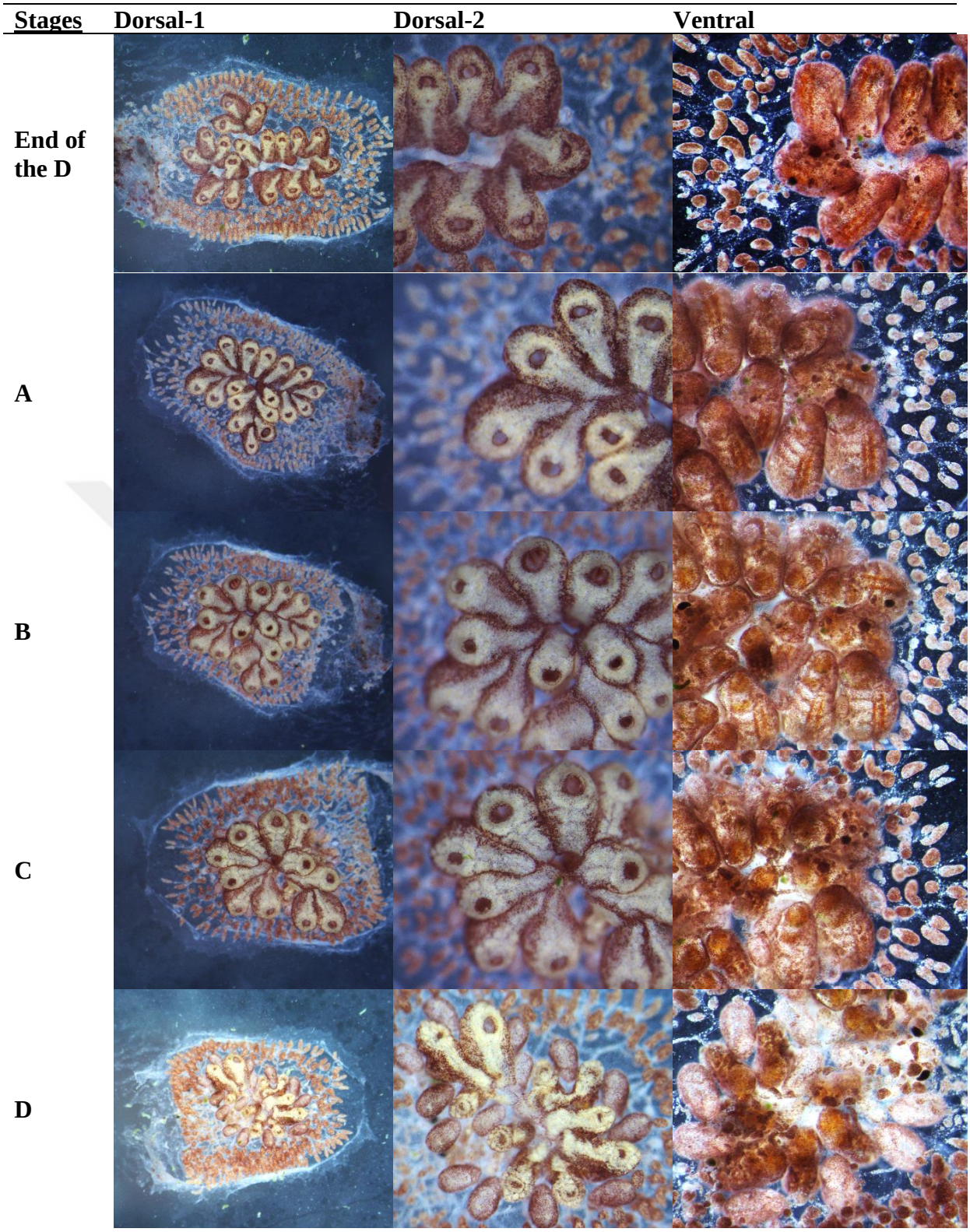


Figure 17. Blastogenic cycle of *B. aff. leachii*. Cycle was monitored daily basis and images were recorded under stereo microscope.

4.3. Hibernation

The living colonies were kept at 20^0C in the IMS-METU aquaculture room. The temperature and light of the room were stable all the time. Salinity of the water was kept at 40 ppt all along. The food concentration and amount were arranged and sustained steadily. Under this constant condition among 21 living colonies, 14 of them were undergo to hibernation during the winter season. Time to time the rest of the colonies were covered with ampullae, like preparing to enter the hibernation stage, but then the blastogenic cycles were continued. Entering the hibernation under the constant ecological conditions may be related with the biological rhythms (circadian/circalunar) of the organism.

During hibernation, there was no observed zooid on the dormant system. The blood circulation was recorded to be low and thicker than normal. Overall morphology was carpet-like due to covered with ampullae (Fig. 18). High pigmentation was also recorded. Termination of hibernation and building new zooids were not recorded since the colony could not recover in aquaculture system.

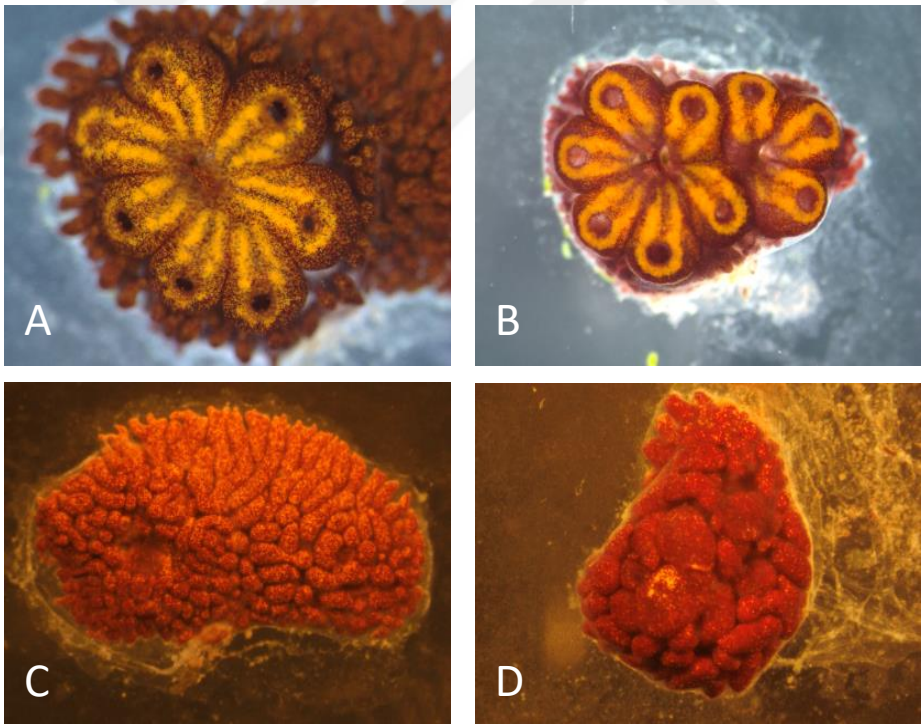
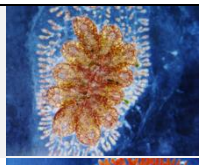
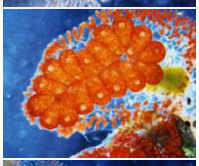
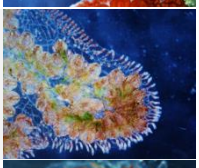
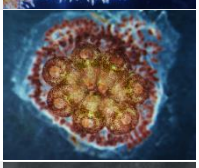


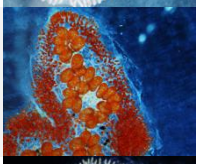
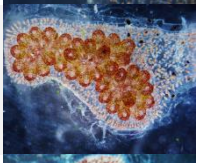
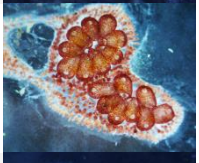
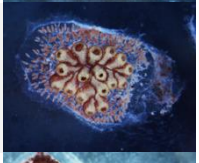
Figure 18. *B. aff. leachii* on hibernation. A) A Typical *B. aff. leachii* morph from Tisan station (specimen code G8). B) Same morph was also taken from Kızkalesi station (specimen code GK13). C) G8 is recorded during hibernation. D) Hibernation morphology of GK13 is also provided.

4.4. Life spans of the living colonies

The living colonies taken from the sampling stations were kept at 20^{O}C degree and used for several assays. In total, 21 colonies were kept and life span of these colonies was recorded and given in the Table 7.

Table 7. The life span of the *B. aff. leachii* colonies those were cultured in IMS-METU aquaculture room.

Code of specimen	Starting day of culture	Day of Death	Approx. month of living	Morph
Z1	03.08.18	14.03.19	7	
Z2	03.08.18	15.02.19	6	
Z4	03.08.18	14.03.19	7	
G1	03.10.18	25.12.18	2	
G8	03.10.18	25.12.18	2	
G13	03.10.18	22.04.19	6	
G15	03.10.18	26.02.19	4	
GK1	03.10.18	22.04.19	6	

GK4	03.10.18	14.03.19	5	
GK7	03.10.18	01.04.19	6	
GK13	03.10.18	07.12.18	2	
GK21	03.10.18	16.05.19	7	
R1	18.09.18	12.02.19	5	
R4	18.09.18	16.05.19	8	
R5	18.09.18	16.05.19	8	
R6	18.09.18	22.04.19	7	
R8	18.09.18	16.05.19	8	
R9	18.09.18	07.12.18	3	
L15	26.09.18	16.05.19	8	
L18	26.09.18	16.05.19	8	

NN	03.08.18	26.02.19	6	

Although they were all kept at the same laboratory conditions, the life span among the living colonies varied from 2-8 months. Only the 8 months living colonies were able to fixed in Bouin's solution (5% acetic acid, 9% formaldehyde, 0.9% picric acid), those samples will be used for further analysis while the others those in the hibernation period (stage H) separated from the slide after a while and washed away during the water replacement process. Only one correlation was observed between G8 and GK13 colonies. Both had same phenotype (dark brown colour with orange stripes) and approximately equal life span (~2 months) (Table 4). For G8 and GK13, regression of zooids and presence of excessive ampullae as a sign of hibernation were recorded which could be interpreted for the reason of short life (Fig. 17). Both organisms were monitored and recorded not to recover from hibernation. However, different morphs were also represented to have same life interval. Moreover, the biggest difference among life spans of two identical morphs was recorded between G1 and R5 as 2 and 8 months respectively. In conclusion, there was no distinct pattern observed between morph variation and life span.

4.5. Molecular Results

4.5.1 Spatial Results

4.5.1.1. Mitochondrial COI Gene Analyses

4.5.1.1.1. Distance Analysis

Final length of aligned and trimmed COI partial sequences was 519 bp. Distance analysis was performed to understand the COI gene divergence among the present study's North-eastern Mediterranean populations (Table 5; from 1 to 8) and the sequences those mined from the GenBank (Table 5; from 9 to 12). Kimura 2-parameter model with Gamma distributed version was used via MEGA 7 (Kumar et al., 2008).

No divergence was recorded among the Tisan, Alanya, Side, Kemer and Kızkalesi populations. Highest difference was observed between the Mezitli and Konacık samples as 0.3%. Around 17% diverge were recorded between the GenBank (Table 5; 10-13) mined samples and present study populations. The closest database sample was *Botrylloides nigrum* that uploaded from USA (Table 5; 9), differentiation ratio of this samples from the present study samples was

recorded as 0.4-0.7%. Differentiation range of the out-group sequence (*Botryllus schlosseri*) was recorded as 20%.

Table 8. Mean distance of between populations are given in the lower triangle, upper triangle shows the standard deviations.

Between	1	2	3	4	5	6	7	8	9	10	11	12	13	14
1.Mezitli		0.002	0	0	0	0	0	0	0.004	0.025	0.025	0.026	0.026	0.028
2.Konacik	0.003		0.002	0.002	0.002	0.002	0.002	0.001	0.002	0.025	0.025	0.027	0.026	0.029
3.Tersane	0.001	0.003		0	0	0	0	0	0.004	0.025	0.025	0.026	0.026	0.029
4.Tisan	0.001	0.003	0		0	0	0	0	0.004	0.025	0.025	0.026	0.026	0.029
5.Alanya	0.001	0.003	0	0		0	0	0	0.004	0.025	0.025	0.026	0.026	0.029
6.Side	0.001	0.003	0	0	0		0	0	0.004	0.025	0.025	0.026	0.026	0.029
7.Kemer	0.001	0.003	0	0	0	0		0	0.004	0.025	0.025	0.026	0.026	0.029
8.Kızkalesi	0.001	0.003	0	0	0	0	0		0.004	0.025	0.025	0.026	0.026	0.029
9.USA- *B. nigrum*	0.007	0.004	0.007	0.007	0.007	0.007	0.007	0.007		0.026	0.026	0.028	0.027	0.03
10.USA-*B. leachii*	0.169	0.174	0.169	0.169	0.169	0.169	0.169	0.169	0.18		0	0.004	0.003	0.03
11.Israel- *B. leachii*	0.169	0.174	0.169	0.169	0.169	0.169	0.169	0.169	0.18	0		0.004	0.003	0.03
12.Spain- *B. leachii*	0.179	0.185	0.18	0.18	0.18	0.18	0.18	0.18	0.191	0.009	0.009		0.004	0.03
13.Italy- *B. leachii*	0.176	0.181	0.177	0.177	0.177	0.177	0.177	0.177	0.188	0.004	0.004	0.009		0.031
14.Out-group	0.21	0.216	0.211	0.211	0.211	0.211	0.211	0.211	0.223	0.216	0.216	0.219	0.224	

4.5.1.1.2. Network Analysis

Network analysis of *B. leachii* and (one) *B. nigrum* sequences based on COI locus clearly states the position of current study haplotypes (Fig. 19). Present study samples were clustered under the four haplotypes; H1, H6, H7 and H8. H6, H7 and H8 are private for the North-eastern Mediterranean (Turkey), H7 is the main haplotype recorded in 217 samples. H6 and H8 those recorded in Mezitli and Kızkalesi samples respectively are differentiated from the main haplotype (H7) with 1 mutation step while the H1 that observed only in Konacık samples was located 3 mutation steps away. On the other hand, the Konacık haplotype (H1) clustered with *B. nigrum* (USA) sample that was mined from the GenBank. Among the recorded data, the Israeli samples was located the closest proximity to the Turkish coastline samples, but at least 60 mutation steps recorded between those samples. Out-group (*Botryllus schlosseri*) was observed to vary from the current study *B. aff. leachii* samples in at least 71 mutation steps.

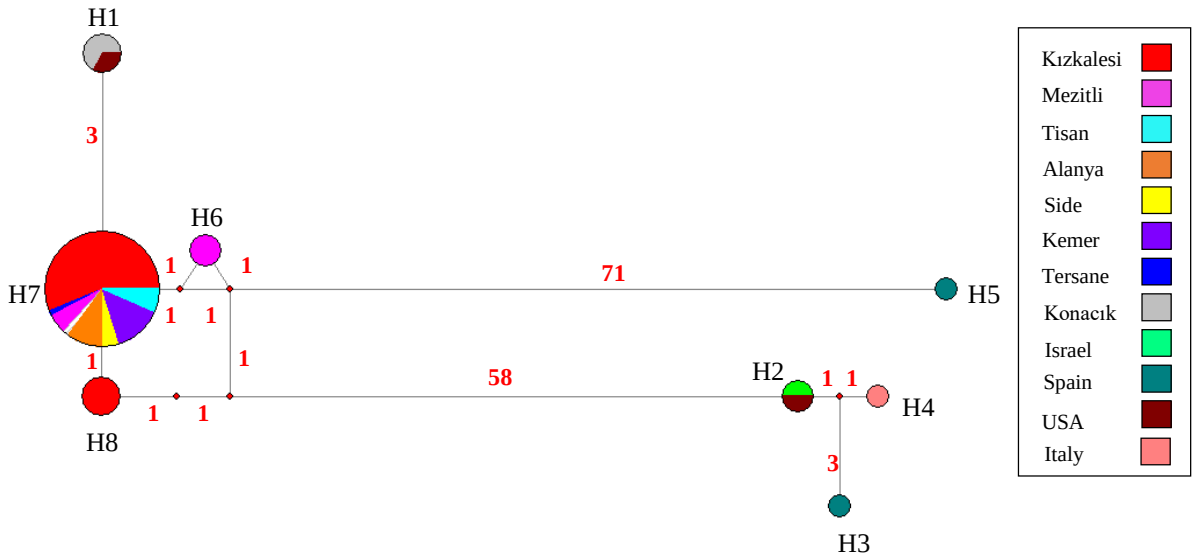
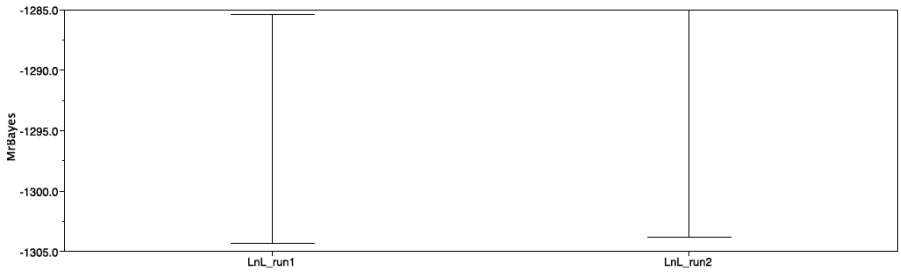


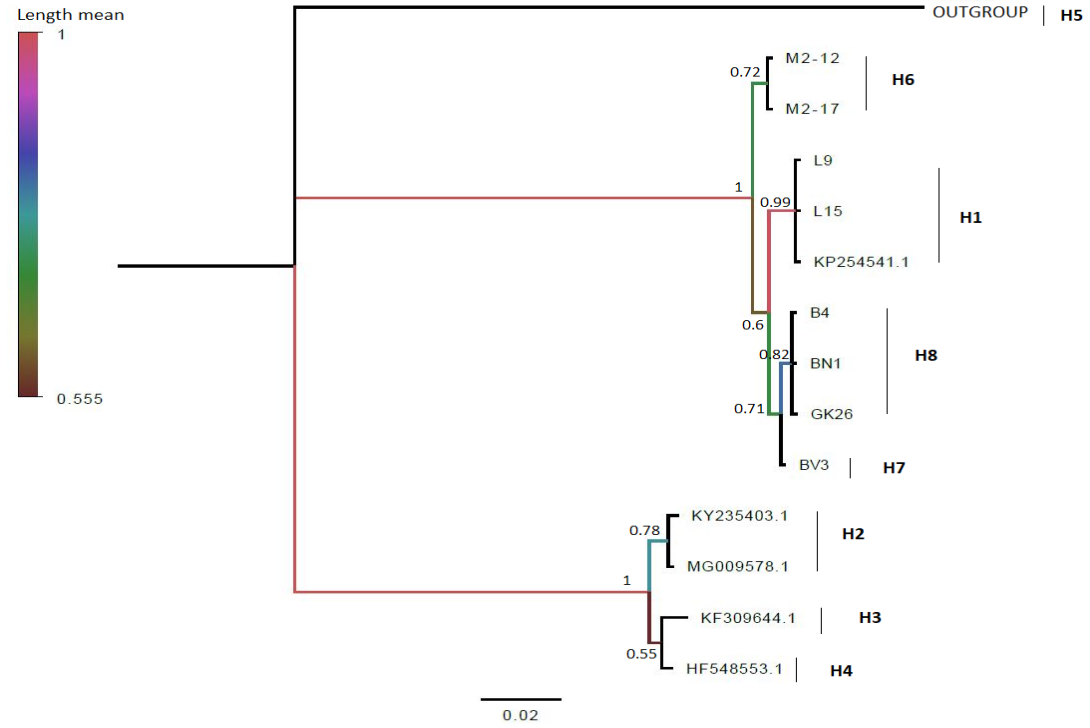
Figure 19. Median Joining Network analysis of *B. aff. leachii* based on COI locus was constructed. Circles were remarked by the haplotype name. Size differences of circles state frequency while colours reflect regions where the haplotype was taken. The region names were seen on the right of the network. Numbers represent mutation steps between the haplotypes. USA samples (brown): sample clustered in H1 is *Botrylloides nigrum*, -H2 is *B. leachii*.

4.5.1.1.3. Bayesian Phylogeographic Analysis

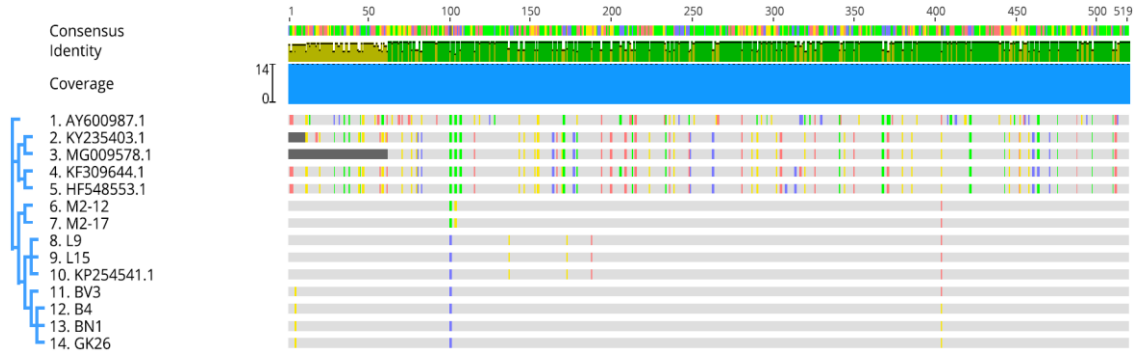
Bayesian tree for 7 network haplotypes (excluding out-group) was presented by using InvGamma model (Fig. 20). Current study haplotypes (H1, H7, H6, H8) and the other *B. leachii* sequences were observed to be monophyletic sister groups considering the distance.



A



B



C

Figure 20. A) Coupled runs were resulted the posterior probabilities of the Bayesian analysis (Summary Statistic: mean = -1294; std. dev. of mean = 8.6; 95% HPD lower = -1304; 95% HPD upper = -1285; auto-correlation time (ACT) = 277.85; effective sample size (ESS) =3289) B) Bayesian phylogeographic analyses based on 519 bp partial COI sequences of haplotypes

was constructed. Distance scale was supplied below the tree and the haplotypes were specified on the tree. Branches were scaled in colour with respect to the length mean. Colour range is provided. C) Bayesian consensus tree with the illustration of polymorphic sites.

4.5.1.1.4. Spatial Populations Parameters

To understand population parameters regionally, sequence numbers (n), number of polymorphic sites (Np), number of haplotypes (Nh), nucleotide diversity (Pi), haplotype diversity (Hd), Fu and Li's D (Fu&LD), Fu and Li's F (Fu&LF) and Tajima's D (Taj. D) were calculated and documented in Table 6. In total, 138 sequences were analysed. Two haplotypes were recorded in Kızkalesi, Mezitli and Konacık populations. Despite the lower number of sample size (5), the highest polymorphism (4), nucleotide diversity (0,0046) and haplotype diversity (0,6) were measured in Konacık population. No polymorphism was documented among Tisan, Alanya, Side, Tersane and Kemer populations.

Table 9. Spatial populations parameters based on the COI locus of the North-eastern Mediterranean populations.

Populations	n	Np	Nh	Pi	Hd	Fu &LD	F&LF	Taj.D
Kızkalesi	38	1	2	0,0001	0,053	$-1,758^{NS}$	$-1,823^{NS}$	$-1,129^{NS}$
Mezitli	14	3	2	0,0015	0,264	$1,070^{NS}$	$0,757^{NS}$	$-0,494^{NS}$
Tisan	14	0	1	0	0	0^{NS}	0^{NS}	0^{NS}
Alanya	24	0	1	0	0	0^{NS}	0^{NS}	0^{NS}
Side	10	0	1	0	0	0^{NS}	0^{NS}	0^{NS}
Tersane	3	0	1	0	0	0^{NS}	0^{NS}	0^{NS}
Kemer	30	0	1	0	0	0^{NS}	0^{NS}	0^{NS}
Konacık	5	4	2	0,0046	0,600	$1,641^{NS}$	$1,670^{NS}$	$1,641^{NS}$
All	138	7	4	0,0004	0,071	$0,257^{NS}$	$-0,557^{NS}$	$-1,857^{*}$

Sequence numbers (n), number of polymorphic sites (Np), number of haplotypes (Nh), nucleotide diversity (Pi), haplotype diversity (Hd), Fu and Li's D (Fu&LD), Fu and Li's F (Fu&LF) and Tajima's D. Window length: 100 Step size: 25. Not significant (NS), $P < 0.05$ (*).

Besides, Fu and Li's D, Fu and Li's F and Tajima's D test were run to examine the neutrality of mutations. The examinations were based on the idea that all the mutations are under neutral selection. Although both are based on the same idea, the approach of Fu&Li's test is coalescent while Tajima's D is not. In this case, significant positive Fu&Li's and Tajima's D values are interpreted as balancing selection while the negative values are indicated as population expansion or negative selection (Tajima, 1989; Fu, 1997). Within this scope and based on the significant negative Tajima's D value (Table 9), it is possible to say that the overall Turkey's North-eastern Mediterranean populations are under negative selection and the population is

expanding. Further mismatch distribution analyses were performed (Fig. 21). Raggedness statistic values for all distributions were resulted with insignificant (r > 0.05).

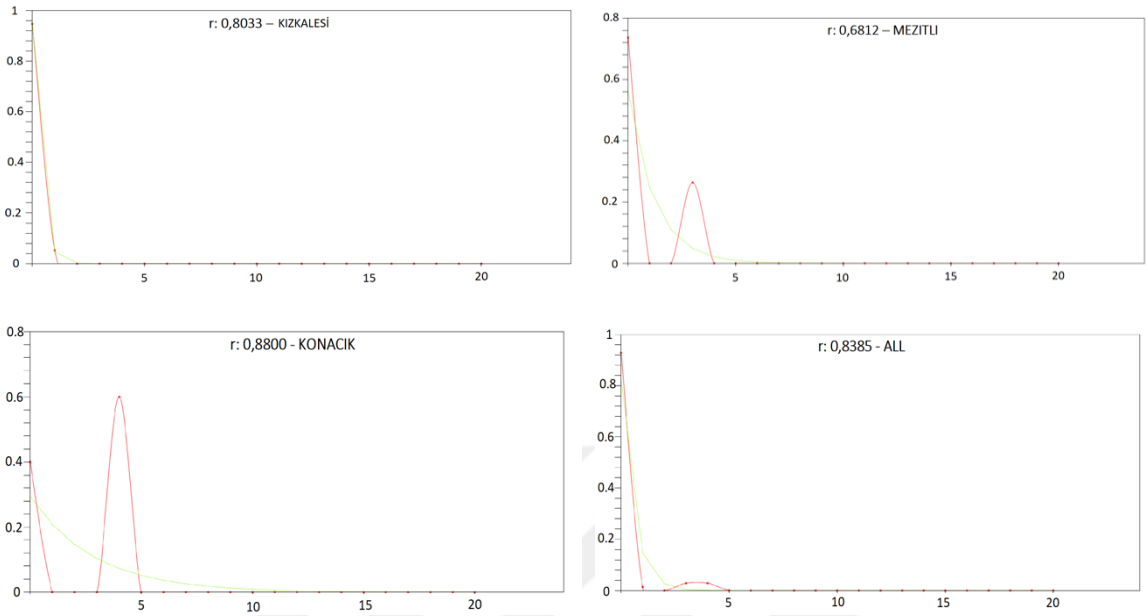


Figure 21. Population size changes were demonstrated based on mismatch distribution of COI gene for Kızkalesi, Mezitli, Konacık and all populations. Raggedness statistic values (r) for each analysis was supplied (r> 0.05). The X-axis states the number of pairwise differences while the Y-axis represents frequency. Red line indicates observed frequency for stable population size and green line shows expected frequency.

Kızkalesi population was observed as unimodal due to a possible population expansion. Multimodal pattern was observed for Mezitli, Konacık and overall populations which might be linked with a population subdivision and a constant population size.

Furthermore, pairwise gene flow (Nm) approximations for 8 spatial stations as listed in the Table 7. Present study samples were demonstrated to divide in two groups. The first one is Tersane, Tisan, Alanya, Side and Kemer and the second Mezitli, Konacık and Kızkalesi populations. While there was no gene polymorphism to conduct this test in the first group, significant gene flow was observed between the all populations of second group. The highest gene flow was measured between the Kızkalesi and Kemer stations.

Following with the gene flow approximations, genetic differentiation analyses on spatial populations were performed (Table 11). Significant gene differentiations were observed in Konacık population. Also, between Kemer and Mezitli stations, significant genetic differentiation was seen.

Table 10. Gene flow (Nm) approximations for spatial stations (Nei, 1973).

Nm	Mezitli	Konacık	Tersane	Tisan	Alanya	Side	Kemer
Mezitli							
Konacık	6.71						
Tersane	8.76	3.75					
Tisan	12	1.92	0				
Alanya	9.16	1.66	0	0			
Side	13.92	2.17	0	0	0		
Kemer	8.29	1.58	0	0	0	0	
Kız Kalesi	16.03	2.61	7.63	96.06	576.98	46.53	2422

Nm <1; there is not enough gene flow to negate the effects of genetic drift – not possible to prevent genetic differentiation; Nm > 1, there is enough gene flow to decrease the effects of genetic drift; Nm > 4, populations involves in one randomly mating population.

Table 11. Pairwise genetic differentiation (F_{st}) within spatial populations. The method is applied for 10.000 permutations (Hudson, Slatkin & Maddison, 1992).

F_{st}	Mezitli	Konacık	Tersane	Tisan	Alanya	Side	Kemer
Mezitli							
Konacık	0.17*						
Tersane	0.08^{NS}	0.25^{NS}					
Tisan	0.08^{NS}	0.25*	-				
Alanya	0.08^{NS}	0.25**	-	-			
Side	0.08^{NS}	0.25*	-	-	-		
Kemer	0.08*	0.25***	-	-	-	-	
Kızkalesi	0.07^{NS}	0.25***	0^{NS}	0^{NS}	0^{NS}	0^{NS}	0^{NS}

(P 0.01<P<0.05) significant (*); (0.001< P < 0.01) significant (**); (P < 0.001) significant (***); not significant (NS).

4.5.1.2. Nuclear H3 Gene Analyses

4.5.1.2.1. Distance Analysis

Aligned and trimmed histone 3 partial sequences were 280 bp. Intraspecific distances among the current study sequences were measured to resolve H3 gene divergences (Table 5; from 1 to 8) by also comparing *B. leachii* H3 sequences from databases (Table 12). Kimura 2-parameter with Gamma distributed model was used via MEGA 7.

Unlike the COI, higher variation in population level was recorded for H3 gene. No divergence was recorded between the Konacık, Mezitli and Tisan populations. Highest divergence among the current study populations was seen between the Side & Alanya (0.8%) populations. One *B. leachii* sequence that mined from the NCBI (Table 12; 8-Israel, Reem et al., 2017) was compared with present study samples and 1.7-2.1% divergence has been observed. Out-group

sequence (*Botryllus schlosseri*) was seen to differ ~14% from all the listed (Table 12; 1-8) populations.

Table 12. Intraspecific mean distance between the present study populations (except Tersane) are shown in the lower triangle, upper triangle reflects the standard deviations.

Between	1	2	3	4	5	6	7	8	9
1.Konacık		0	0.001	0	0.003	0.002	0.001	0.008	0.028
2.Mezitli	0		0.001	0	0.003	0.002	0.001	0.008	0.028
3.Kızkalesi	0.001	0.001		0.001	0.003	0.002	0.001	0.008	0.028
4.Tisan	0	0	0.001		0.003	0.002	0.001	0.008	0.028
5.Alanya	0.004	0.004	0.005	0.004		0.003	0.003	0.009	0.028
6.Side	0.004	0.004	0.005	0.004	0.008		0.002	0.008	0.028
7.Kemer	0.001	0.001	0.002	0.001	0.005	0.005		0.008	0.028
8.Israel	0.017	0.017	0.018	0.017	0.021	0.021	0.017		0.029
9.Out-group	0.136	0.136	0.137	0.136	0.134	0.141	0.137	0.137	

4.5.1.2.2. Network Analysis

Network estimation based on Histone 3 gene was performed including a *B. leachii* and an out-group (*Botryllus schlosseri)* H3 sequences both from Israel coast of Mediterranean (Fig. 22). In total fourteen haplotypes (H1-H14) were recorded for current study samples. Three main haplotypes H1, H2 and H4 were observed. The rest of the eleven haplotypes were measured to differ from the main haplotypes within 1 to 8 mutation steps. No distinct regional separation was observed among the current study populations. Furthermore, one Kemer haplotype (H14) was seen separated from the other populations in minimum 8 mutation steps. The *B. leachii* haplotype (H15) from Israel was seen differentiate from the Turkey haplotypes with minimum 5 mutation steps. Thirty-three mutation steps variation was observed between the present study samples and out-group species (*Botryllus schlosseri*).

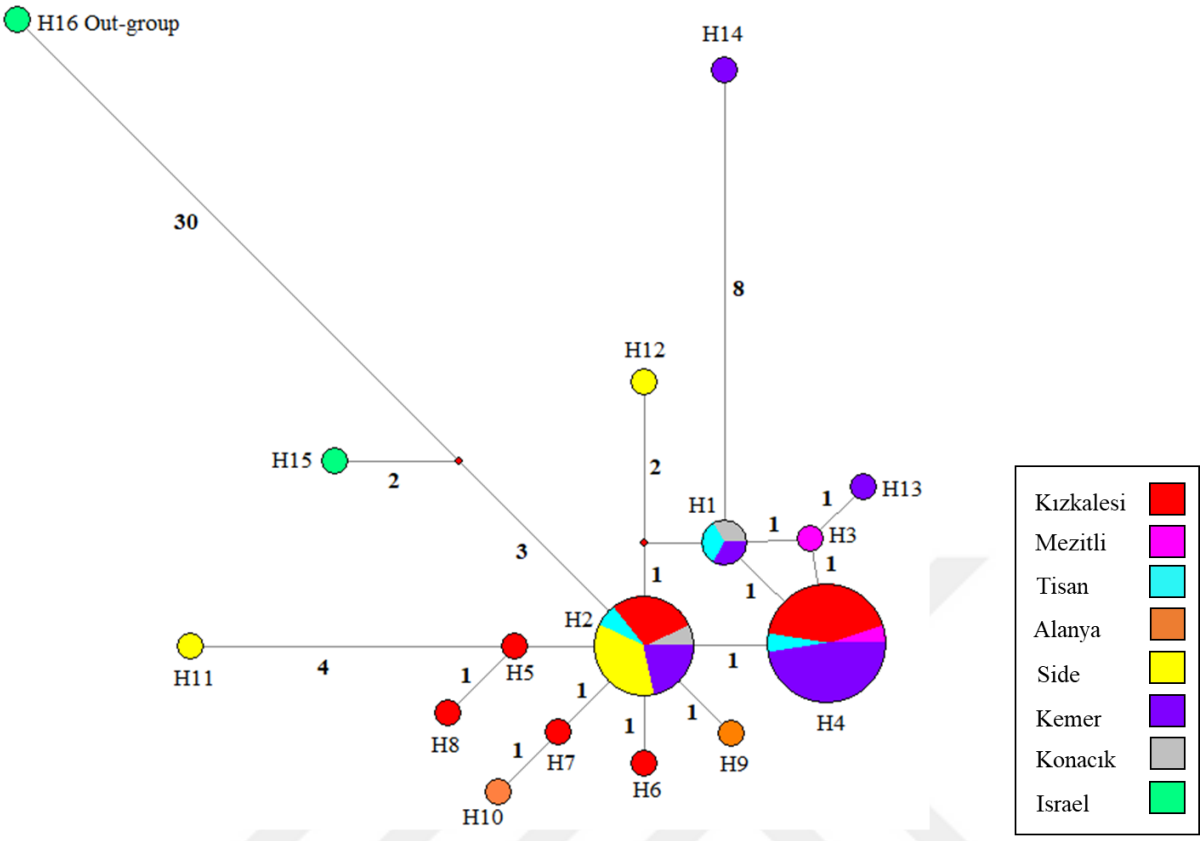


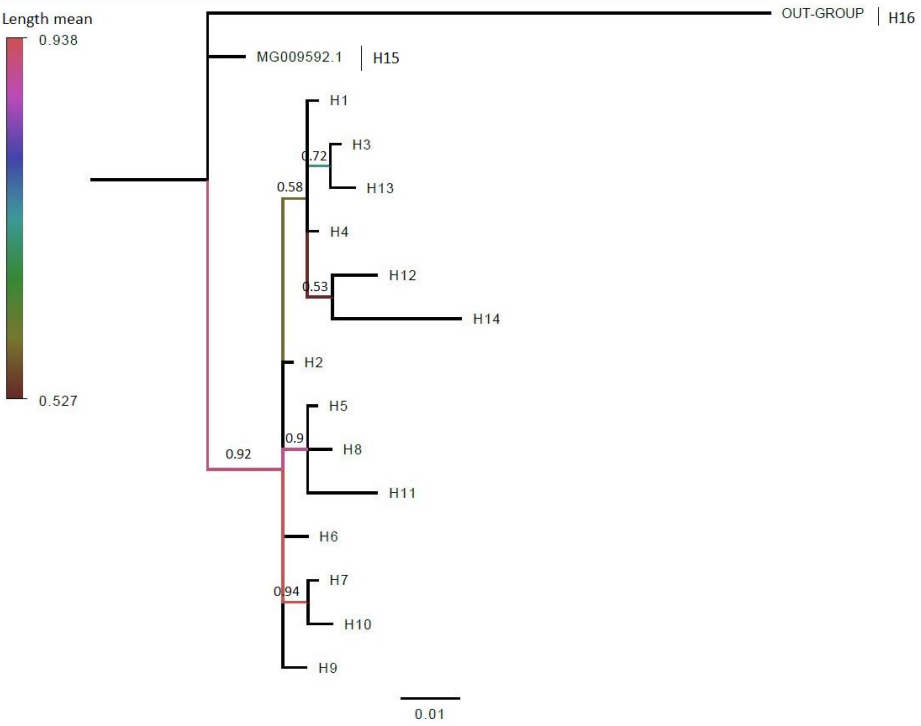
Figure 22. Median Joining Network estimation of *B. aff. leachii* based on H3 locus was illustrated. Circles reflects the haplotype name. Size differences of circles represent frequency. Colours depicts regions where the haplotype was located. The region names were given on the right side of the network. Numbers shows mutation steps between the haplotypes.

4.5.1.2.3. Bayesian Phylogeographic Analyses

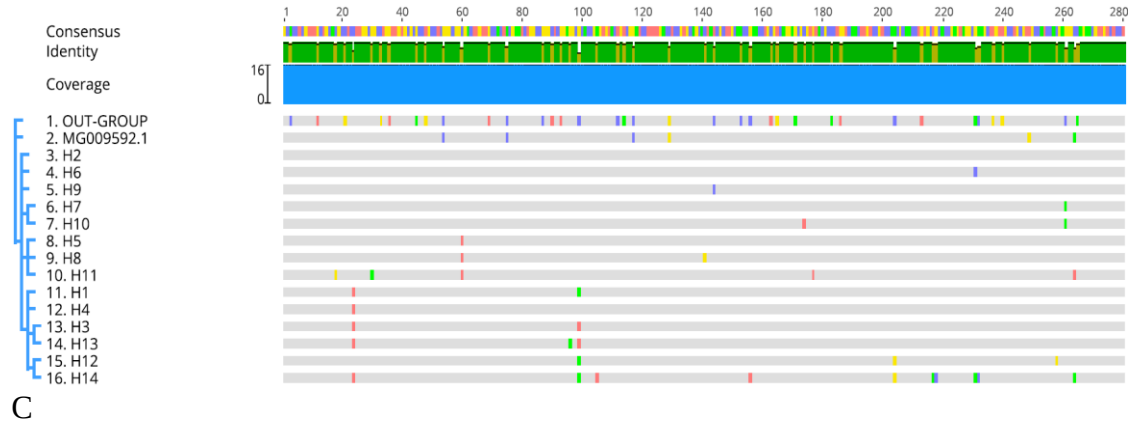
Bayesian tree for 15 H3 haplotypes (excluding out-group) was presented by InvGamma model (Fig. 23). Current study haplotypes (H1-H14) were recorded to cluster in one group. Besides, haplotype 11 and 14 were seen to diverge clearly within the cluster. Compared to the *B. leachii* sequence from Israel, the Turkey cluster were observed to be monophyletic sister group based on the evolutionary distance.



A



B



C

Figure 23. A) The posterior probabilities of the Bayesian analysis were calculated for coupled runs (Summary Statistic: mean = -722; std. dev. of mean = 0.114; 95% HPD lower = -733; % HPD upper =-713; auto-correlation time (ACT) = 425.858; effective sample size (ESS) =2113)

B) Bayesian phylogeographic analyses based on 280 bp partial H3 sequences of haplotypes was modelled. Distance scale was provided below the tree and the haplotypes were stated on the tree. Branches were scaled in colour with respect to the length mean. Colour range is given. C) Bayesian consensus tree with the illustration of polymorphic sites.

4.5.1.2.4. Spatial Populations Analyses

Spatial population parameters based on H3 gene were calculated (Table 13). In total, 47 sequences were analysed and 14 haplotypes were observed. In total 20 polymorphic sites were recorded. The highest nucleotide diversity was seen within Alanya population (Pi = 0.011) while the lowest (Pi = 0.004) was observed in Mezitli population. The haplotype diversity (Hd) of Mezitli, Tisan, Alanya and Konacık populations were counted as 1. The highest polymorphism was seen in the Kemer population (Np=11).

Table 13. Spatial population parameters based on the H3 gene of the North-eastern Mediterranean populations.

Populations	n	Np	Nh	Pi	Hd	Fu&LD	F&LF	Taj.D
Kızkalesi	16	5	6	0.004	0.717	-1,052^{NS}	-1,128^{NS}	-2,149*
Mezitli	2	1	2	0.004	1	-	-	-
Tisan	3	2	3	0.005	1	-	-	-
Alanya	2	3	2	0.011	1	-	-	-
Side	7	8	3	0.008	0.524	-1,666^{NS}	-1,800^{NS}	-1,576^{NS}
Kemer	15	11	5	0.007	0.629	-2,234^{NS}	-2,455^{NS}	-1,885*
Konacık	2	2	2	0.007	1	-	-	-
All	47	20	14	0.006	0.755	-3,799**	-3,830*	-2,149*

Sequence numbers (n), number of polymorphic sites (Np), number of haplotypes (Nh), nucleotide diversity (Pi), haplotype diversity (Hd), Fu and Li's D (Fu&LD), Fu and Li's F (Fu&LF) and Tajima's D. Window length: 100 Step size: 25. Not significant (NS), P < 0.05 (*), P <0.02 (**)

Regarding to significant negative Fu and Li's D, Fu and Li's F and Tajima's D results, it can say that all populations are under the gene hitchhiking or population expansion. On the other hand, Kemer and Kızkalesi populations are found to be expanding. Additionally, mismatch distribution analyses were applied (Fig. 24). Raggedness statistic values for all distributions were found to be not significant (r > 0.05). Unimodal distribution were observed for Alanya, Kızkalesi, Konacık and Mezitli populations, the results might state expansion for these populations. On the other hand, multimodal distribution was recorded for Kemer, Side and overall North-eastern populations that demonstrate a possible population subdivision. Especially the Side population was seen to have the highest number of subdivisions.

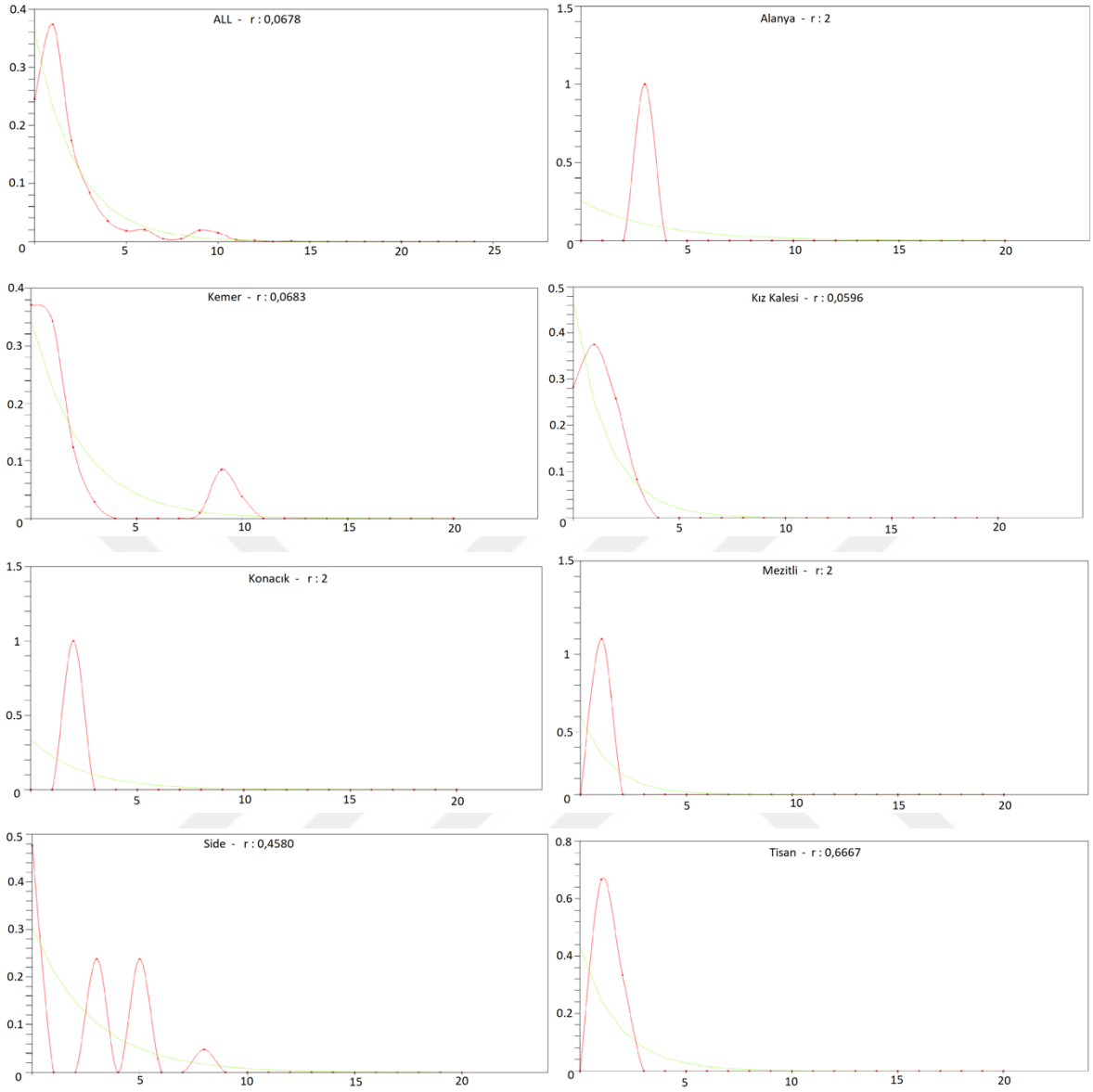


Figure 24. Population size changes were illustrated based on mismatch distribution of H3 for all populations. Raggedness statistic values (r) for each analysis was provided ($r > 0.05$). The X-axis shows the number of pairwise differences while the Y-axis states frequency. Red line infers observed frequency for stable population size and green line represents expected frequency.

Furthermore, pairwise gene flow (Nm) for H3 locus was calculated and listed in the Table 14. Highest gene flow was recorded between the Kemer and Tisan populations (85.11). No gene flow was observed between Alanya, Mezitli and Konacık populations.

Table 14. Gene flow (Nm) estimation based on H3 gene (Nei, 1973).

Nm	Konacık	Tisan	Kemer	Kızkalesi	Alanya	Side	Mezitli
Konacık							
Tisan	-1.65						
Kemer	2.52	85.11					
Kızkalesi	4.85	29.45	-14.95				
Alanya	0	30	1.78	2.04			
Side	-15.87	13.12	1.18	1.82	1.39		
Mezitli	0	-3.49	5.26	4.43	0	1.39	

Nm<1; there is not enough gene flow to negate the effects of genetic drift – not possible to prevent genetic differentiation; Nm > 1, there is enough gene flow to decrease the effects of genetic drift; Nm > 4, populations are within random mating population, not possible to block genetic differentiation.

Genetic differentiation (Fst) between the spatial populations were also calculated. As a result, significant positive values as a sign of differentiation was recorded the between several populations which are Alanya & Kemer (0.209), Side & Kemer (0.214) and Kızkalesi & Alanya (0.08).

Table 15. Pairwise genetic differentiation (Fst) analysis based on H3. The method is applied for 10.000 permutations (Hudson, Slatkin & Maddison, 1992).

Fst	Konacık	Tisan	Kemer	Kızkalesi	Alanya	Side
Konacık						
Tisan	-0.667^{NS}					
Kemer	-0.195^{NS}	-0.138^{NS}				
Kızkalesi	-0.197^{NS}	-0.080^{NS}	0.053^{NS}			
Alanya	0^{NS}	0.133^{NS}	0.209**	0.080*		
Side	-0.071^{NS}	0.116^{NS}	0.214*	0.107^{NS}	0^{NS}	
Mezitli	-0.200^{NS}	-0.167^{NS}	-0.063^{NS}	0.184^{NS}	0.333^{NS}	0.361^{NS}

(P 0.01<P<0.05) significant (*); (0.001< P < 0.01) significant (**); not significant (NS).

4.5.1.3. Nuclear ANT Gene Analyses

4.5.1.3.1. BLAST Analyses

BLAST analysis through NCBI was performed for the ANT sequences of current study. As the result, only the first 63 bases of the present study were matched with the database *B. leachii* sample (JF962229.1; Teske et al., 2011) (Fig. 25).

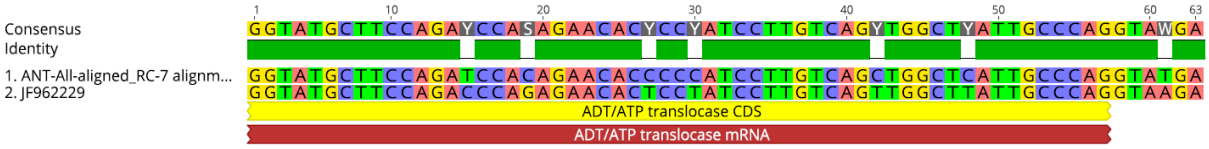


Figure 25. The BLAST result of the ANT sequence of present study and the database sequence (JF962229.1; Teske et al., 2011).

4.5.1.3.2. Distance Analysis

Aligned and trimmed ANT partial sequences were measured to range within 300-1000 bp. Pairwise genetics distances among the ANT sequences of current study were calculated to resolve the nuclear gene divergences (Table 16). Kimura 2-parameter with Gamma distributed model was used via MEGA 7.

Unlike the COI and H3, very high variation was recorded for ANT and the distance was ranging from 0.2% to 20%. Due to high level of variation clustering of populations has not been possible.

Table 16. Intraspecific mean distance between the present study samples based on ANT gene region are shown in the lower triangle.

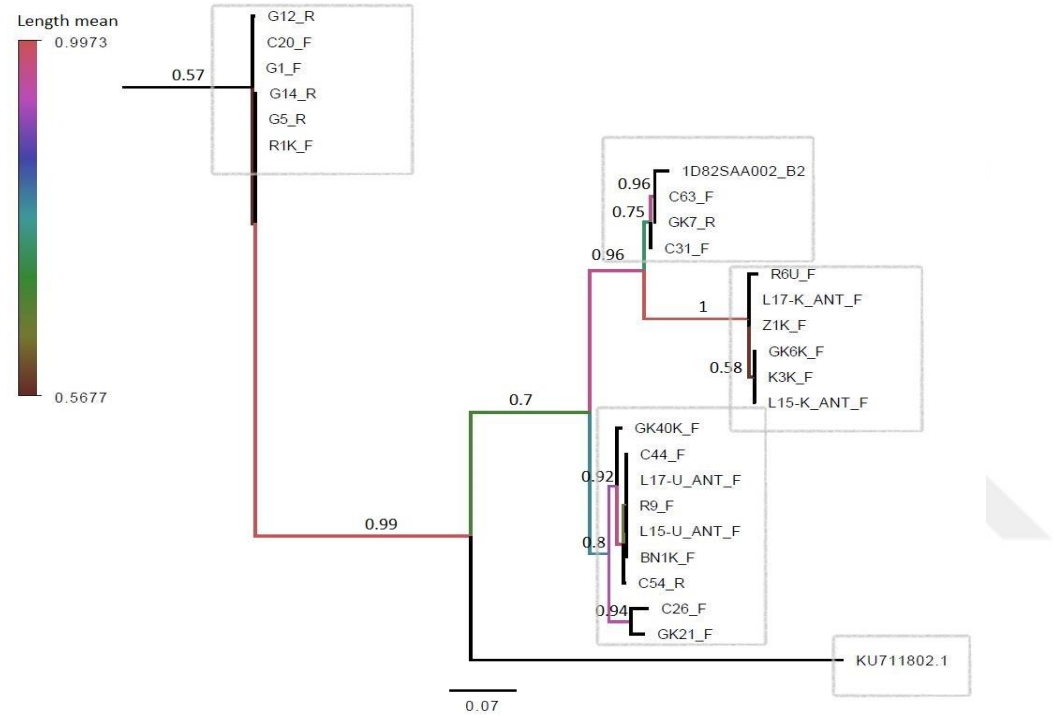
	1	2	3	4	5	6	7	8	9	10	11	12	13	14	15	16	17	18	19	20	21	22	23	24	25
1. G12																									
2. G14	0.002																								
3. G5	0.002	0.002																							
4. R1K	0.007	0.008	0.008																						
5. C20	0.007	0.008	0.008	0.014																					
6. G1	0.001	0.001	0.001	0.007	0.007																				
7. C39	0.244	0.245	0.245	0.237	0.251	0.244																			
8. C31	0.229	0.23	0.23	0.222	0.235	0.229	0.016																		
9. C63	0.233	0.234	0.234	0.226	0.239	0.232	0.012	0.005																	
10. GK7	0.233	0.234	0.234	0.226	0.24	0.233	0.012	0.005	0.001																
11. R6U	0.238	0.239	0.239	0.231	0.245	0.238	0.039	0.023	0.027	0.027															
12. L17K	0.241	0.241	0.241	0.233	0.247	0.24	0.041	0.025	0.029	0.03	0.011														
13. Z1K	0.238	0.238	0.239	0.23	0.244	0.237	0.038	0.022	0.026	0.027	0.008	0.003													
14. GK6K	0.244	0.245	0.245	0.237	0.251	0.244	0.044	0.029	0.033	0.033	0.015	0.004	0.007												
15. K3K	0.244	0.244	0.244	0.236	0.25	0.243	0.044	0.028	0.032	0.033	0.014	0.003	0.006	0.001											
16. L15K	0.242	0.243	0.243	0.235	0.249	0.242	0.042	0.027	0.031	0.031	0.013	0.002	0.004	0.002	0.001										
17. GK40K	0.192	0.193	0.193	0.185	0.199	0.192	0.109	0.093	0.097	0.097	0.103	0.105	0.102	0.108	0.108	0.106									
18. C44	0.194	0.194	0.195	0.186	0.2	0.193	0.11	0.095	0.099	0.099	0.104	0.106	0.103	0.11	0.109	0.108	0.014								
19. L17U	0.194	0.194	0.195	0.186	0.2	0.193	0.11	0.095	0.099	0.099	0.104	0.106	0.103	0.11	0.109	0.108	0.014	0.001							
20. R9	0.193	0.194	0.194	0.186	0.2	0.193	0.11	0.094	0.098	0.099	0.104	0.106	0.103	0.11	0.109	0.108	0.014	0	0						
21. C54	0.202	0.202	0.203	0.194	0.208	0.201	0.118	0.103	0.107	0.107	0.112	0.114	0.111	0.118	0.117	0.116	0.022	0.009	0.009	0.008					
22. L15U	0.193	0.194	0.194	0.186	0.2	0.193	0.11	0.094	0.098	0.099	0.104	0.106	0.103	0.11	0.109	0.108	0.014	0	0	0	0.008				
23. BN1K	0.197	0.198	0.198	0.19	0.204	0.197	0.114	0.098	0.102	0.102	0.108	0.11	0.107	0.113	0.113	0.111	0.017	0.004	0.004	0.004	0.005	0.004			
24. C26	0.201	0.202	0.202	0.194	0.208	0.201	0.118	0.102	0.106	0.106	0.112	0.114	0.111	0.117	0.117	0.115	0.044	0.045	0.045	0.045	0.053	0.045	0.049		
25. GK21	0.194	0.195	0.195	0.187	0.201	0.194	0.111	0.095	0.099	0.1	0.105	0.107	0.104	0.111	0.11	0.109	0.037	0.039	0.039	0.038	0.046	0.038	0.042	0.028	

4.5.1.3.3. Bayesian Tree

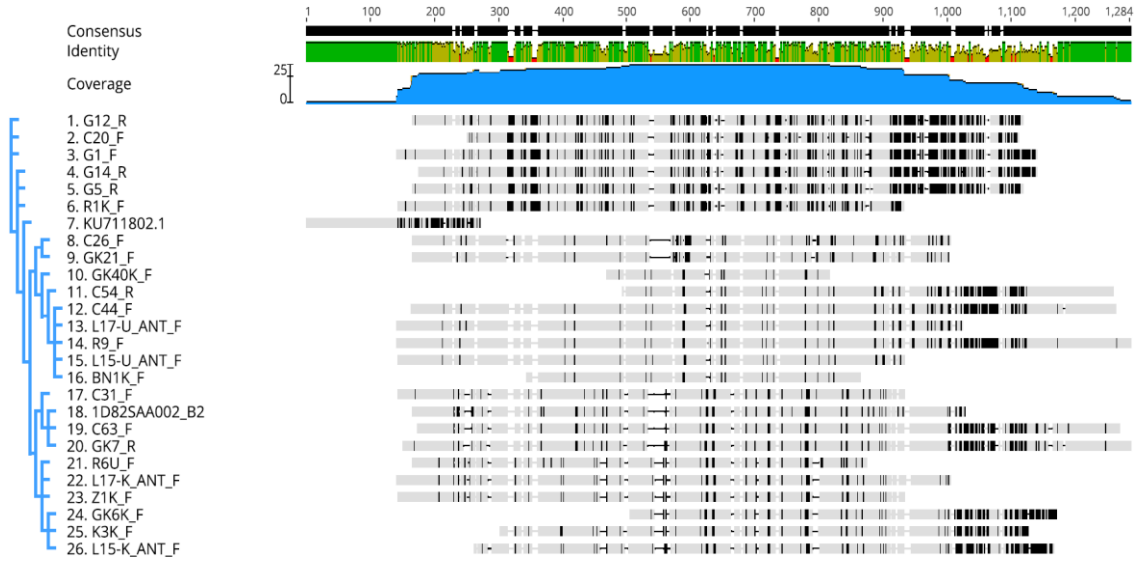
Bayesian tree for all ANT sequences was illustrated by using InvGamma model. Posterior probabilities of the Bayesian analysis were also demonstrated (Fig 26). As a result, four possible sub-clusters were caught. The region was seen to have ultra-variation with many polymorphisms, possibly due to multiple recombination events.


-3880.0
-3885.0
-3890.0
-3895.0
-3900.0
-3905.0
-3910.0
-3915.0
MrBayes
LnL_run1
LnL_run2

A


Length mean
0.9973
0.5677
G12_R
C20_F
G1_F
G14_R
G5_R
R1K_F
0.57
1D82SAA002_B2
C63_F
GK7_R
C31_F
0.96
0.75
0.96
R6U_F
L17-K_ANT_F
Z1K_F
GK6K_F
K3K_F
L15-K_ANT_F
1
0.58
0.7
GK40K_F
C44_F
L17-U_ANT_F
R9_F
L15-U_ANT_F
BN1K_F
C54_R
C26_F
GK21_F
0.92
0.8
0.94
0.99
KU711802.1
0.07

B


Consensus
Identity
Coverage
1
100
200
300
400
500
600
700
800
900
1,000
1,100
1,200
1,284
25
0
1. G12_R
2. C20_F
3. G1_F
4. G14_R
5. G5_R
6. R1K_F
7. KU711802.1
8. C26_F
9. GK21_F
10. GK40K_F
11. C54_R
12. C44_F
13. L17-U_ANT_F
14. R9_F
15. L15-U_ANT_F
16. BN1K_F
17. C31_F
18. 1D82SAA002_B2
19. C63_F
20. GK7_R
21. R6U_F
22. L17-K_ANT_F
23. Z1K_F
24. GK6K_F
25. K3K_F
26. L15-K_ANT_F

C

Figure 26. A) The posterior probabilities of the Bayesian analysis were measured for coupled runs (Summary Statistic: mean = -3897; std. dev. of mean = 0.277; 95% HPD lower = -3912; % HPD upper =-3884; auto-correlation time (ACT) = 675.078; effective sample size (ESS) =666). B) Bayesian phylogeographic analyses based on ~300-1200 bp partial ANT sequences of *B. aff leachii* was drawn. Distance scale was provided below the tree and the haplotypes were represented on the tree. Branches were scaled in colour with respect to the length mean. Colour range is supplied C) Bayesian consensus tree based on ANT locus is supplied with the illustration of the polymorphic sites.

4.5.2. Temporal Results

4.5.2.1. Mitochondrial COI Gene

4.5.2.1.1. Temporal Population Parameters

Temporal population parameters based on COI gene was calculated for Kızkalesi time series station (Table 17). In total, 103 sequences were analysed. Two haplotypes were observed. Solely one polymorphic site was seen. The highest nucleotide and haplotype diversity were observed within November-2017 population while no diversity was observed for July-August-September-2018 period. Significantly, the same polymorphism was recorded within November-2017 and September-2018 populations.

Table 17. Kızkalesi time series population parameters

Populations	n	Np	Nh	Pi	Hd	Fu &LD	F&LF	Taj.D
November-2017	18	1	2	0,0002	0,111	$-1{,}450^{NS}$	$-1{,}612^{NS}$	$-1{,}165^{NS}$
July-2018	4	0	1	0	0	0^{NS}	0^{NS}	0^{NS}
August-2018	17	0	1	0	0	0^{NS}	0^{NS}	0^{NS}
September-2018	26	0	1	0	0	0^{NS}	0^{NS}	0^{NS}
October-2018	38	1	2	0,0001	0,053	$-1{,}758^{NS}$	$-1{,}823^{NS}$	$-1{,}129^{NS}$
All	103	1	2	0,0001	0,038	$0{,}491^{NS}$	$0{,}080^{NS}$	$-0{,}912^{NS}$

Sequence numbers (n), number of polymorphic sites (Np), number of haplotypes (Nh), nucleotide diversity (Pi), haplotype diversity (Hd), Fu and Li's D (Fu&LD), Fu and Li's F (Fu&LF) and Tajima's D. Window length: 100 Step size: 25. Not significant (NS), $P < 0.05$ (*).

Furthermore, negative Fu and Li's D, Fu and Li's F and Tajima's D values show that November-2017 and October-2018 populations were not rejected to be under gene hitchhiking or population expansion due to the non-significant values. Based on Fu and Li's D and Fu and Li's F, through one year, it can be said that Kızkalesi time series samples are under the

balancing selection and hence the polymorphism could be conserved, although negative Tajima's D test result is stated the opposite situation.

Population changes were illustrated in Fig. 27. The value of the population those don't have any polymorphic site were not be estimated. All the populations were displayed unimodal graphs, it is indicating that populations are expanding.

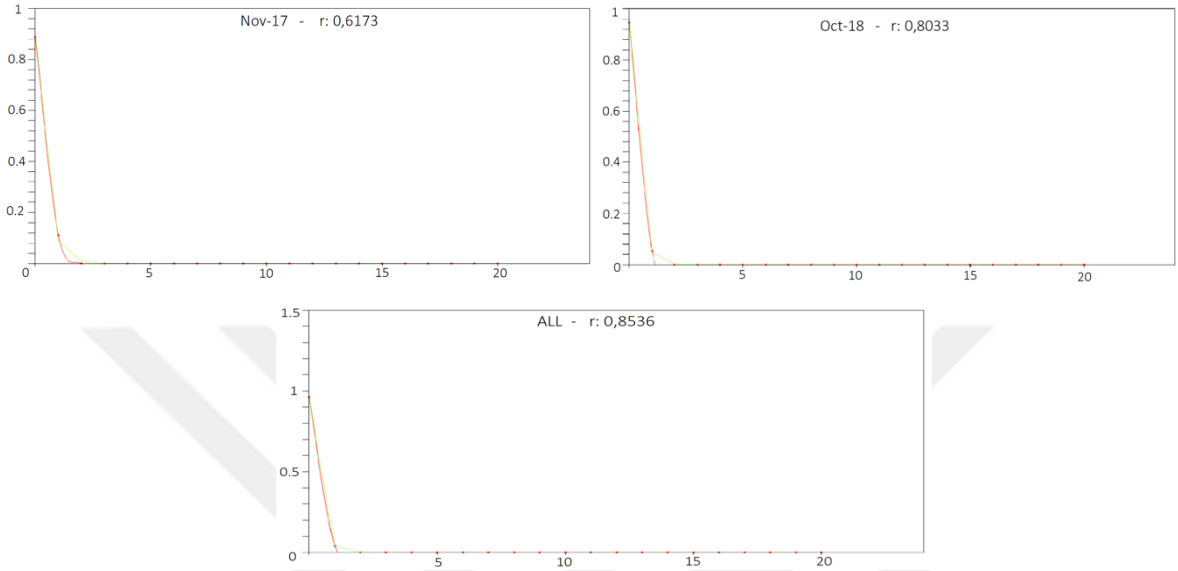


Figure 27. Population size changes of Kızkalesi time series station based on mismatch distribution of COI. Raggedness statistic values (r) for each analysis were seen on the graph (r>0.05). The X-axis shows the number of pairwise differences while the Y-axis states frequency. Red line shows observed frequency for stable population size and green line represents expected frequency.

Pairwise correlation between each station was performed to understand the presence of gene flow (Table 18). Highest gene flow was seen between the November and August samples (21420). Negative result between the November and October (-32.79) can be sign of hybridization phenomenon.

Table 18. Gene flow (Nm) approximations for temporal stations (Nei, 1973).

Nm	Nov-2017	July-2018	Aug-2018	Sept-2018	Oct-2018
November-2017					
July-2018	16.16				
August-2018	21420	0			
September-2018	643	0	0		
October-2018	-32.79	11.04	161.13	878.22	

Nm<1; there is not enough gene flow to negate the effects of genetic drift – not possible to prevent genetic differentiation; Nm > 1, there is enough gene flow to decrease the effects of genetic drift; Nm > 4, populations are within random mating population, not possible to block genetic differentiation.

Table 19. Pairwise genetic differentiation (Fst) within the temporal populations from Kızkalesi time series station. The method is applied for 10.000 permutations (Hudson, Slatkin & Maddison, 1992).

Fst	Nov-2017	July-2018	Aug-2018	Sept-2018	Oct-2018
November-2017					
July-2018	0^{NS}				
August-2018	0^{NS}	-			
September-2018	0^{NS}	-	-		
October-2018	-0.037^{NS}	0^{NS}	0^{NS}	0^{NS}	

(P 0.01<P<0.05) significant (*); (0.001< P < 0.01) significant (**); not significant (NS).

Additionally, the genetic differentiation was analysed between the monthly populations. Overall, no genetic differentiation was recorded for this annual period.

4.5.3. Additional Nuclear Gene (18S rRNA & 28S rRNA) analyses

Three 18S rRNA and two 28S rRNA sequences belonging to samples from Kızkalesi station were additionally analysed. The sequences after alignment and trimming were counted as 964 bp for 18S and 648 bp for 28S. Following the BLAST analyses were applied to identify the sequences. Regarding to the results, 18S sequences were matched 99.60% with the database *B. aff. leachii* sequence (Acc. No: MG009589.1; Reem et al., 2017). However, blasted sequence was also recorded to match 99.90% with other compound ascidians, *B. schlosseri* (Acc. No: FM244858.1; Tsagkogeorga et al., 2009). On the other hand, 28S sequence of current study sample was found to be particularly matching the *B. aff. leachii* sequence 99.84%.

5. DISCUSSION

In the present study, three main (COI, H3 & ANT) and two additional molecular markers (18S & 28S) were used to understand genetic characterization of *B. aff. leachii* from the Levantine coasts of Turkey. The first assignment of the species was concluded as *Botrylloides sp.* (either *B. leachii* or *B. nigrum)* based on the colonial phenotype during the samplings. The duality was due to the lack of certain morphological distinction between these two species (Brunetti, 2009).

Although, processes of larval incubation and structure of pyloric caecum are suggested to use as anatomical distinction features which might vary between these two species (Brunetti, 2009), the genetic divergence was calculated to estimate the separation in the current study. Additionally, the morphological identification and phenotypic characterization of the organism were provided.

According to the morphological examination, *B. leachii* type zooid organization was found for all of the colonies. More than 9 major morphs with various different types of striped pigmentation as sub-morphs were recorded in the Turkey colonies. The morphological diversity was found to be greater than the description of Brunetti (2009) who solely indicated 4 morphotypes. Although the genetic markers could not resolve the phenotypic variation, it is possible both genetic and environmental parameters such as diet could be related with this and further investigation is needed. Yet, according to Van Name, (1945) and Boyd et al., (1990) morphological variations are accepted to have no taxonomic importance for ascidians. On the other hand, Tarjuelo et al. (2004) suggested that it is possible to differentiate the colour morphs of *Pseudodistoma crucigaster* (a colonial ascidian), based on the COI locus. Also similar to Israeli colonies (Brunetti, 2009), Turkey colonies were found to be dwarf form of *B. leachii* regarding to the tallness of zooids (~1.5mm). Brunetti (2009) stated that the downsizing was probably as a result of high salinity and temperature. Considering the high temperature and salinity values in the North-eastern Mediterranean of Turkey coasts during the summer period like Israel, the results are seen to be congruent with each other.

Similar to the observations of Brunetti (2009), 4 larger and 4 smaller in total 8 tentacles and also very small ones varying in number were recorded in the current study zooids' buccal syphon. Similar results have been gained from the monitoring of the blastogenic cycles of different morphs. The stages (A-D) are sequential for the all of the colonies and the duration are varying from 4 to 7 days. These results are congruent with the previously suggested cycle duration as about one week (Berrill, 1947). The shorter cycles are probably related with the hibernation (Hyams et al., 2017). Along with these, several colonies that entered hibernation were monitored. Most of them could not be recovered under the aquaculture system conditions. Hyams et al., (2017) stated ~80% of the 39 hibernating colonies were degenerated and died eventually within the five months after the hibernation period. As a result, hibernation was concluded as one of the main reasons of short life span for this animal. The variation in the life

history characteristics of these animal are probably shaped by the high phenotypic plasticity resulting from the environmental changes (Rinkevich et al., 1995).

According to the molecular results, COI sequences of the present study samples were matched 100% with *B. nigrum* during the BLAST analysis, on the other hand H3 sequences paired with *B. leachii* 99.25%. With the support of other two other gene regions (18 rRNA-99.60% and 28 rRNA-99.84%) the samples were identified as *B. aff. leachii*. There have been debates about whether or not *B. leachii* and *B. nigrum* (Hartmeyer & Michaelsen, 1928) are the same species. Brunetti (2009) states that the two species were different based on the type of larval incubation. Along with the present study results, the Median Joining Network and Bayesian analysis for COI gene is clearly showed that in the case all GenBank sequences denominated properly, *B. leachii* and *B. nigrum* is not the same species, they are monophyletic sister groups.

Further molecular comparisons with the GenBank data has showed that current study samples differ approximately 17% from *B. leachii* and less than 1% from *B. nigrum* based on the COI locus. When this result was compared with the intraspecific distance of metazoans (2%; Hebert et al., 2003) and the interspecific distances of ascidians (14-16%; Bock et al., 2012), it can be stated that the current study samples are carrying the *B. nigrum* mtDNA based on the DNA barcoding region (COI). The earliest samplings in the region is dated back to 2012 by Karahan, it has also shown that those colonies have also *B. nigrum* mtDNA. In addition, intraspecific divergence of the current study populations was ranged between 0 - 0.3%. This shows the *B. aff. leachii* populations from the North-eastern Mediterranean of Turkey are in the single cluster with low genetic variation based on the COI locus.

Along with COI, nuclear H3 distances were also measured to understand nuclear DNA at some level. Intraspecific distance among the Turkey colonies were found within 0 - 0.8% range. Compared to COI, H3 is found to demonstrate higher variation rate. Like COI locus, H3 also confirms the presence of single cluster in the Turkey coasts with low evolutionary distance. The higher variation rate for H3 could be explained by the necessity of different types of histone proteins which is found to be particularly important during the whole body regeneration process (Zondag et al., 2019).

Also, the GenBank mined *B. leachii* sequence (Israel) showed 1.7-2.1% distance from the current study populations. Considering the H3 intraspecific distance for *B. leachii* stated by Reem et al. (2.5%; 2017), our result (0.8%) confirms the lower divergence for the current study populations compared to Israeli populations. However, due to absence of *B. nigrum* H3 sequence in the GenBank, the resolution is only framed in terms of present *B. leachii* sequences. Within this scope, it is concluded that current study populations possess *B. leachii* nuclear genome and confirming the presence of single species based on H3 locus. In addition, the populations from 2014 have resulted to possess *B. leachii* H3 gene, by confirming at least since 2014, these colonies do exist in the form of a chimera considering the presence of *B. nigrum* mtDNA in the Levantine basin colonies since 2012.

To further sustain this assumption, ANT, 18S and 28S sequences were investigated. Both 18S and 28S were found to be matching congruently with the Israeli *B. leachii* sequences (Reem et al., 2017). Based on the NCBI BLAST results, it is concluded that the 18S rRNA resolution for species identification is lower than the 28S RNA locus because of the high mismatch ratio. Besides, BLAST analyses of consensus ANT sequences of present study gave very short coverage (63 bp from 1000 bp) with Teske et. Al. (2011)'s *B. leachii* sample (Australia – JF962229.1). No considerable match was observed between the present study ANT sequences with *B. nigrum* ANT sequence from Florida (Sheets et al., 2016; KU711800.1). On the other hand, based on this very short coverage (63 bp from 1000 bp) it is not possibly to make any interpretation about resolution of this gene.

Considering natural chimerism (the co-occurrence of different species' cells/strains in the same organism) is a common phenomenon, the presence of different genotypes might be resulted from germline parasitism (Rinkevich, 2005; Voskoboynik et al., 2018). The presence of different genotypes would be specified as a result of germline stem cell competition (Rinkevich, 2005; Voskoboynik et al., 2018). The competition indicates the takeover of germline or somatic descendance and the results might indicate the non-chimeric colony due to the disposal of the other colony's genome or a chimeric colony that possesses a mixture of different strains (Voskoboynik et al., 2018). As a result, a chimera would possess more diverse genetic variation than non-chimeric one, and this might increase the tolerance of the colony to adapt different environmental conditions. In addition, Rinkevich (2005) suggested that environmental changes could lead genotypic shifts in the somatic components of chimeric

zooids. Regarding the habitable surface is limited in the natural habitat of these organisms, natural chimerism may results in the elimination of less adaptive/heterozygote colonies or creation of more adaptive/heterozygote entities.

This general assessment was also investigated in detailed to search the genetic variation among the Turkey's North-eastern Mediterranean *B. aff. leachii* populations and resulted with 4 and 14 haplotypes based on COI and H3 loci respectively. Among the COI haplotypes, Konacık haplotype was clustered together with the *B. nigrum* from Florida. Sheets et al. (2016) stated 8 COI haplotypes globally for *B. nigrum*. Considering the zone width, it can be said that Levantine basin colonies have a great diversity. The other three novel haplotypes, one as the main haplotype, was concluded with low level of variation on COI locus for Turkey's North-eastern Mediterranean samples that has shown no demographic pattern. Additionally, Mezitli and Kızkalesi haplotypes were found to diverge from the main haplotype with one mutation step. Within this content, the low diversity might be result of a recent introduction from a single species or the frame of sampling was not covered to estimate the native population dynamics (Dlugosch & Parker, 2008; Sheets et al., 2016).

Besides, the overall haplotype diversity of current study COI sequences were detected to be very low (Pi_{COI}: 0.0004) compared to H3 (Pi_{H3}:0.0063) which might stem from a recent bottleneck for the mitochondrial genome. Similarly, Sheets et al. (2016) also found low diversity for the *B. nigrum* populations in the Atlantic and Pacific coasts both at COI and ANT loci. However, considering the differences in diversity for COI, H3 and ANT sequences, it seems 'the possible bottleneck' functioned differently on the mitochondrial and nuclear loci.

Considering the significant negative Tajima's D values, the null hypothesis of neutral theory by indicating that overall colonies of Turkey's Levantine basin were under negative selection for COI and H3 loci was not rejected. Although not significant for COI, significant negative Fu and Li's F and D values for H3 are found to reinforcing this negative selection hypothesis. Additionally, based on H3, Kızkalesi and Kemer populations are observed to be under negative selection along with overall Levantine basin populations. Likewise, Sheets et al. (2016) found the *B. nigrum* populations in the Atlantic coast of Panama, the Pacific coast of Panama and Mexico were also under negative selection for the COI locus by suggesting to may result from small population size, founder effect or low dispersal. Considering the mtDNA is under natural

selection, our results are coherent and indicate that one possible reason of low diversity at mtDNA is selection, and the selective forces most probably coming from the environmental stressors in this case it might be salinity or temperature (Morin et al., 2018; Wei et al., 2019).

Following, the demographic population analyses based on COI gene has shown that overall the Turkey's North-eastern Mediterranean *B. aff. leachii* populations might had slight population subdivisions due to possible coastal ecological fluctuations. One of the reasons of the Side population subdivision can be related with a major freshwater input (Manavgat stream) to the sampling area which is not valid for the other sampling areas of the present study, although any underground water source is not known well. Supportively, the freshwater input is known to fluctuate coastal salinity values seasonally and Karahan et al. (2016) stated that dynamics of *B. schlosseri* populations from the California coasts was dramatically affected due to flooding events and even after eradication of local population, high salinity deep-water colonies or a closely located population that could elude from the low salinity exposure could lead in resettlement.

Cytochrome oxidase subunit I and H3 gene flow estimations were conducted to elucidate the population interactions but, no phylogeographic pattern was observed. COI haplotype containing populations (Kızkalesi, Mezitli and Konacık) are found to have gene flow between each other and the other populations. The high gene flow estimations based on COI explains the low genetic diversity in the Levantine basin colonies considering the highest distance between sampling stations (Kemer-Konacık) is around 800 kilometres and the regional maritime traffic possibly affects the larval dispersal from the colonies that attached on hulls (Lambert, 2011). Negative Nm values were probably resulted from introgressive hybridization (Nydam et al., 2011). In adition, genetic differentiation is observed only between several populations where no significant gene flow was present. Due to the significant differentiation values of COI (Fst), Konacık population seems to be isolated. As expected, COI haplotype involving populations were differentiated from each other except Kızkalesi and Mezitli, probably because of distance and significant gene flow. Even though their close proximity when compared to other populations, Alanya and Side populations were found to be isolated from the Kemer population based on H3 locus. Sheets et al. (2016) also stated that *B. nigrum* populations demonstrate low isolation levels based on the distance value of COI and ANT loci.

Along with COI and H3, nuclear ANT gene was found to have intraspecific divergence within 0.2-20% range. Possibly, because of having both exon and intron regions high variation was observed for ANT gene. Although the intraspecific divergence was given as 1% by Sheets et al. (2016) and they did not record any recombination for *B. nigrum* based on ANT locus. The multi-variation of the present study ANT locus is probably a result of introgression or incomplete lineage sorting.

In regard to the temporal results, the colonies were found to be present except the winter and spring period in Kızkalesi time series station between the October 2017 and November 2018. Considering the possibility of under-sampling, it can be stated that the colonies were not present in the intertidal zone during the winter period when the environmental conditions were not suitable. Another possibility can be the migration to deep waters where the salinity high enough (Karahan et al., 2016). It is possible to say that, when the environmental conditions are favourable, the colonies are settling the shore areas again. Besides, the molecular analyses demonstrated that during the November and October period the colonies were expanding and exposed to introgression possibly due to high level of asexual reproduction and colonial fission (Brunetti, 1976; Rinkevich et al., 1995).

6. CONCLUSION

In this study, population structures and interactions of North-eastern Mediterranean *B. aff. leachii* were investigated by using five molecular markers for eight spatial stations and one time series station along with the morphological records. Morphological results showed similar colonial characteristics regarding on the blastogenic cycle and hibernation but with a greater number of new morphotypes records. Regarding the ambiguities in classification of *B. leachii,* previously suggested molecular markers were used to reveal the differences whether a clear identification would be acquired or not for the Turkey populations. As a result, varied differentiation levels were found for these DNA markers. COI, H3 and 28S were observed to provide adequate identification of the species. H3 was seen to have greater resolution compared to COI. Great level of variation was determined for ANT locus and only very low coverage was gained for taxon identification. Distinctively, the mitochondrial marker matched with *B. nigrum* while the nuclear markers was paired with *B. leachii* sequences. In conclusion, no phylogeographic pattern was observed between the populations.

REFERENCES

Arnback-Christie-Linde, A. (1923). *Tunicata*. Almqvist och Wiksells.

Assembler, D. B. S. (2012). Heracle BioSoft SRL Romania.

Avise, J. C., Arnold, J., Ball, R. M., Bermingham, E., Lamb, T., Neigel, J. E., … Saunders, N. C. (1987). Intraspecific Phylogeography: The Mitochondrial DNA Bridge Between Population Genetics and Systematics. *Annual Review of Ecology and Systematics*, *18*(1), 489–522. https://doi.org/10.1146/annurev.es.18.110187.002421

Avise, J. C. (2009). Phylogeography: Retrospect and prospect. *Journal of Biogeography*, *36*(1), 3–15. https://doi.org/10.1111/j.1365-2699.2008.02032.x

Azzurro, E., Goren, M., Diamant, A., Galil, B., & Bernardi, G. (2015). Establishing the identity and assessing the dynamics of invasion in the Mediterranean Sea by the dusky sweeper, Pempheris rhomboidea Kossmann & Räuber, 1877 (Pempheridae, Perciformes). *Biological Invasions*, *17*(3), 815–826. https://doi.org/10.1007/s10530-014-0836-5

Ballard, J. W. O., & Kreitman, M. (1995). Is mitochondrial DNA a strictly neutral marker? *Trends in Ecology & Evolution*, *10*(12), 485–488. https://doi.org/10.1016/S0169-5347(00)89195-8

Bandelt, H. J., Forster, P., & Röhl, A. (1999). Median-joining networks for inferring intraspecific phylogenies. *Molecular biology and evolution*, *16*(1), 37-48.

Bariche, M., Torres, M., Smith, C., Sayar, N., Azzurro, E., Baker, R., & Bernardi, G. (2015). Red Sea fishes in the Mediterranean Sea: A preliminary investigation of a biological invasion using DNA barcoding. *Journal of Biogeography*, *42*(12), 2363–2373. https://doi.org/10.1111/jbi.12595

Berrill, N. J. (1947). The developmental cycle of Botrylloides. *Journal of Cell Science*, *3*(4), 393-407.

Berrill, N. J. (1950). The Tunicata with an account of the British species. *Ray Society*.

Blanchoud, S., Rinkevich, B., & Wilson, M. J. (2018a). Whole-body regeneration in the colonial tunicate Botrylloides leachii. In *Marine Organisms as Model Systems in Biology and Medicine* (pp. 337-355). Springer, Cham.

Blanchoud, S., Rutherford, K., Zondag, L., Gemmell, N. J., & Wilson, M. J. (2018b). De novo draft assembly of the Botrylloides leachii genome provides further insight into tunicate evolution. *Scientific Reports*, *8*(1), 1–18. https://doi.org/10.1038/s41598-018-23749-w

Bock, D. G., Macisaac, H. J., & Cristescu, M. E. (2012). Multilocus genetic analyses differentiate between widespread and spatially restricted cryptic species in a model ascidian. *Proceedings of the Royal Society B: Biological Sciences*, *279*(1737), 2377–2385. https://doi.org/10.1098/rspb.2011.2610

Boyd, H. C., Weissman, I. L., & Saito, Y. (2007). Morphologic and Genetic Verification That Monterey Botryllus and Woods Hole Botryllus are the Same Species . *The Biological Bulletin*, *178*(3), 239–250. https://doi.org/10.2307/1541825

Brunetti, R. (1976). Biological Cycle of *Botrylloides leachii* (Savigny)(Ascidiacea) In Venetian Lagoon. *Vie et Milieu Serie A-Biologie Marine*, *26*(1), 105.

Brunetti, R., Beghi, L., Bressan, M., & Marin, M. (2007). Combined Effects of Temperature and Salinity on Colonies of Botryllus schlosseri and Botfylloides leachi (Ascidiacea) from the Venetian Lagoon. *Marine Ecology Progress Series*, *2*, 303–314. https://doi.org/10.3354/meps002303

Brunetti, R. (2009). Botryllid species (Tunicata, Ascidiacea) from the Mediterranean coast of Israel... *Zootaxa*, *32*, 18–32.

Bucklin, A., Steinke, D., & Blanco-Bercial, L. (2011). DNA Barcoding of Marine Metazoa. *Annual Review of Marine Science*, *3*(1), 471–508. https://doi.org/10.1146/annurev-marine-120308-080950

Chen, J.-Y., Huang, D.-Y., Peng, Q.-Q., Chi, H.-M., Wang, X.-Q., & Feng, M. (2003). The first tunicate from the Early Cambrian of South China. *Proceedings of the National Academy of Sciences*, *100*(14), 8314–8318. https://doi.org/10.1073/pnas.1431177100

Cloney, R. A. (1982). Ascidian larvae and the events of metamorphosis. *Integrative and Comparative Biology*, *22*(4), 817–826. https://doi.org/10.1093/icb/22.4.817

Delsuc, F., Brinkmann, H., Chourrout, D., & Philippe, H. (2006). Tunicates and not cephalochordates are the closest living relatives of vertebrates. *Nature*, *439*(7079), 965–968. https://doi.org/10.1038/nature04336

Dlugosch, K. M., & Parker, I. M. (2008). Founding events in species invasions: Genetic variation, adaptive evolution, and the role of multiple introductions. *Molecular Ecology*, *17*(1), 431–449. https://doi.org/10.1111/j.1365-294X.2007.03538.x

Eryilmaz, L., & Dalyan, C. (2006). First record of Apogon queketti Gilchrist (Osteichthyes: Apogonidae) in the Mediterranean Sea. *Journal of Fish Biology*, *69*(4), 1251–1254. https://doi.org/10.1111/j.1095-8649.2006.01185

Fu, Y. X. (1997). Statistical tests of neutrality of mutations against population growth, hitchhiking and background selection. *Genetics*, *147*(2), 915-925.

Folmer, O. Black M. Hoeh W. Lutz R. Vrijenhoek R. 1994. DNA primers for amplification of mitochondrial cytochrome c oxidase subunit I from diverse metazoan invertebrates. *Molecular Marine biology and biotechnology*, *3*(5), 294-299.

Ghobashy, A. F. A., & Adbel Messeih, M. K. (1991). Ascidians in Egyptian waters. *J Egypt Ger Soc Zool*, *4*, 313-326.

Gissi, C., Iannelli, F., & Pesole, G. (2008). Evolution of the mitochondrial genome of Metazoa as exemplified by comparison of congeneric species. *Heredity*, *101*(4), 301–320. https://doi.org/10.1038/hdy.2008.62

Glaser, O., & Anslow, G. A. (1949). Copper and Ascidian metamorphosis. *Journal of Experimental Zoology*, *111*(1), 117–139. https://doi.org/10.1002/jez.1401110107

Goldstien, S. J., Dupont, L., Viard, F., Hallas, P. J., Nishikawa, T., Schiel, D. R., … Bishop, J. D. D. (2011). Global phylogeography of the widely introduced North West Pacific ascidian Styela clava. *PLoS ONE*, *6*(2). https://doi.org/10.1371/journal.pone.0016755

Golestani, H., Crocetta, F., Padula, V., Camacho-García, Y., Langeneck, J., Poursanidis, D., … valdés, Á. (2019). The little Aplysia coming of age: from one species to a complex of species complexes in Aplysia parvula (Mollusca: Gastropoda: Heterobranchia). *Zoological Journal of the Linnean Society*, (June), 1–52. https://doi.org/10.1093/zoolinnean/zlz028

Govindarajan, A. F., Bucklin, A., & Madin, L. P. (2011). A molecular phylogeny of the Thaliacea. *Journal of Plankton Research*, *33*(6), 843–853. https://doi.org/10.1093/plankt/fbq157

Halim, Y., & Abdel Messeih, M. (2016). Aliens in Egyptian waters. A checklist of ascidians of the Suez Canal and the adjacent Mediterranean waters. *Egyptian Journal of Aquatic Research*, *42*(4), 449–457. https://doi.org/10.1016/j.ejar.2016.08.004

Hall, T. A. (1999, January). BioEdit: a user-friendly biological sequence alignment editor and analysis program for Windows 95/98/NT. In *Nucleic acids symposium series* (Vol. 41, No. 41, pp. 95-98). [London]: Information Retrieval Ltd., c1979-c2000..

Hartmeyer, R. & Michaelsen, W. (1928) Ascidiae Diktyobranchiae und Ptychobranchiae. Fauna Südwest-australiens, 5, 251–460

Haydar, D., Hoarau, G., Olsen, J. L., Stam, W. T., & Wolff, W. J. (2011). Introduced or glacial relict? Phylogeography of the cryptogenic tunicate Molgula manhattensis (Ascidiacea, Pleurogona). *Diversity and Distributions*, *17*(1), 68–80. https://doi.org/10.1111/j.1472-4642.2010.00718.x

Hebert, P. D. N., & Gregory, T. R. (2005). The promise of DNA barcoding for taxonomy. *Systematic Biology*, *54*(5), 852–859. https://doi.org/10.1080/10635150500354886

Hyams, Y., Paz, G., Rabinowitz, C., & Rinkevich, B. (2017). Insights into the unique torpor of Botrylloides leachi, a colonial urochordate. *Developmental Biology*, *428*(1), 101–117. https://doi.org/10.1016/j.ydbio.2017.05.020

Karahan, A., Douek, J., Paz, G., & Rinkevich, B. (2016). Population genetics features for persistent, but transient, Botryllus schlosseri (Urochordata) congregations in a central

Californian marina. *Molecular Phylogenetics and Evolution*, *101*(May), 19–31. https://doi.org/10.1016/j.ympev.2016.05.005

Karahan, A., Douek, J., Paz, G., Stern, N., Kideys, A. E., Shaish, L., … Rinkevich, B. (2017). Employing DNA barcoding as taxonomy and conservation tools for fish species censuses at the southeastern Mediterranean, a hot-spot area for biological invasion. *Journal for Nature Conservation*, *36*, 1–9. https://doi.org/10.1016/j.jnc.2017.01.004

Kassmer, S. H., Rodriguez, D., & De Tomaso, A. W. (2016). Colonial ascidians as model organisms for the study of germ cells, fertility, whole body regeneration, vascular biology and aging. *Current Opinion in Genetics and Development*, *39*, 101–106. https://doi.org/10.1016/j.gde.2016.06.001

Keskin, E., & Atar, H. H. (2013). DNA barcoding commercially important fish species of Turkey. *Molecular Ecology Resources*, *13*(5), 788–797. https://doi.org/10.1111/1755-0998.12120

Kott, P. (1985). The Australian ascidiacea part IP, Phlebobranchia and Stolidobranchia. *Mem. Qd Mus.*, *23*.

Kumar, S., Nei, M., Dudley, J., & Tamura, K. (2008). MEGA: a biologist-centric software for evolutionary analysis of DNA and protein sequences. *Briefings in bioinformatics*, *9*(4), 299-306.

Lambert, G. (2001). A global overview of ascidian introductions and their possible impact on the endemic fauna. In *The biology of ascidians* (pp. 249-257). Springer, Tokyo.

Lejeusne, C., Bock, D. G., Therriault, T. W., MacIsaac, H. J., & Cristescu, M. E. (2011). Comparative phylogeography of two colonial ascidians reveals contrasting invasion histories in North America. *Biological Invasions*, *13*(3), 635–650. https://doi.org/10.1007/s10530-010-9854-0

Leray, M., & Knowlton, N. (2015). DNA barcoding and metabarcoding of standardized samples reveal patterns of marine benthic diversity. *Proceedings of the National Academy of Sciences*, *112*(7), 2076-2081.

López-Legentil, S., Legentil, M. L., Erwin, P. M., & Turon, X. (2015). Harbor networks as introduction gateways: contrasting distribution patterns of native and introduced ascidians. *Biological Invasions*, *17*(6), 1623-1638.

Millar, R. H. (1971). The Biology of Ascidians. *Adv. Marine Biology*, *9*, 1.

Milne-Edwards, H. (1841) Observations sur les ascidies composées des côtes de la Manche. Mémoires de l'Académie des Sciences de l'Institut de France, 18, 1–117.

Monniot, C. (1987). Les ascidies de Polynéie française. *Mém Mus Natn Hist Nat A*, *136*, 1-155.

Morin, P. A., Foote, A. D., Baker, C. S., Hancock-Hanser, B. L., Kaschner, K., Mate, B. R., ... & Alexander, A. (2018). Demography or selection on linked cultural traits or genes? Investigating the driver of low mtDNA diversity in the sperm whale using complementary mitochondrial and nuclear genome analyses. *Molecular ecology*, *27*(11), 2604-2619.

Mukai, H., & Watanabe, H. (1976). Studies on the formation of germ cells in a compound ascidian Botryllus, primigenus oka. *Journal of morphology*, *148*(3), 337-361.

Mukai, H. (1977). Comparative studies on the structure of reproductive organs of four botryllid ascidians. *Journal of morphology*, *152*(3), 363-379.

Nei, M. (1973). Analysis of gene diversity in subdivided populations. *Proceedings of the National Academy of Sciences*, *70*(12), 3321-3323.

Neigel, J., Domingo, A., & Stake, J. (2007). DNA barcoding as a tool for coral reef conservation. *Coral Reefs*, *26*(3), 487–499. https://doi.org/10.1007/s00338-007-0248-4

Nydam, M. L., & Harrison, R. G. (2011). Introgression despite substantial divergence in a broadcast spawning marine invertebrate. *Evolution*, *65*(2), 429–442. https://doi.org/10.1111/j.1558-5646.2010.01153.x

Oter, K., Gunay, F., Tuzer, E., Linton, Y.-M., Bellini, R., & Alten, B. (2013). First Record of Stegomyia albopicta in Turkey Determined By Active Ovitrap Surveillance and DNA Barcoding. *Vector-Borne and Zoonotic Diseases*, *13*(10), 753–761. https://doi.org/10.1089/vbz.2012.1093

Paz, G., & Rinkevich, B. (2002). Morphological consequences for multi-partner chimerism in Botrylloides, a colonial urochordate. *Developmental and Comparative Immunology*, *26*(7), 615–622. https://doi.org/10.1016/S0145-305X(02)00022-8

Paz, G., Douek, J., Mo, C., Goren, M., & Rinkevich, B. (2003). Genetic structure of Botryllus schlosseri (Tunicata) populations from the Mediterranean coast of Israel. *Marine Ecology Progress Series*, *250*, 153-162.

Pınar, E. (1974). Türkiye'nin bazı limanlarında Fouling-Boring organizmalar ve Antifouling-Antiboring boyaların fibular üzerine etkisi. *EÜ Fen Fak. İlmi Rap. Ser*, *170*(113), 1-67.

Pineda, M. C., López-Legentil, S., & Turon, X. (2011). The Whereabouts of an Ancient Wanderer: Global Phylogeography of the Solitary Ascidian Styela plicata. *PLoS ONE*, *6*(9), e25495. https://doi.org/10.1371/journal.pone.0025495

Rambaut, A. (2012). FigTree v1. 4.

Reem, E., Douek, J., & Rinkevich, B. (2018). Ambiguities in the taxonomic assignment and species delineation of botryllid ascidians from the Israeli Mediterranean and other coastlines. *Mitochondrial DNA Part A: DNA Mapping, Sequencing, and Analysis*, *29*(7), 1073–1080. https://doi.org/10.1080/24701394.2017.1404047

Rinkevich, B., Shlemberg, Z., & Fishelson, L. (2006). Whole-body protochordate regeneration from totipotent blood cells. *Proceedings of the National Academy of Sciences*, *92*(17), 7695–7699. https://doi.org/10.1073/pnas.92.17.7695

Rinkevich, B. (1995). Characteristics of allogeneic resorption in Botrylloides from the Mediterranean coast of Israel. *Developmental and Comparative Immunology*, *19*(1), 21–29. https://doi.org/10.1016/0145-305X(94)00050-P

Rinkevich, B., Lilker-Levav, T., & Goren, M. (1994). Allorecognition/xenorecognition responses in Botrylloides (ascidiacea) subpopulations from the mediterranean coast of Israel. *Journal of Experimental Zoology*, *270*(3), 302–313. https://doi.org/10.1002/jez.1402700309

Ronquist, F., Teslenko, M., Van Der Mark, P., Ayres, D. L., Darling, A., Höhna, S., ... & Huelsenbeck, J. P. (2012). MrBayes 3.2: efficient Bayesian phylogenetic inference and model choice across a large model space. *Systematic biology*, *61*(3), 539-542.

Rozas, J., Sánchez-DelBarrio, J. C., Messeguer, X., & Rozas, R. (2003). DnaSP, DNA polymorphism analyses by the coalescent and other methods. *Bioinformatics*, *19*(18), 2496-2497.

Ruiz, G. M., Carlton, J. T., Grosholz, E. D., & Hines, A. H. (1997). Global Invasions of Marine and Estuarine Habitats by Non-Indigenous Species : Mechanisms , Extent , and Consequences Linked references are available on JSTOR for this article : *American Zoologist*, *37*(6), 621–632.

Saito, Y., Hirose, E., & Watanabe, H. (2002). Allorecognition in compound ascidians. *International Journal of Developmental Biology*, *38*(2), 237-247.

Sasakura, Y., & Hozumi, A. (2018). Formation of adult organs through metamorphosis in ascidians. *Wiley Interdisciplinary Reviews: Developmental Biology*, *7*(2), e304. https://doi.org/10.1002/wdev.304

Scofield, V. L., Schlumpberger, J. M., West, L. A., & Weissman, I. L. (1982). Protochordate allorecognition is controlled by a MHC-like gene system. *Nature*, *295*(5849), 499.

Sheets, E. A., Cohen, C. S., Ruiz, G. M., & da Rocha, R. M. (2016). Investigating the widespread introduction of a tropical marine fouling species. *Ecology and Evolution*, *6*(8), 2453–2471. https://doi.org/10.1002/ece3.2065

Shenkar, N., & Swalla, B. J. (2011). Global Diversity of Ascidiacea. *PLoS ONE*, *6*(6), e20657. https://doi.org/10.1371/journal.pone.0020657

Shenkar, N., Gittenberger, A., Lambert, G., Rius, M., Moreira Da Rocha, R., Swalla, B. J., & Turon, X. (2019). Ascidiacea World Database. *Internet]. World Register of Marine Species*.

Smith, M. A., Poyarkov, N. A., & Hebert, P. D. N. (2008). CO1 DNA barcoding amphibians: Take the chance, meet the challenge. *Molecular Ecology Resources*, *8*(2), 235–246. https://doi.org/10.1111/j.1471-8286.2007.01964

Tajima, F. (1989). Statistical method for testing the neutral mutation hypothesis by DNA polymorphism. *Genetics*, *123*(3), 585-595.

Tarjuelo, I., Posada, D., Crandall, K. A., Pascual, M., & Turon, X. (2004). Phylogeography and speciation of colour morphs in the colonial ascidian Pseudodistoma crucigaster. *Molecular Ecology*, *13*(10), 3125–3136. https://doi.org/10.1111/j.1365-294X.2004.02306.x

Teske, P. R., Rius, M., McQuaid, C. D., Styan, C. A., Piggott, M. P., Benhissoune, S., … Beheregaray, L. B. (2011). Nested cryptic diversity in a widespread marine ecosystem engineer: A challenge for detecting biological invasions. *BMC Evolutionary Biology*, *11*(1), 176. https://doi.org/10.1186/1471-2148-11-176

Tsagkogeorga, G., Turon, X., Hopcroft, R. R., Tilak, M. K., Feldstein, T., Shenkar, N., … Delsuc, F. (2009). An updated 18S rRNA phylogeny of tunicates based on mixture and secondary structure models. *BMC Evolutionary Biology*, *9*(1), 1–16. https://doi.org/10.1186/1471-2148-9-187

Turon, X., & Becerro, M. (1992). Growth and survival of several asoidian species from Ihe northwestern Mediterranean. *Marine Ecology Progress Series*, *82*(3), 235–247. https://doi.org/10.3354/meps082235

Turon, X., & López-Legentil, S. (2004). Ascidian molecular phylogeny inferred from mtDNA data with emphasis on the Aplousobranchiata. *Molecular Phylogenetics and Evolution*, *33*(2), 309–320. https://doi.org/10.1016/j.ympev.2004.06.011

Uysal, A. (1976). Türkiye suları Ascidia'ları. *İst Üniv Fen Fak Hid Araş Enst Yay*, *15*, 1-29.

Voskoboynik, A., Newman, A. M., Kowarsky, M., & Weissman, I. L. (2018). Urochordata: Botryllus–Natural Chimerism and Tolerance Induction in a Colonial Chordate. In *Advances in Comparative Immunology* (pp. 503-519). Springer, Cham.

Weissman, I. L., Saito, Y., & Rinkevich, B. (1990). Allorecognition Histocompatibility in a Protochordate Species: Is the Relationship to MHC Somatic or Structural? *Immunological Reviews*, *113*(1), 227–241. https://doi.org/10.1111/j.1600-065X.1990.tb00043.x

Wei, W., Tuna, S., Keogh, M. J., Smith, K. R., Aitman, T. J., Beales, P. L., ... & Brennan, P. (2019). Germline selection shapes human mitochondrial DNA diversity. *Science*, *364*(6442), eaau6520.

Zaniolo, G., Manni, L., & Burighel, P. (1994). Ovulation and embryo-parent relationships in Botrylloides leachi (Ascidiacea, Tunicata). *Invertebrate Reproduction & Development*, *25*(3), 215–225. https://doi.org/10.1080/07924259.1994.9672388

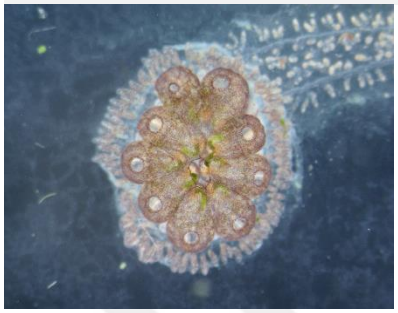
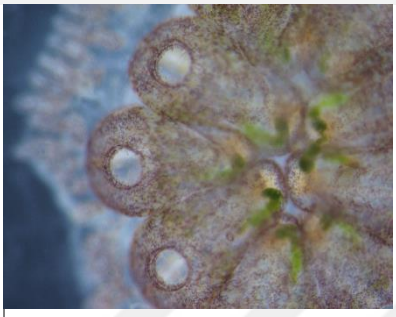
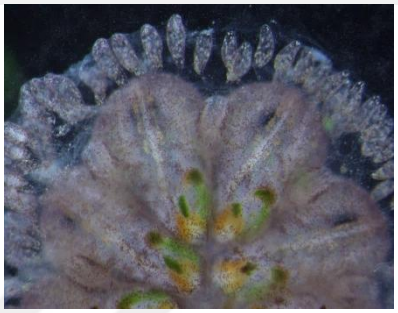
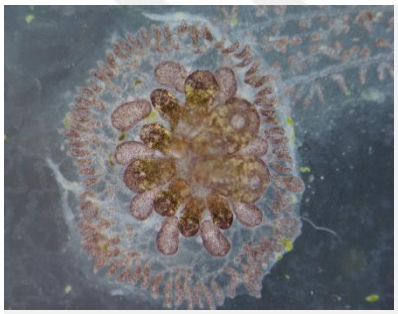
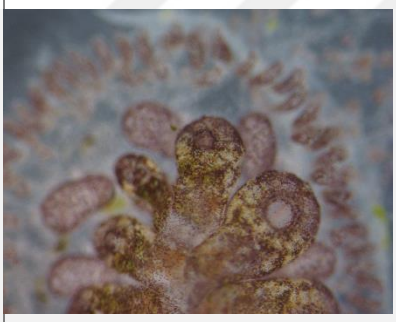
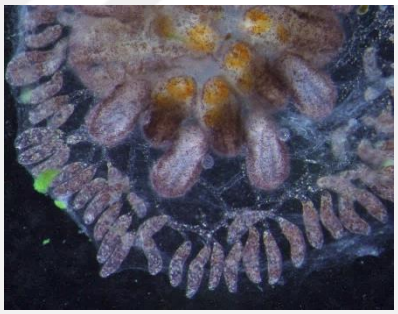
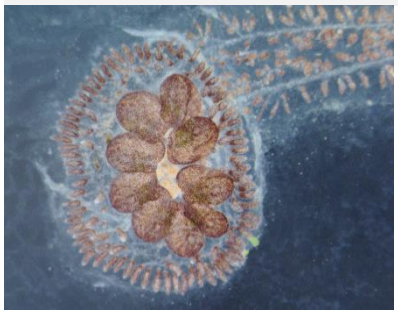
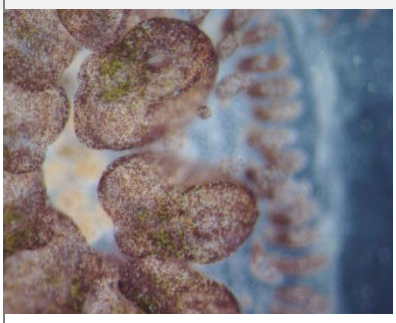
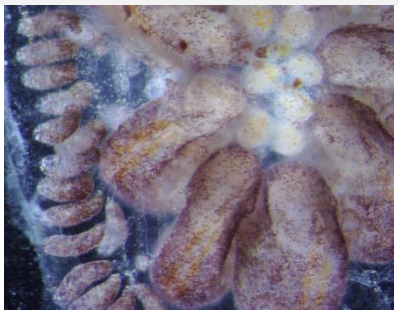
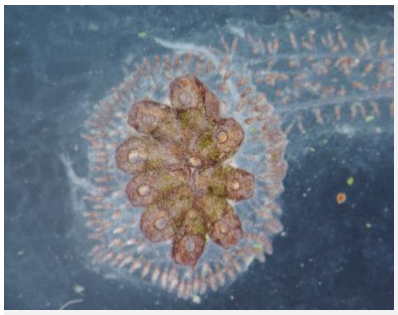
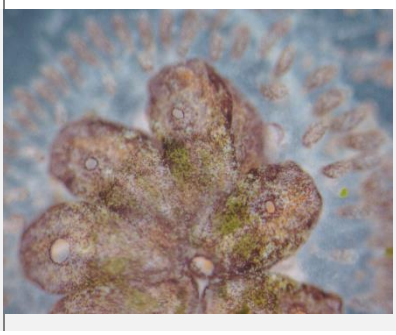
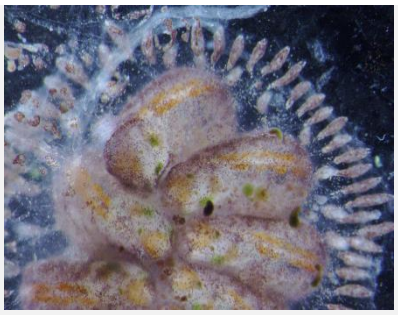
Zondag, L. E., Rutherford, K., Gemmell, N. J., & Wilson, M. J. (2016). Uncovering the pathways underlying whole body regeneration in a chordate model, Botrylloides leachi using de novo transcriptome analysis. *BMC Genomics*, *17*(1), 1–11. https://doi.org/10.1186/s12864-016-2435-6

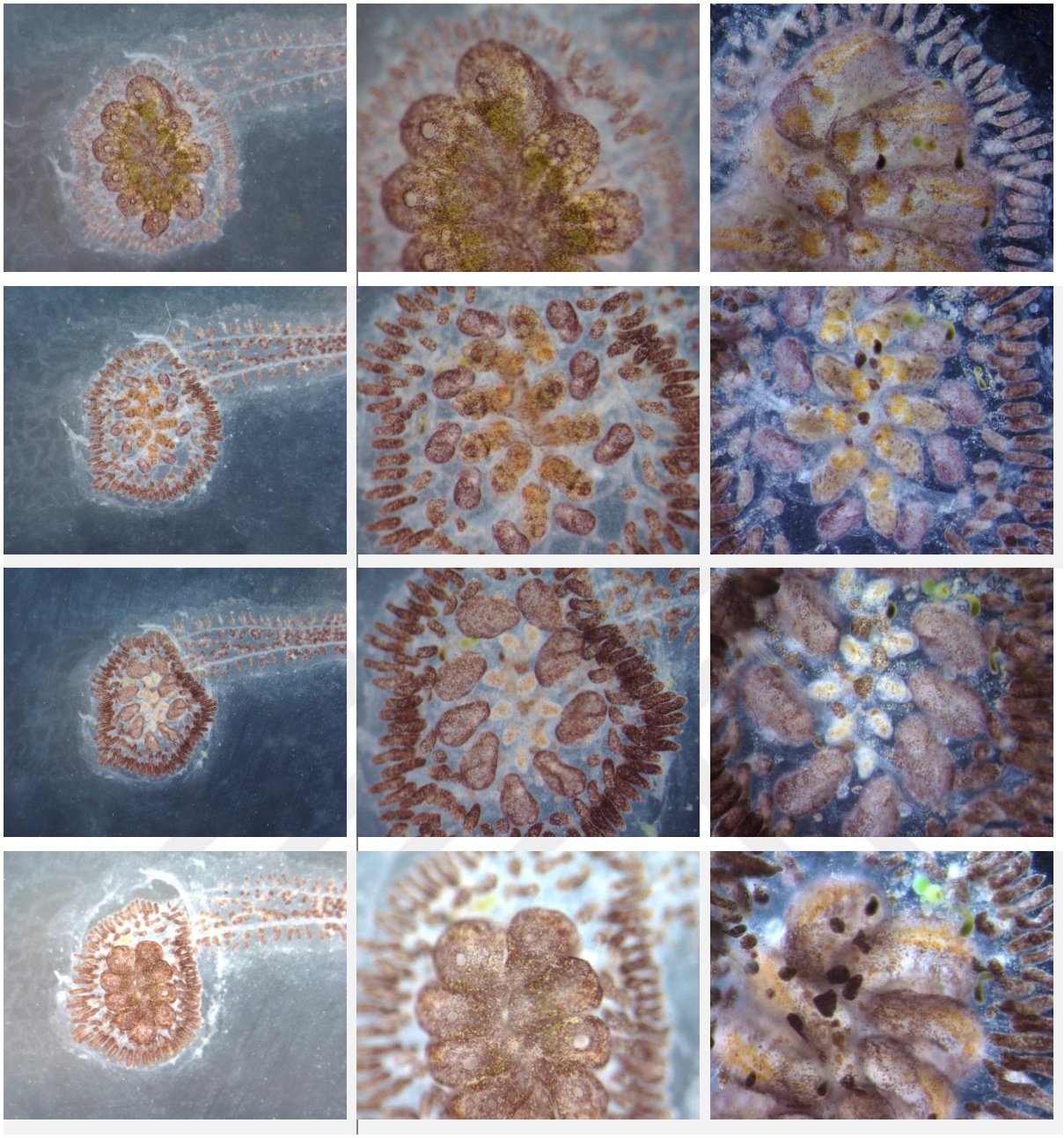
APPENDICES

APPENDIX A

Blastogenic cycles

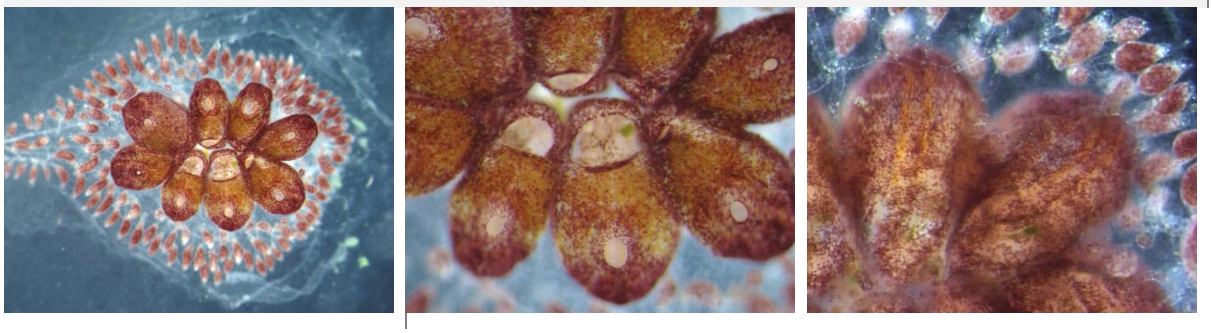
Each day is represented by three aligned columns per row.

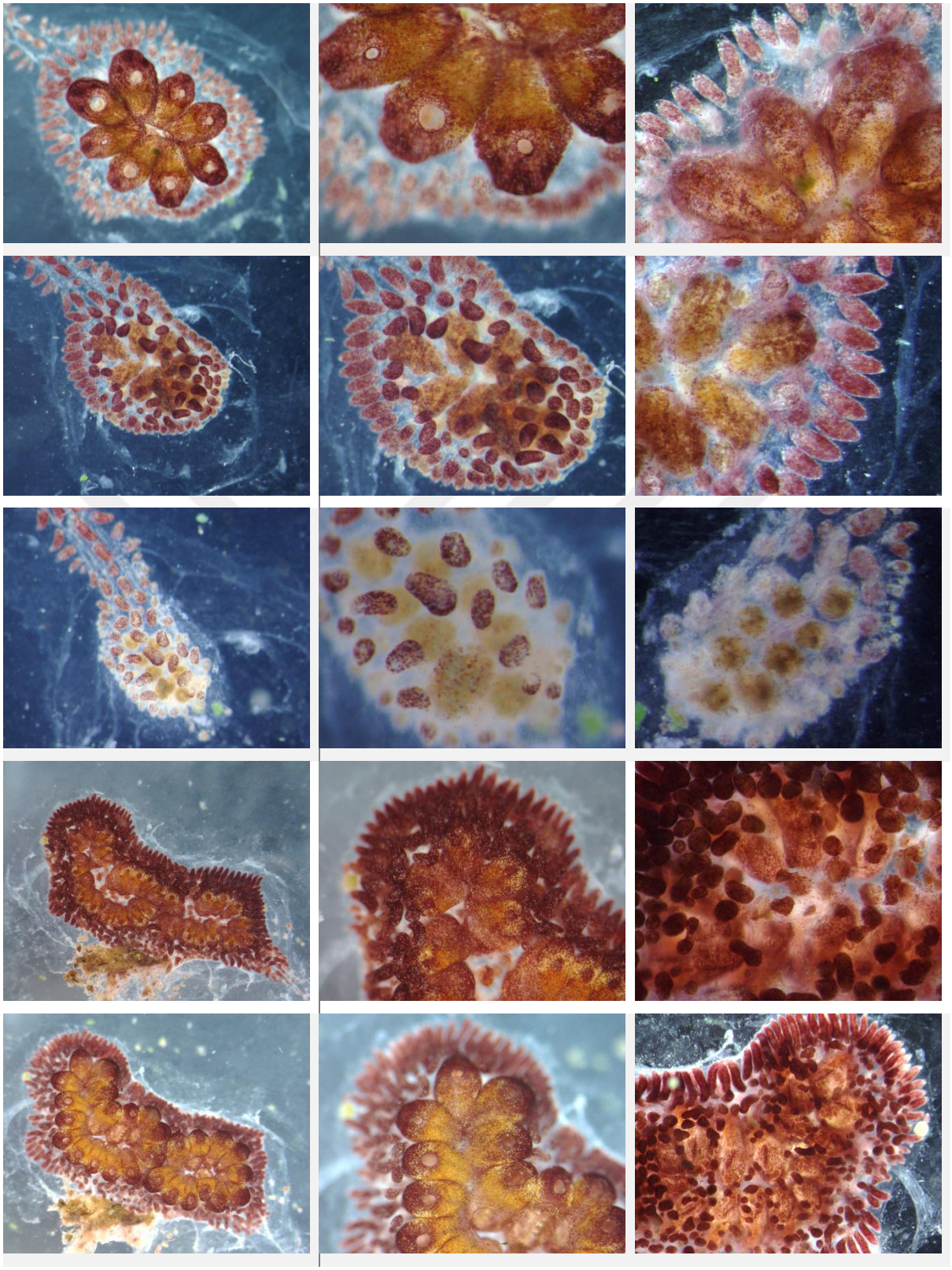
DORSAL - 1	DORSAL - 2	VENTRAL
SAMPLE ID - R5		
		
		
		
		

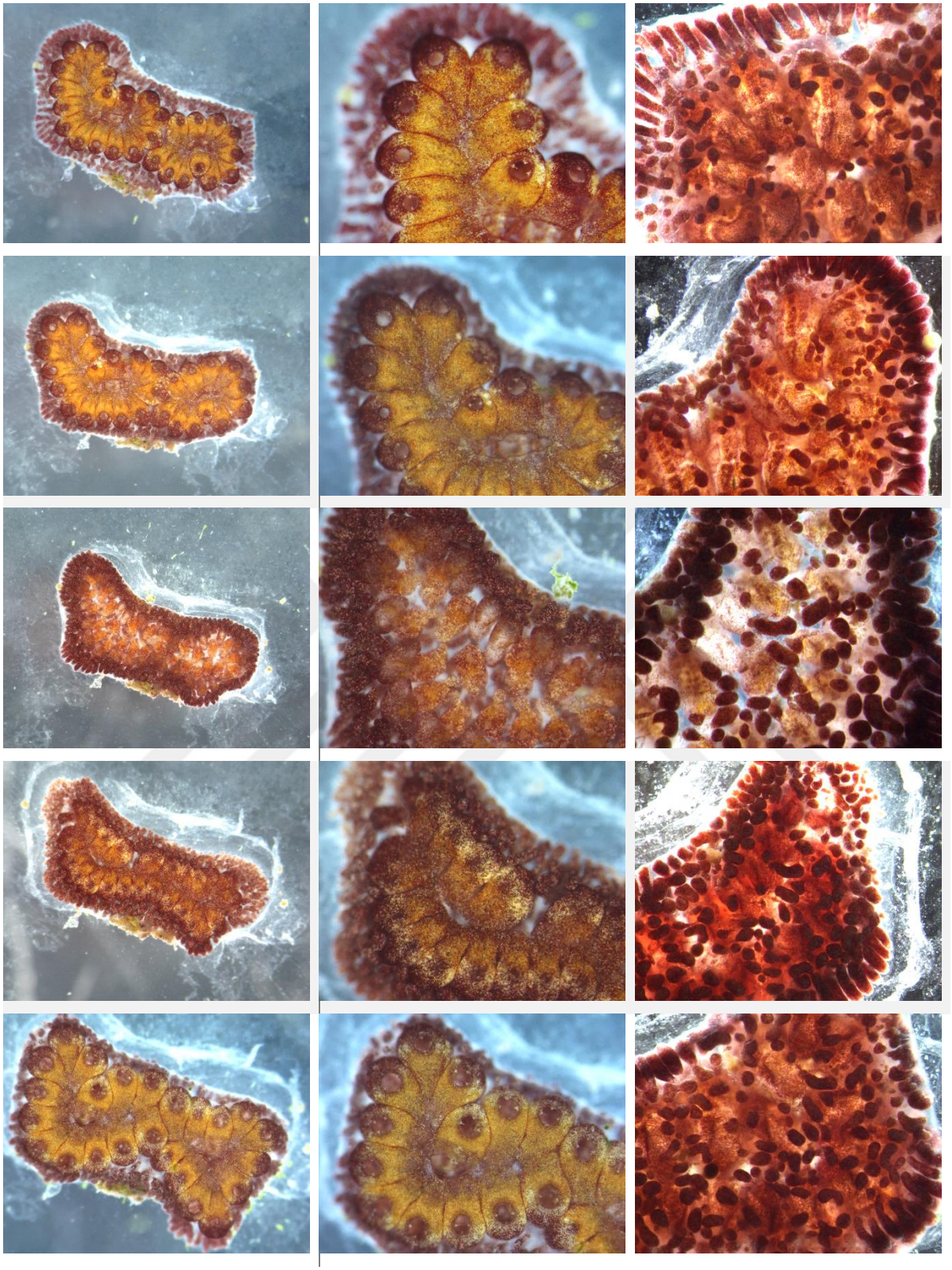


DORSAL - 1 **DORSAL - 2** **VENTRAL**

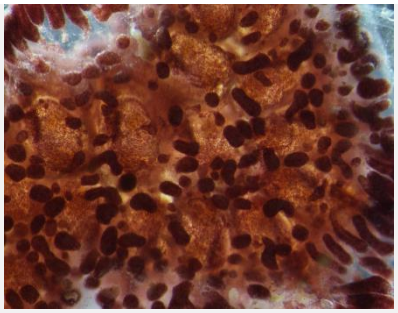
SAMPLE ID – L18





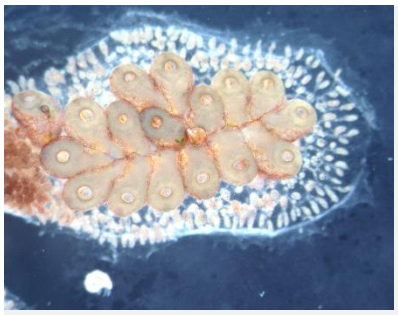
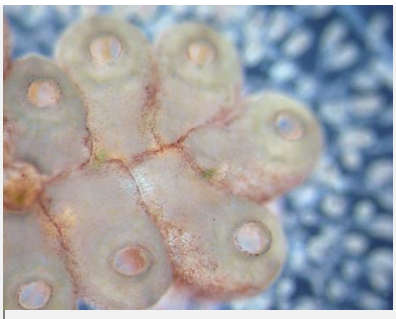
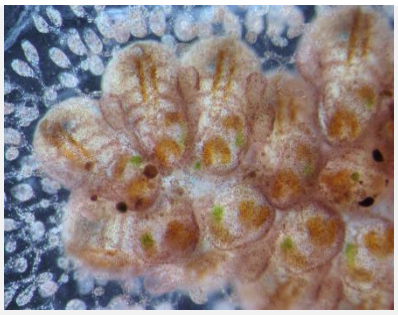
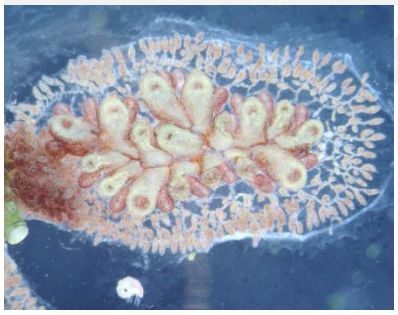
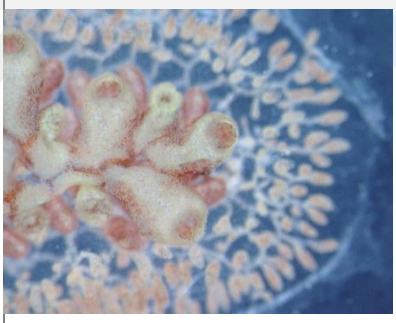
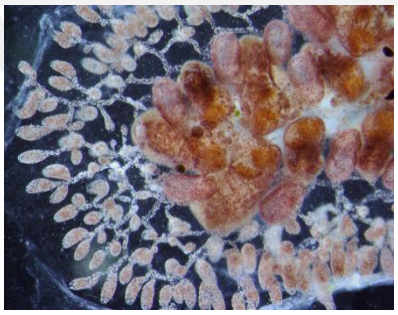
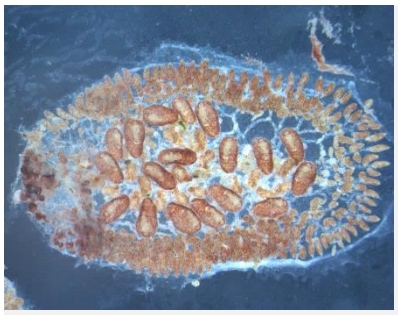


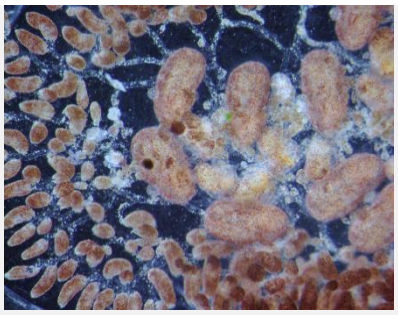


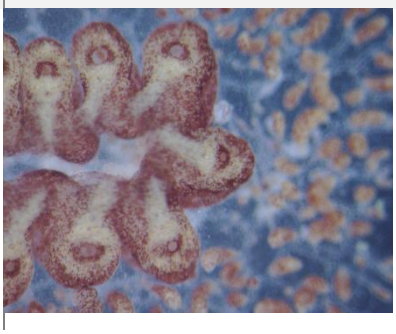
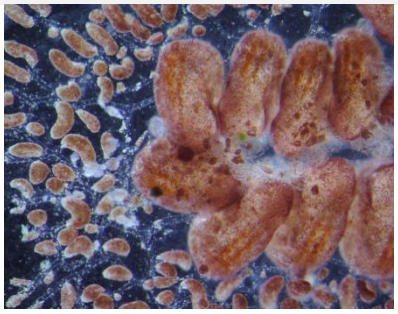


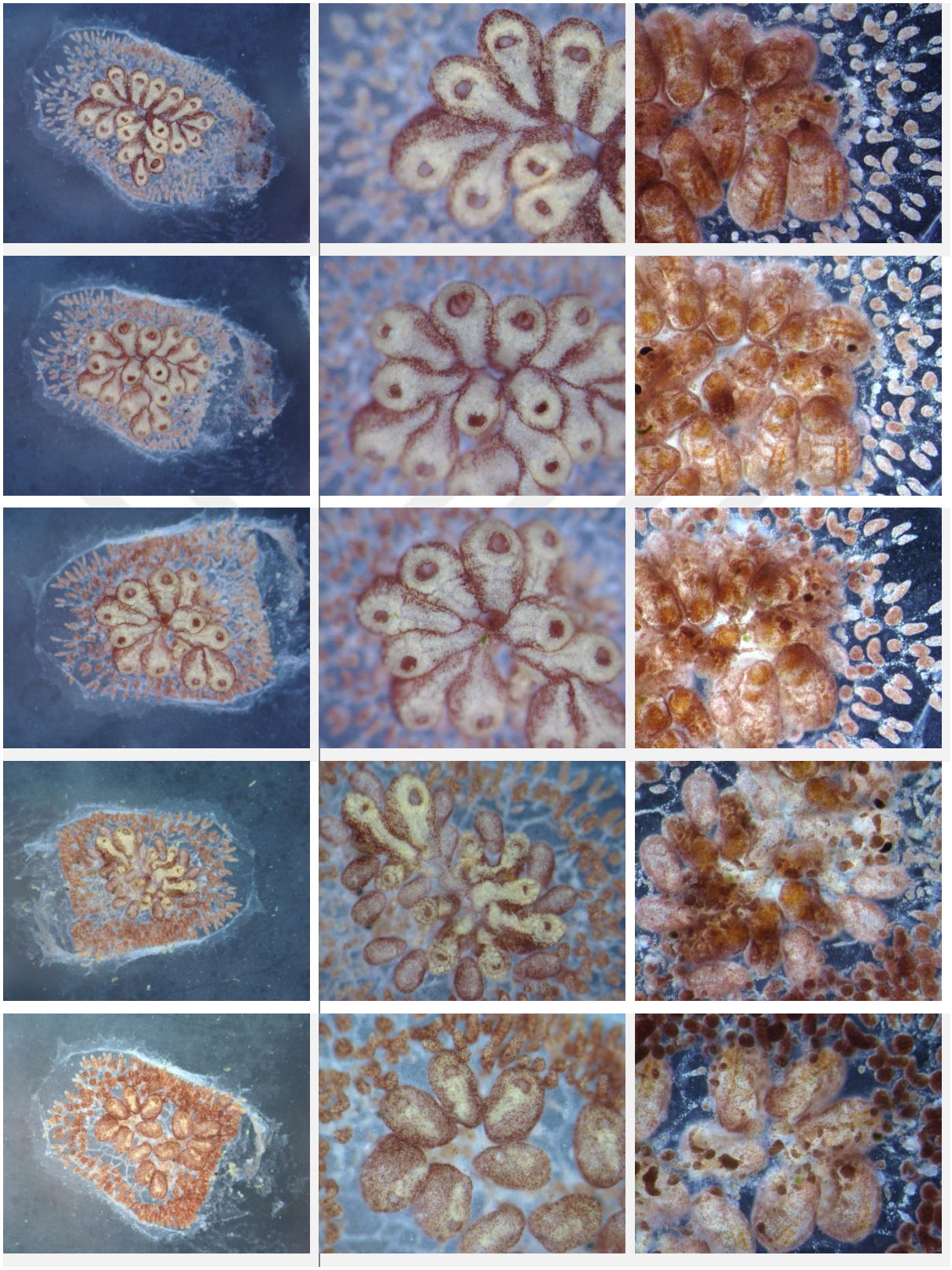
DORSAL - 1	DORSAL - 2	VENTRAL

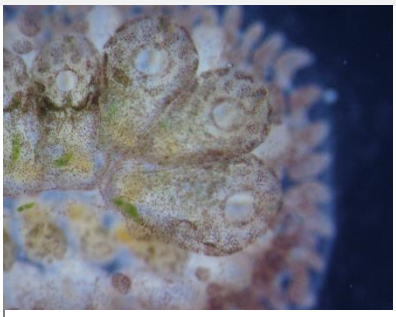
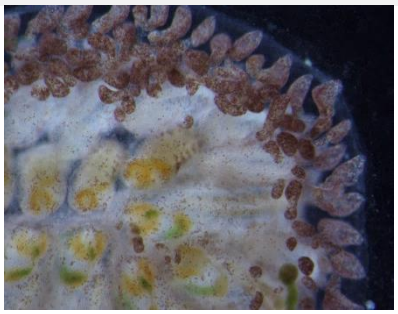
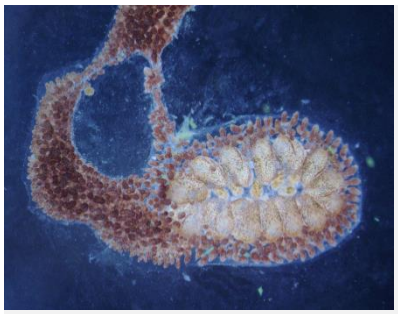
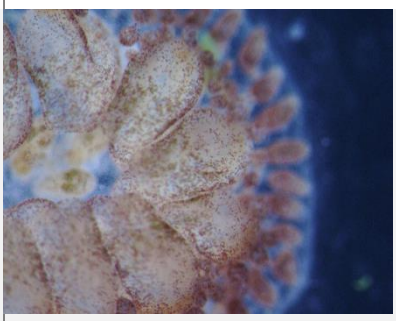
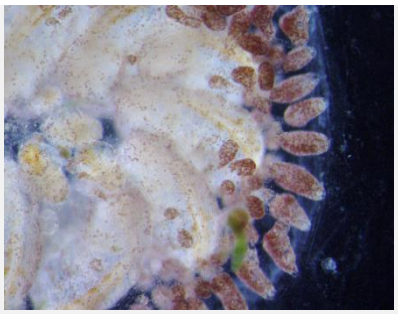
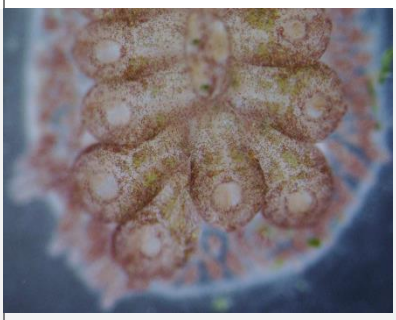
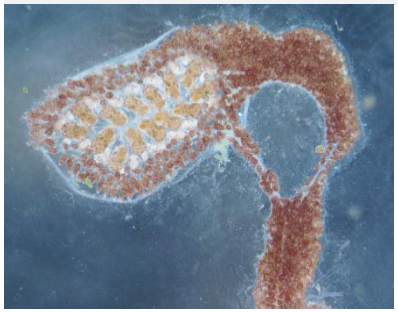
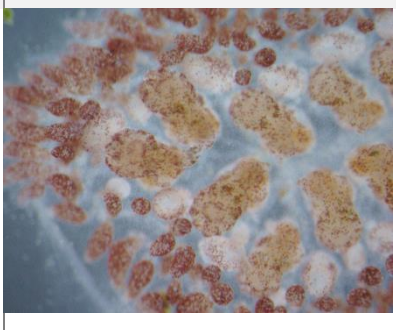
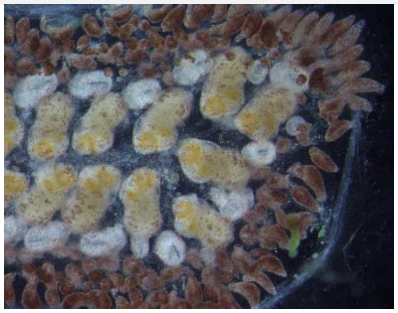
SAMPLE ID – L15

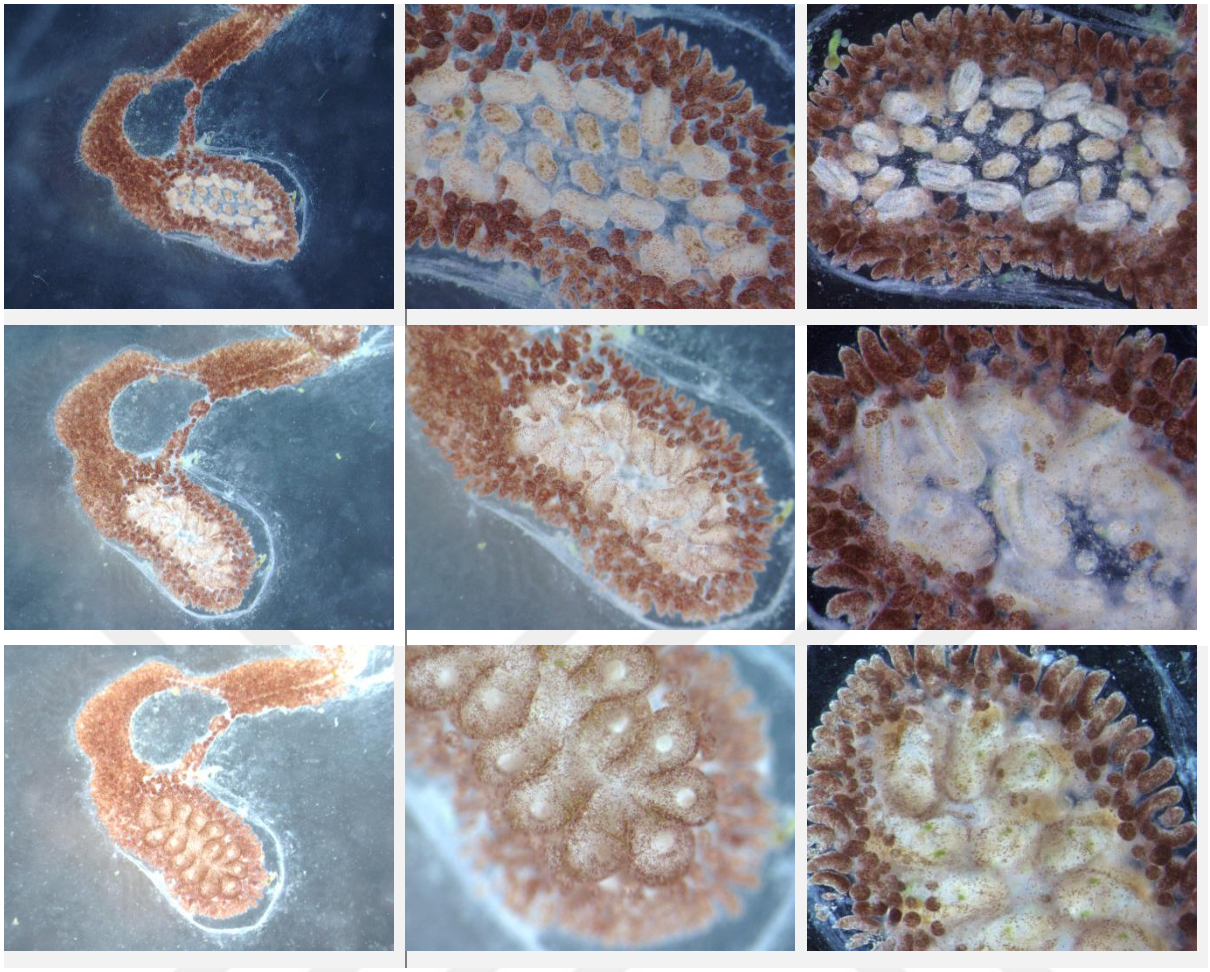










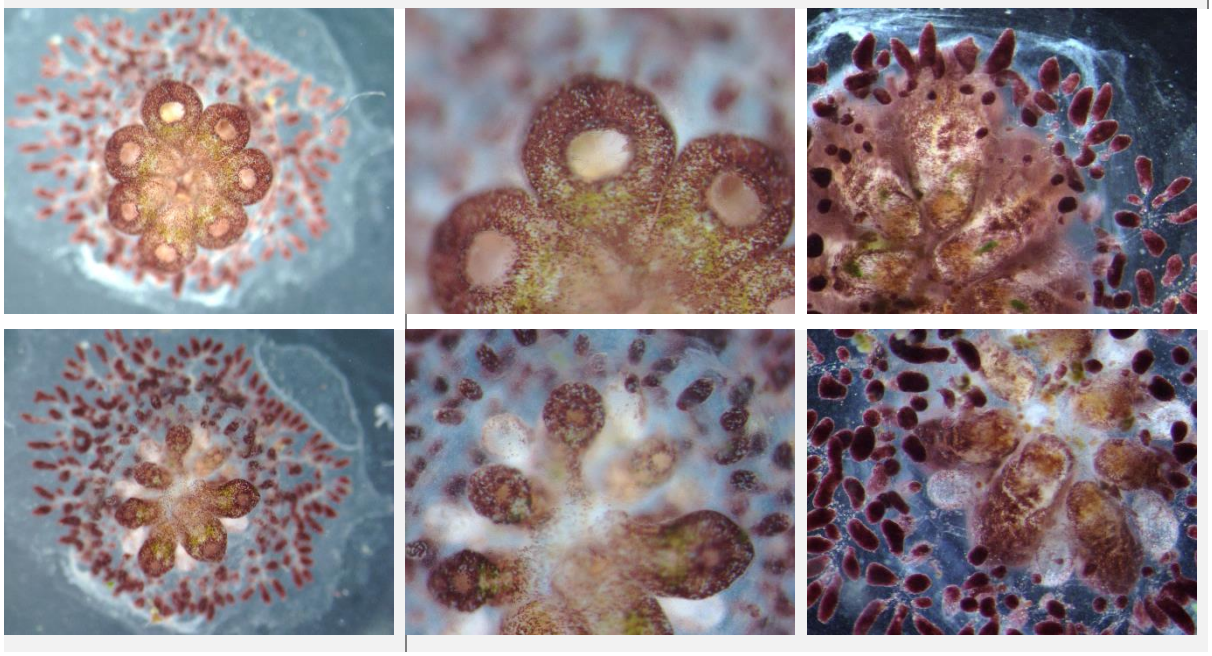


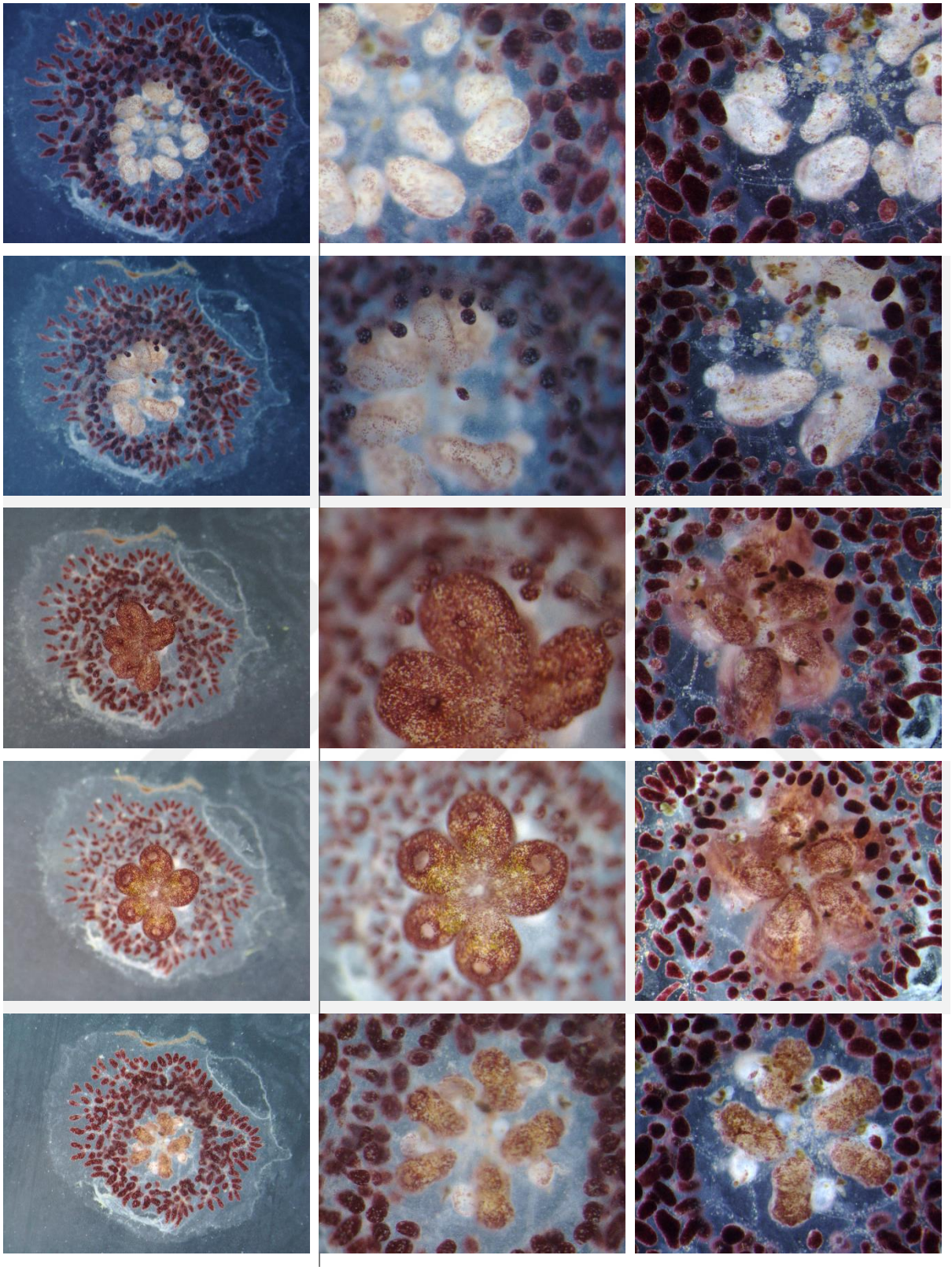
DORSAL - 1	DORSAL - 2	VENTRAL
SAMPLE ID – GK7		
		
		
		
		
		

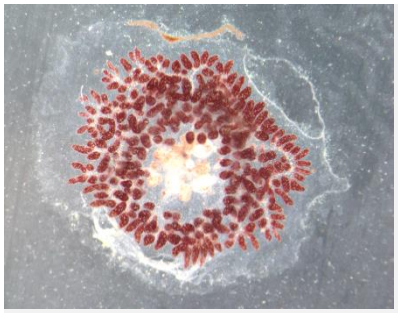
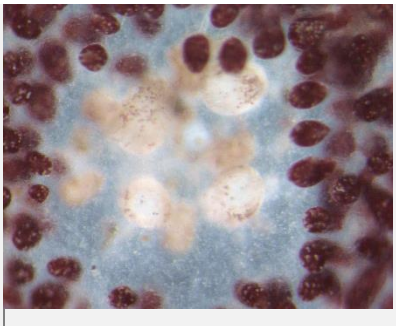
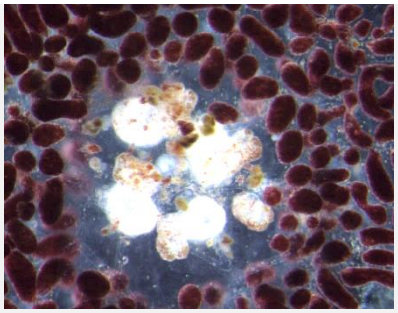


DORSAL - 1 **DORSAL - 2** **VENTRAL**

SAMPLE ID – G1_RIGHT

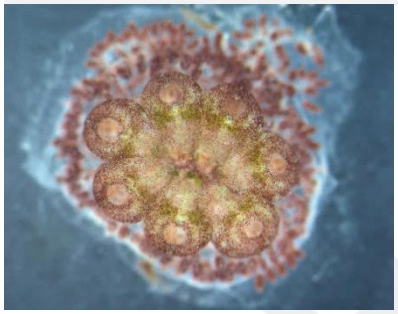
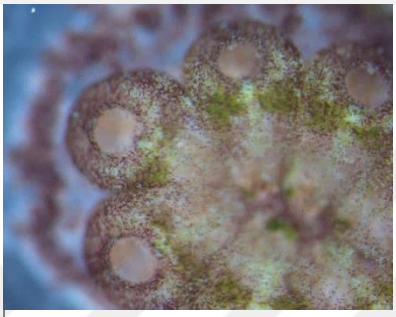
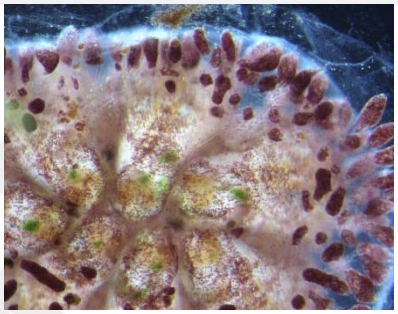
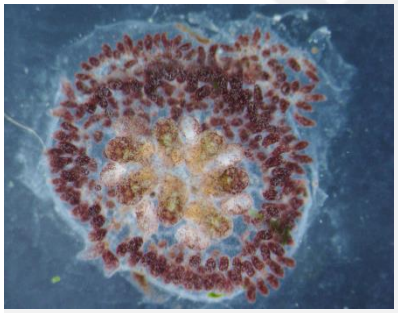
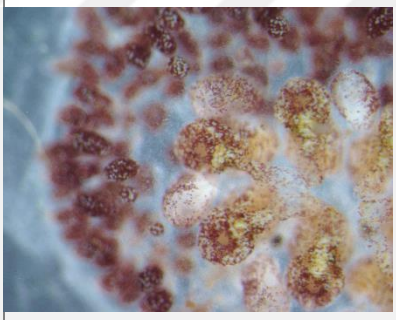
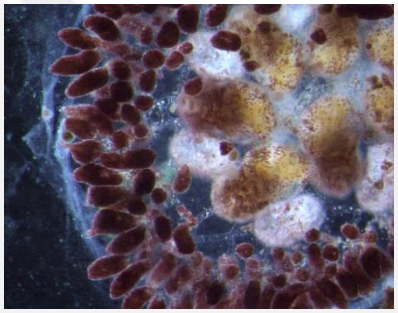
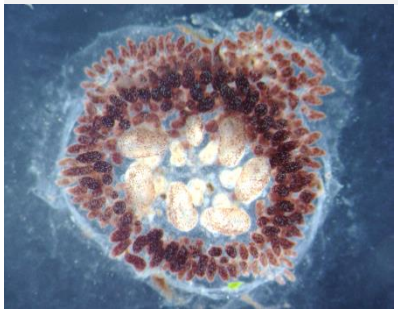
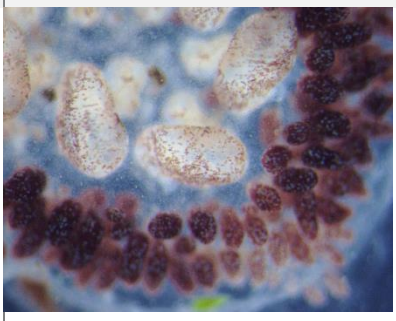
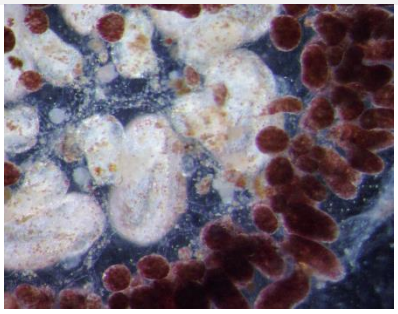
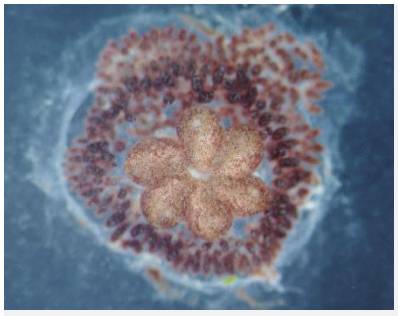
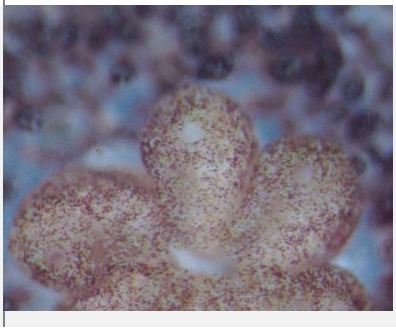
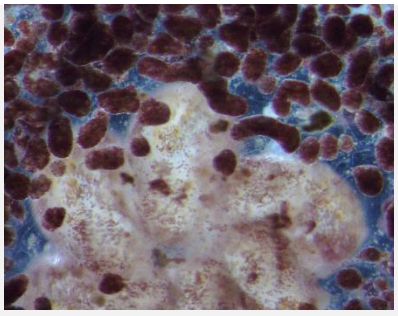


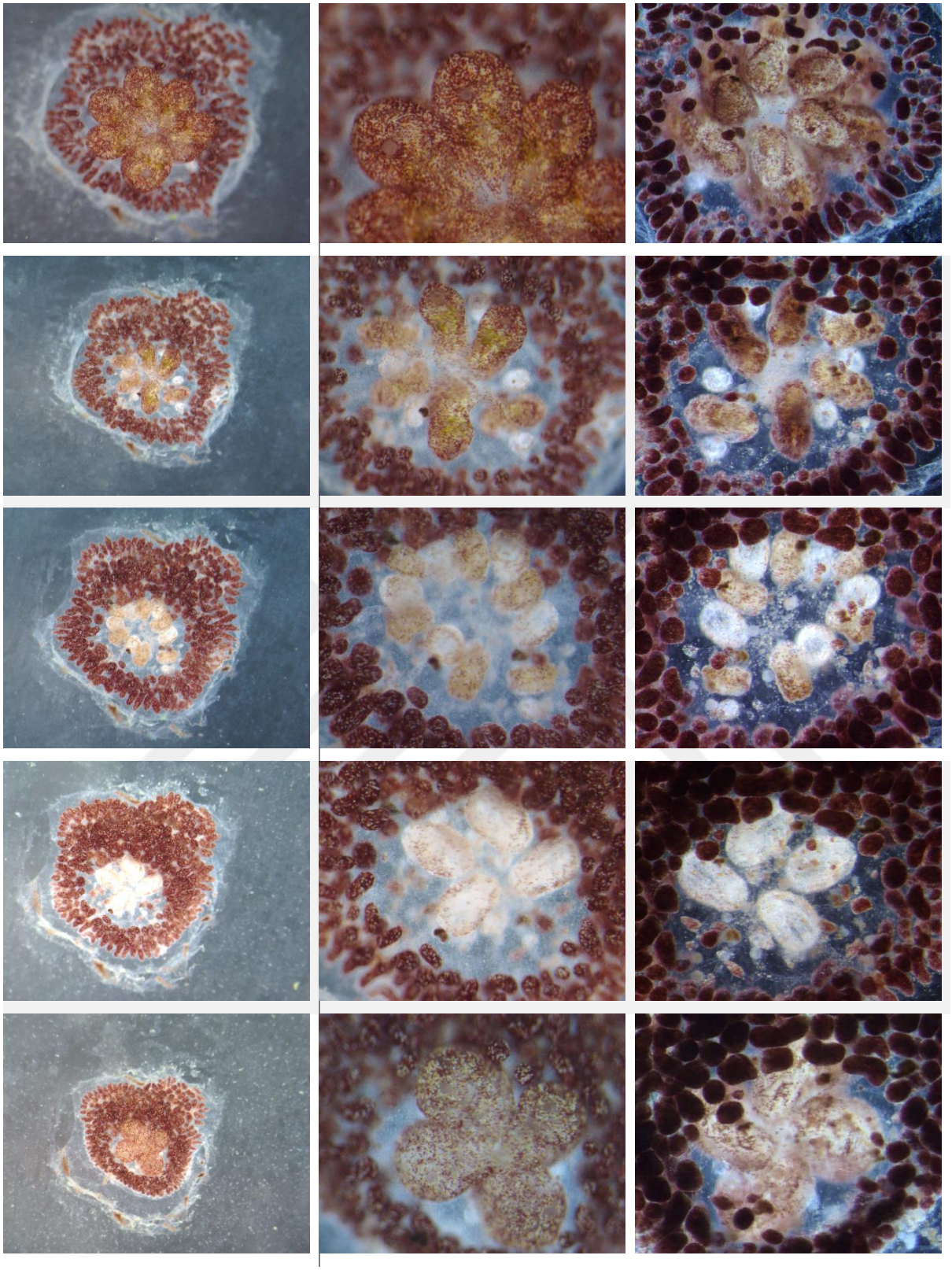


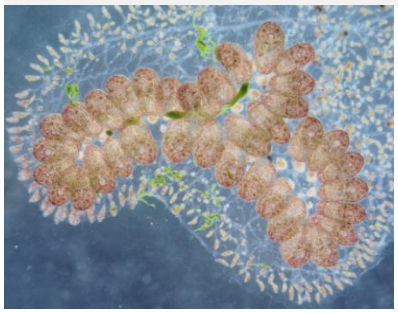
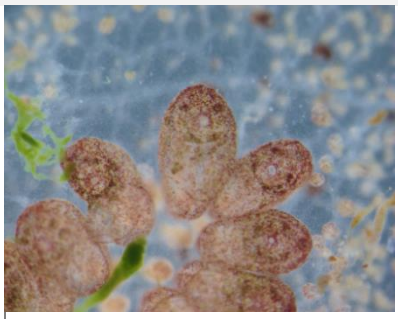
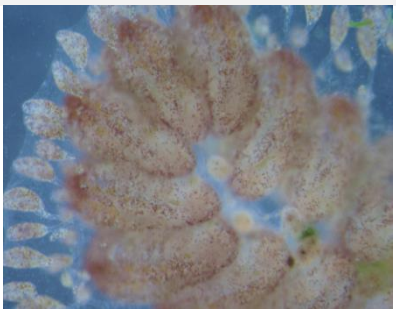
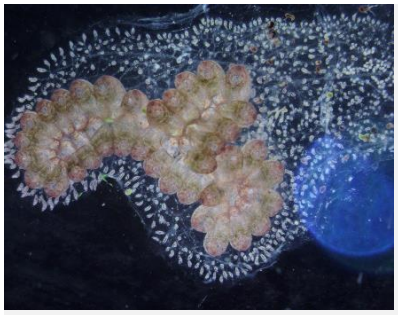
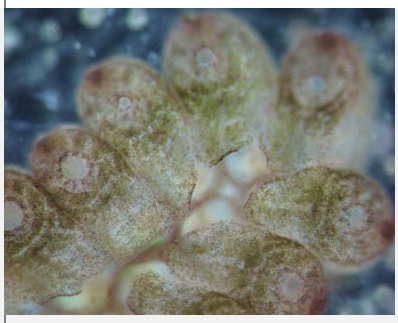
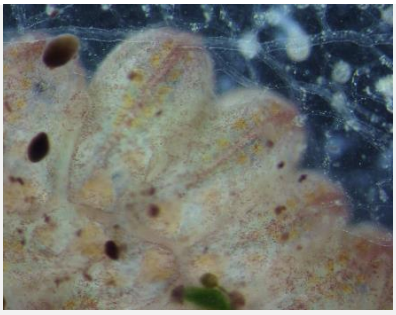
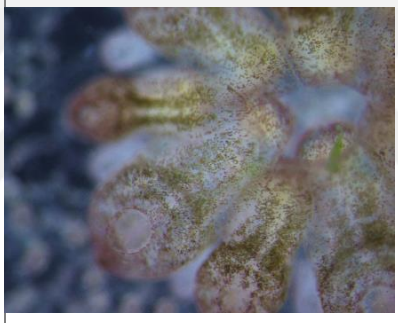
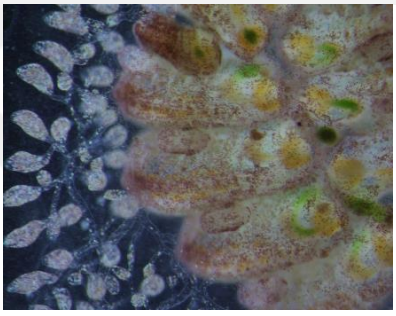
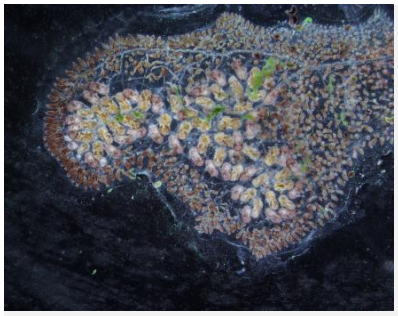
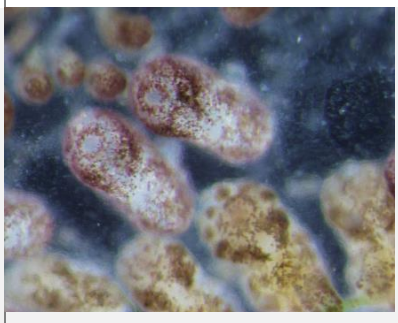
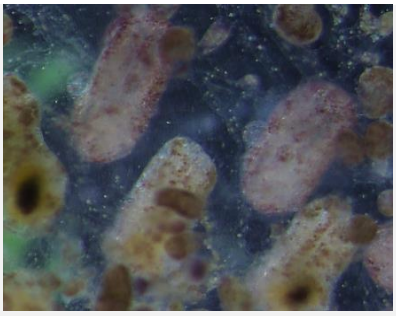
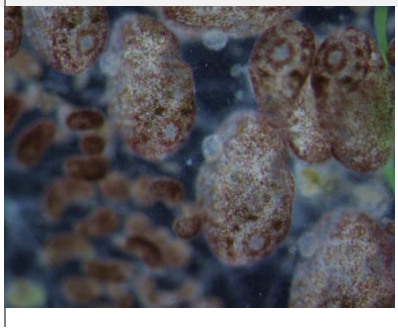
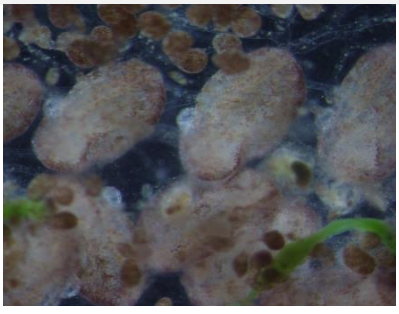




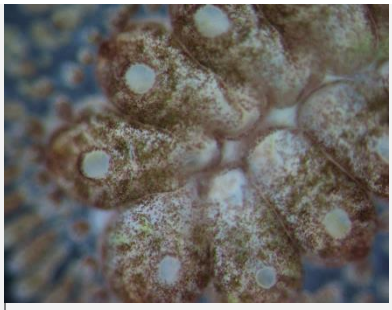
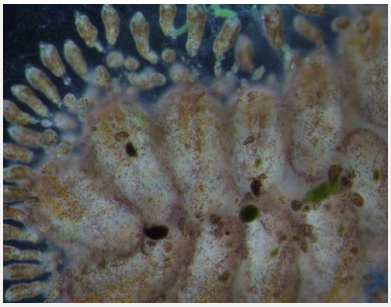
DORSAL - 1 **DORSAL - 2** **VENTRAL**

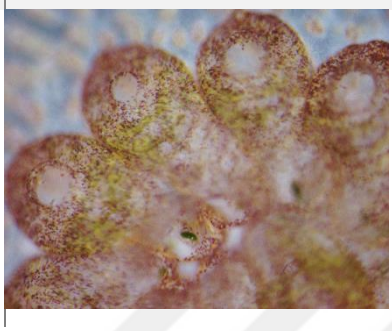
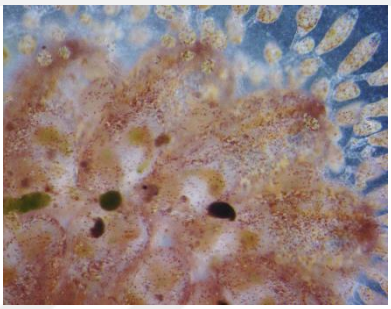
SAMPLE ID – G1_LEFT



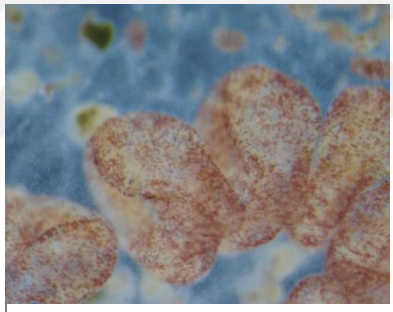
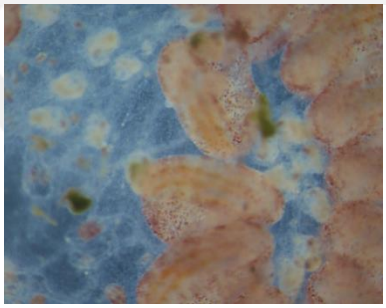
DORSAL - 1	DORSAL - 2	VENTRAL
SAMPLE ID – R8		
		
		
		
		
		

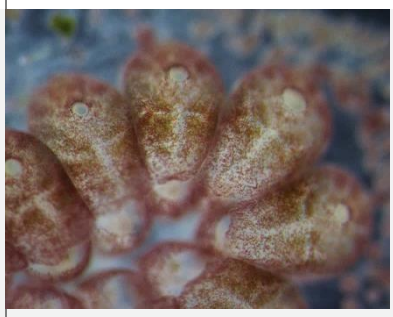
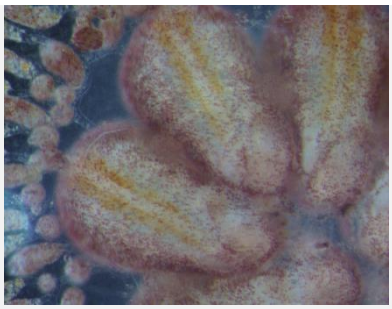
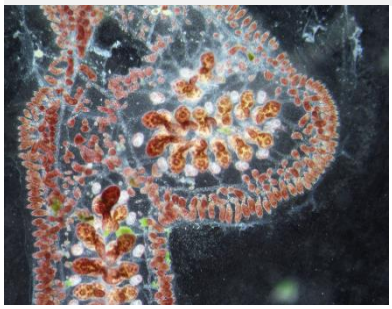
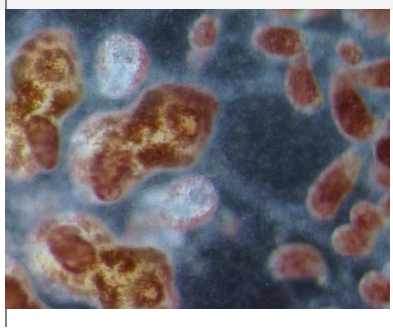
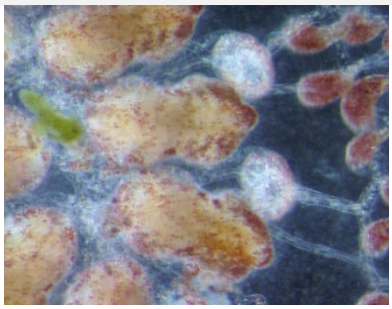




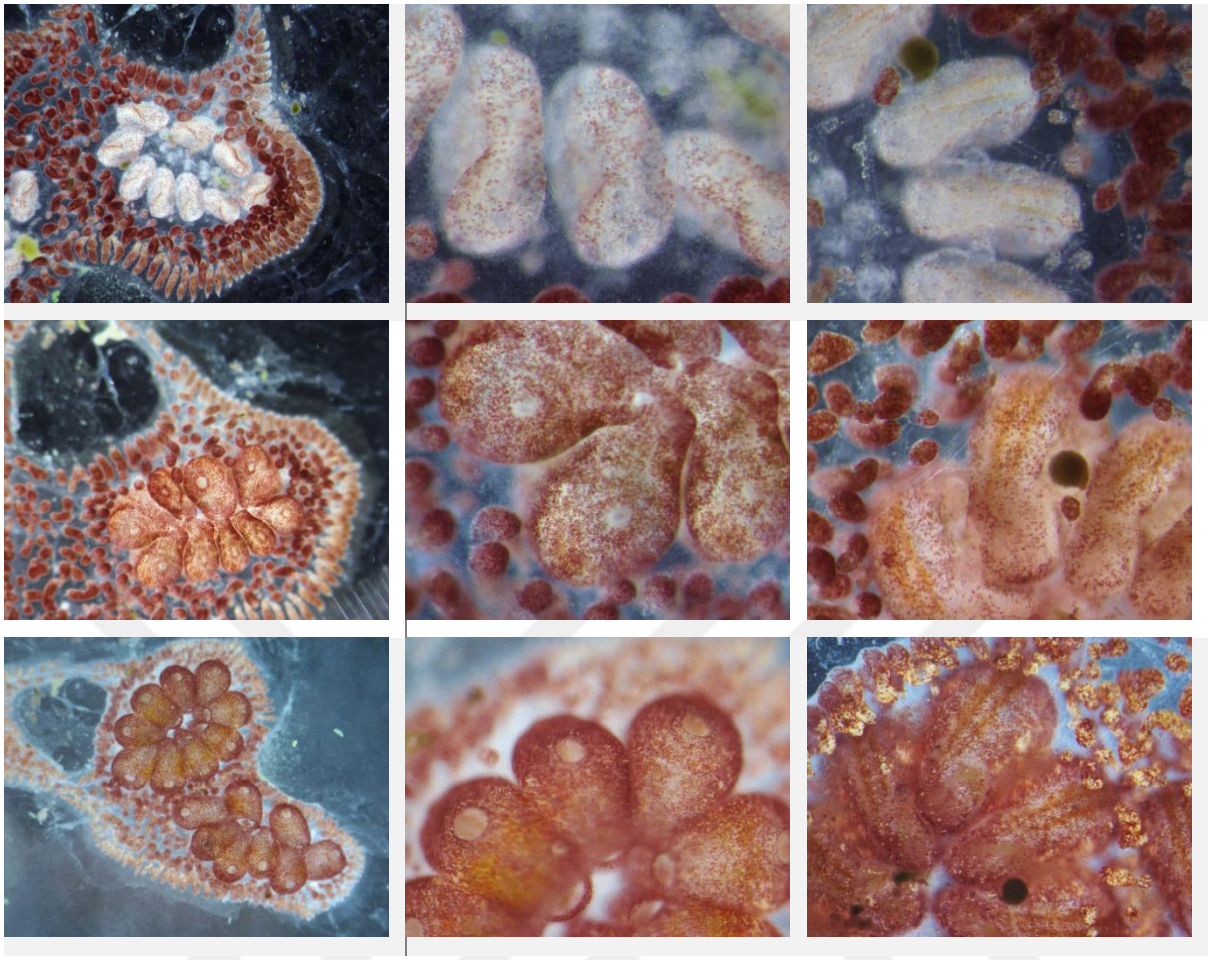



DORSAL - 1 **DORSAL - 2** **VENTRAL**

SAMPLE ID – R9

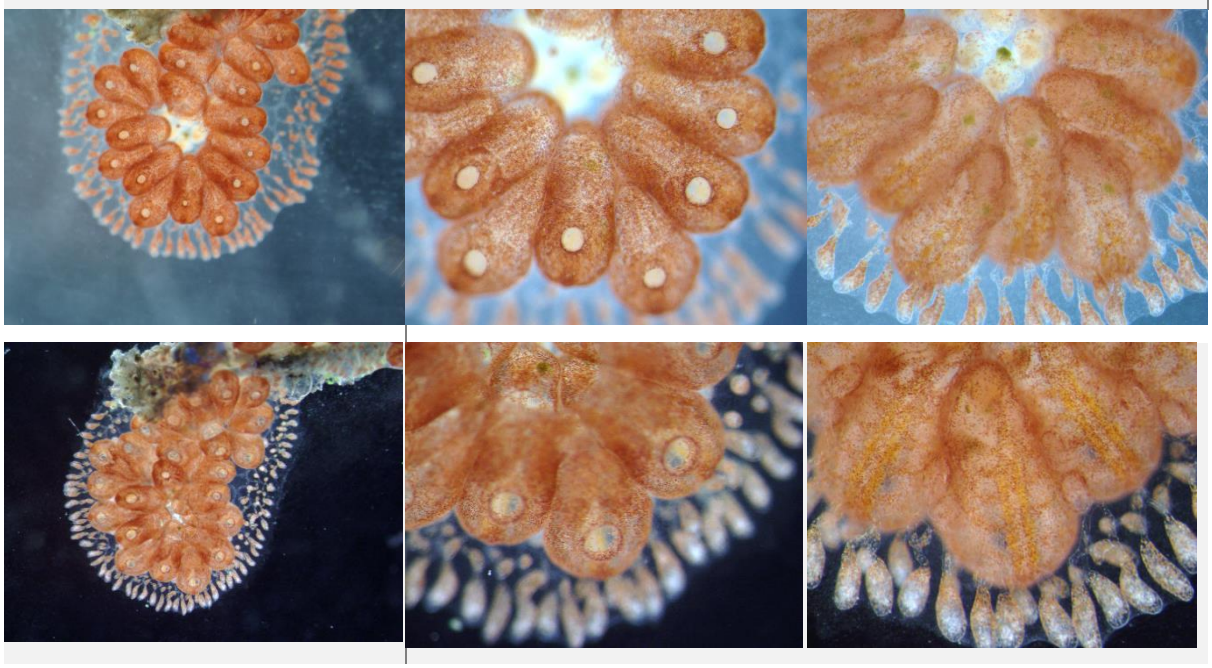




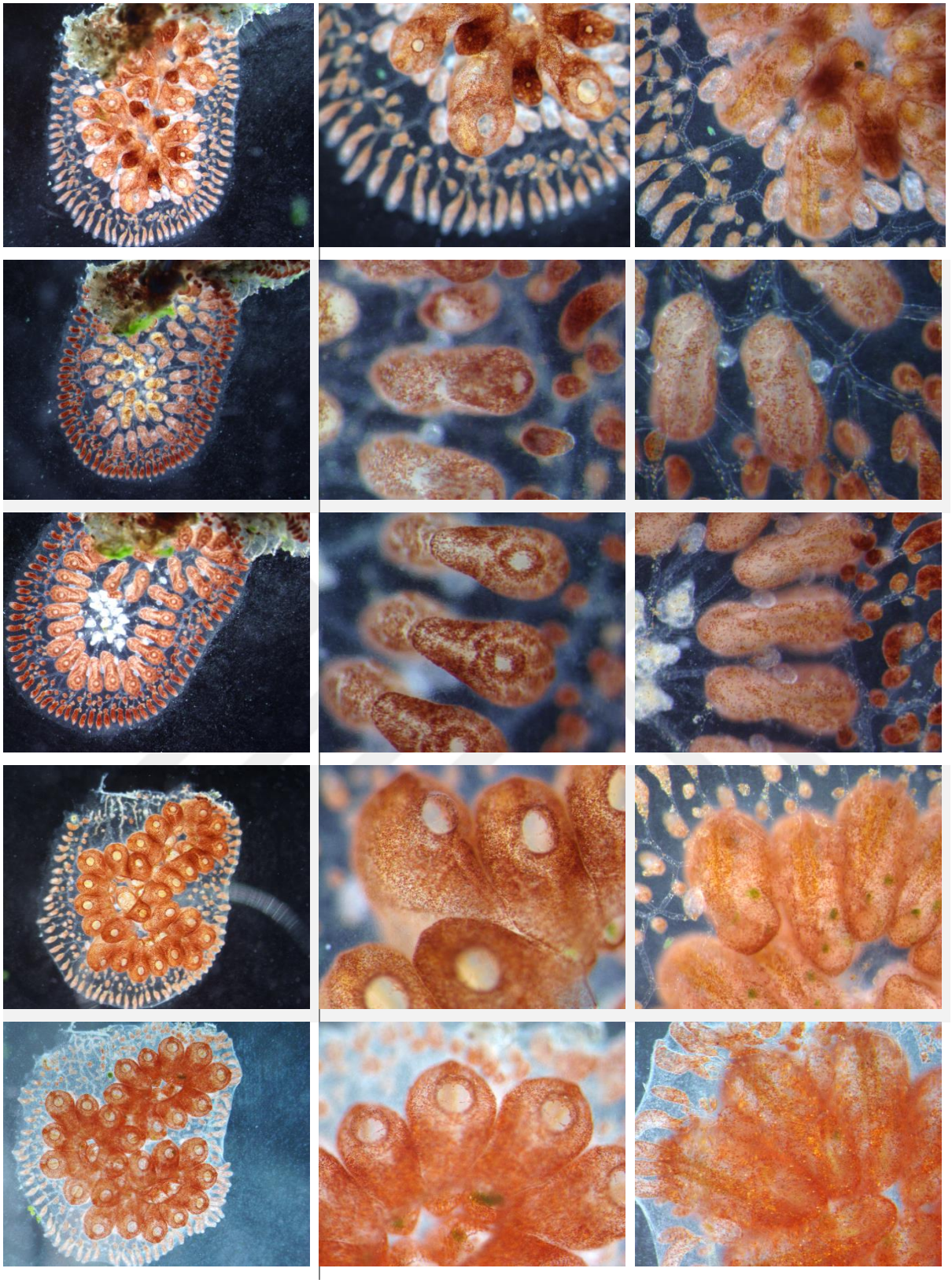






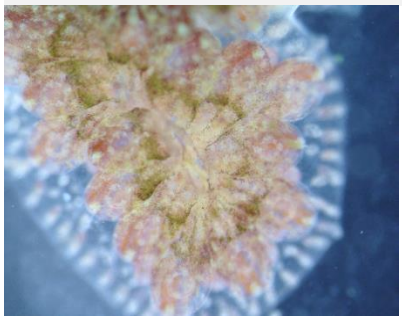
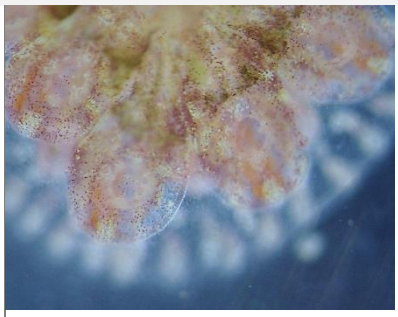
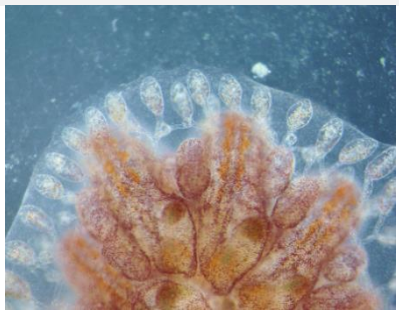
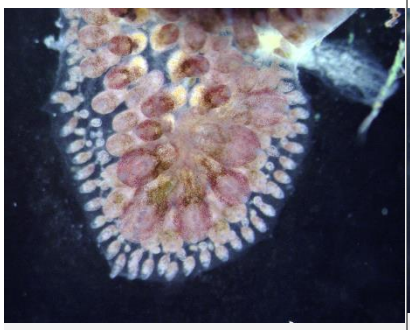
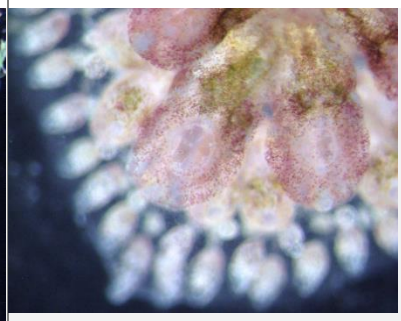
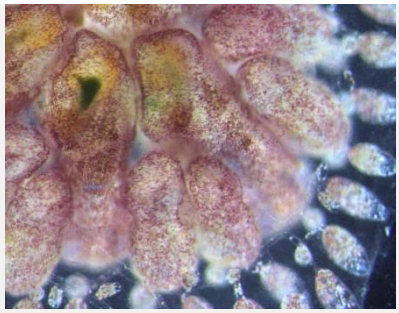
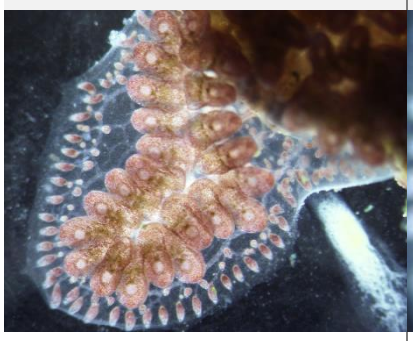
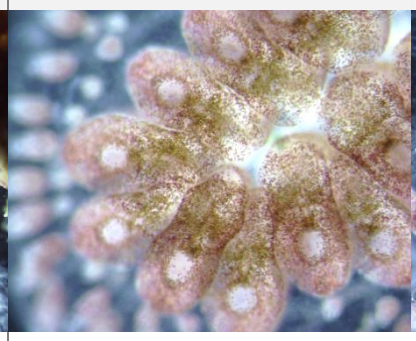
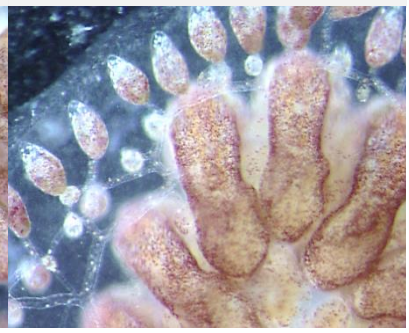
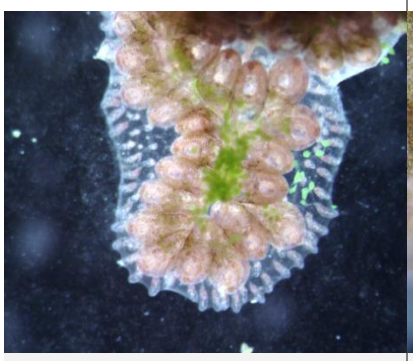
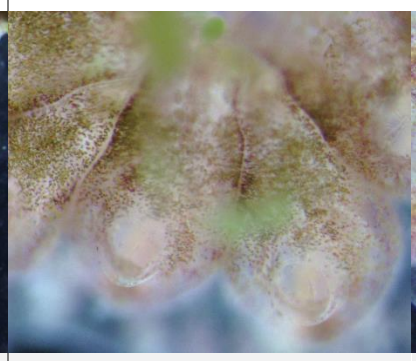
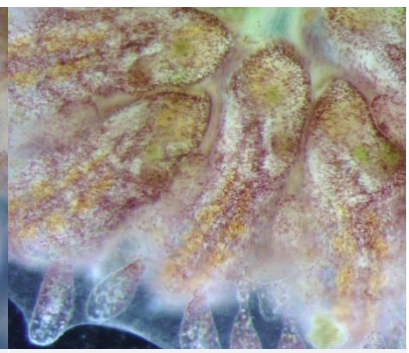
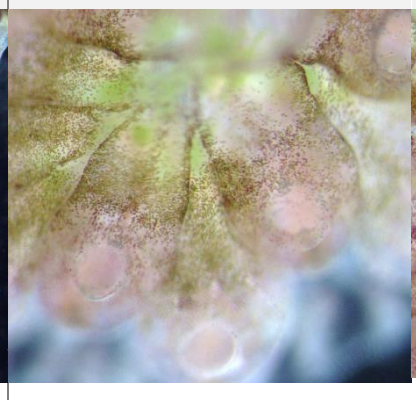
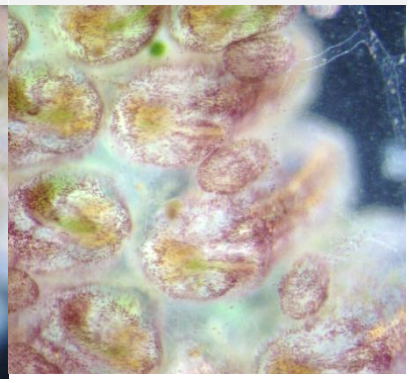


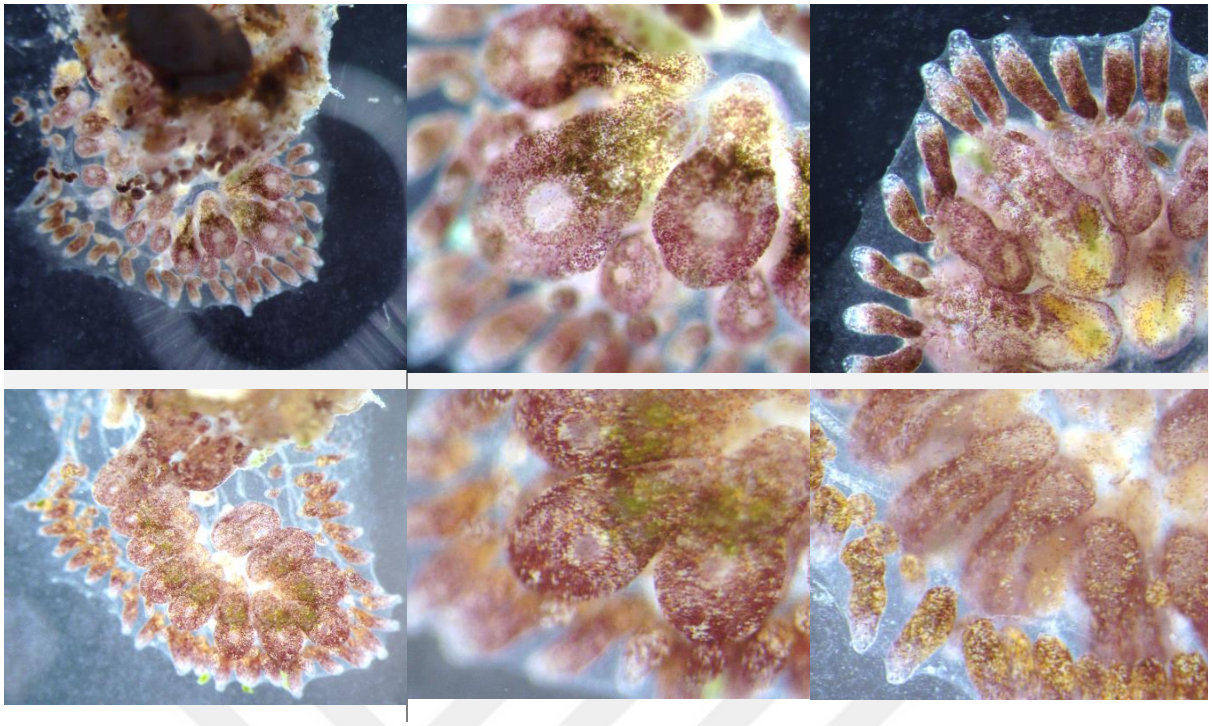
DORSAL - 1 DORSAL - 2 VENTRAL

SAMPLE ID – GK21



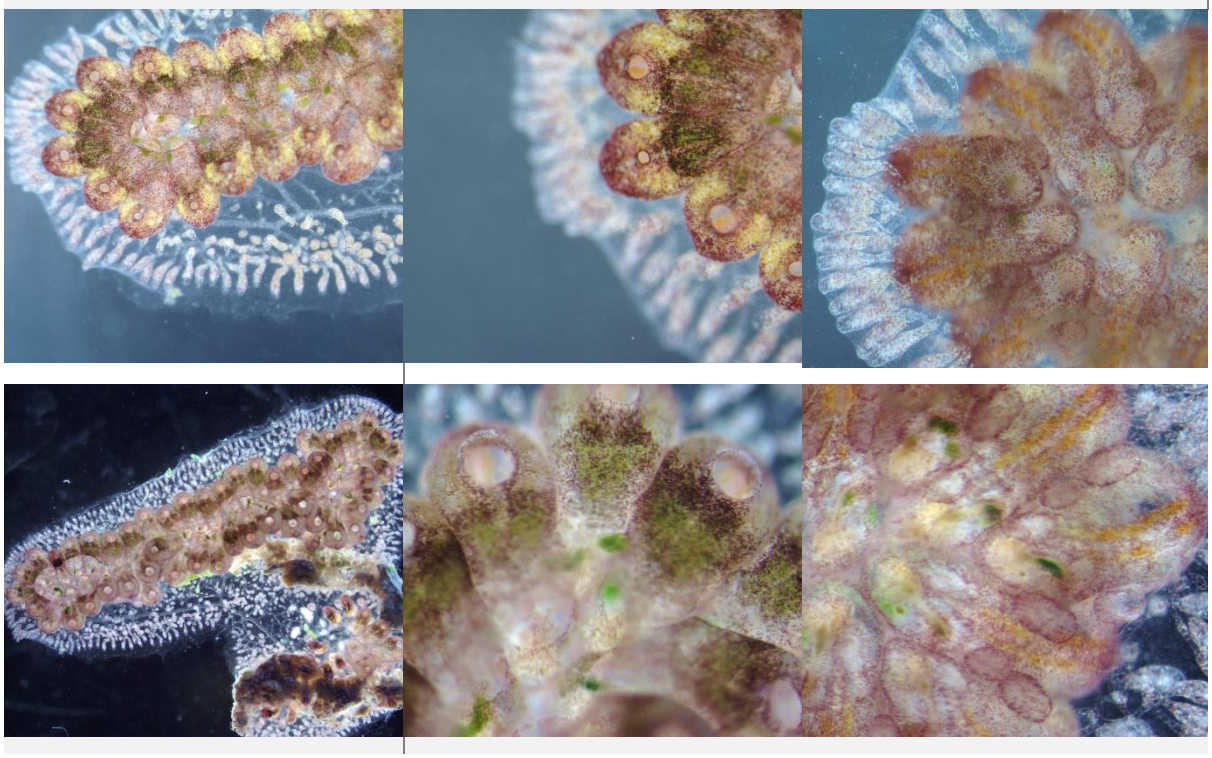


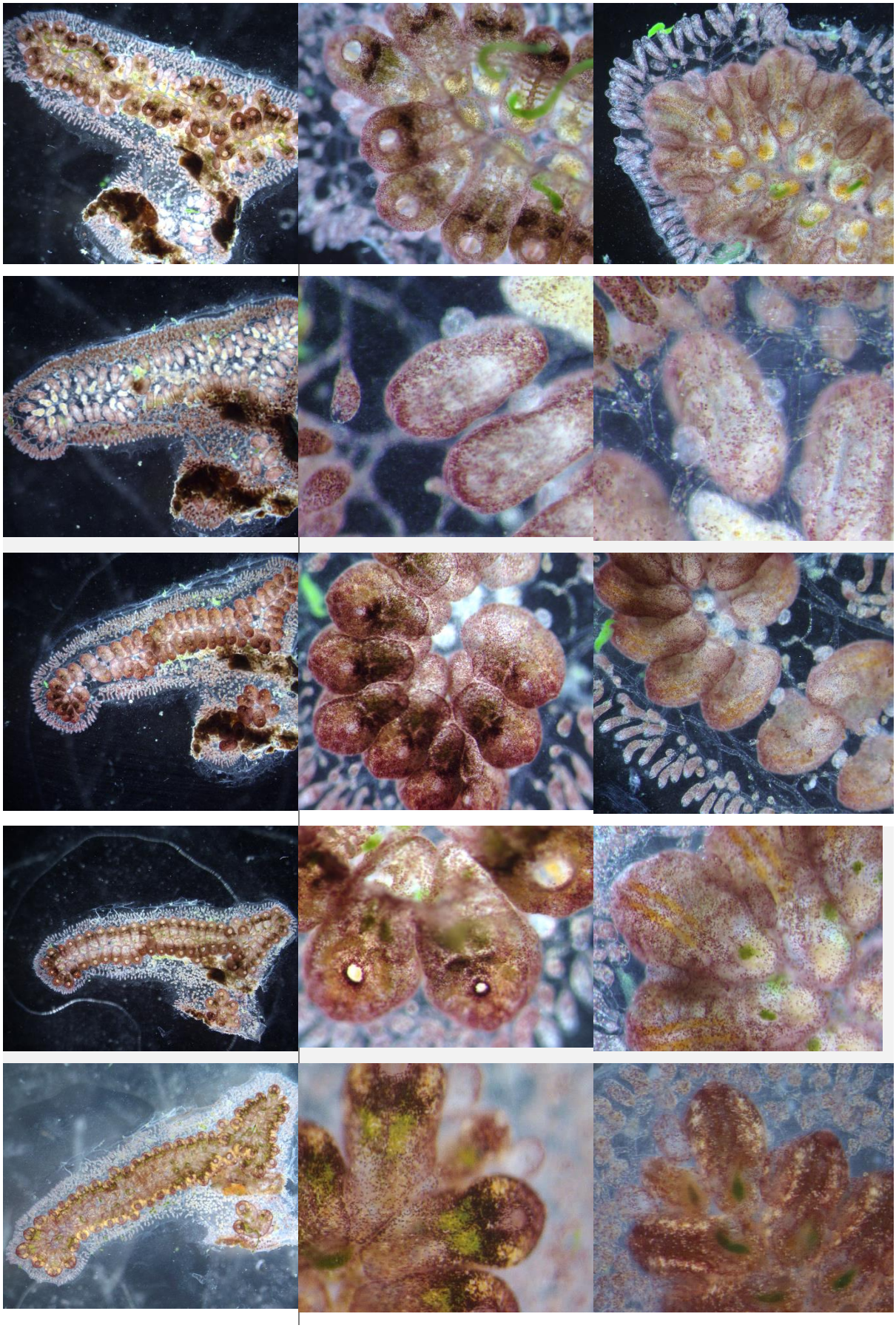
DORSAL - 1	DORSAL - 2	VENTRAL
SAMPLE ID – GK4		
		
		
		
		
		

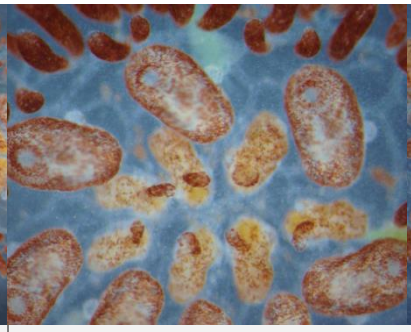
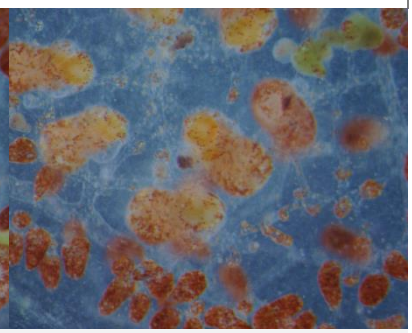
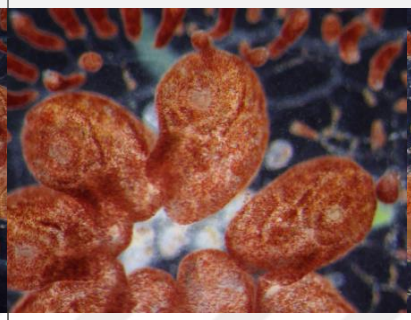
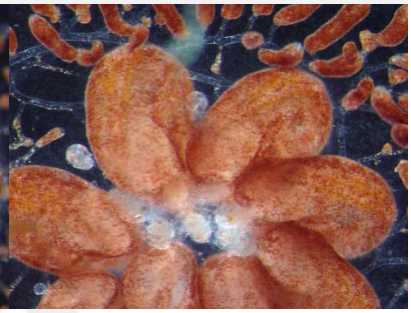
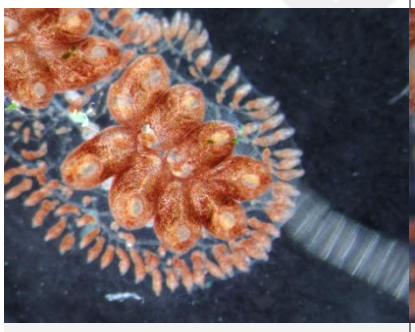
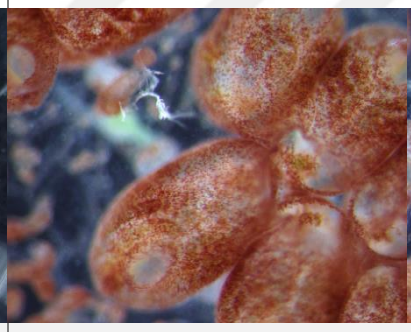
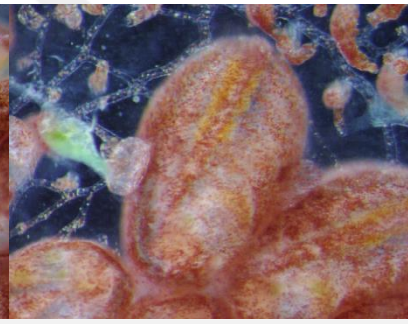
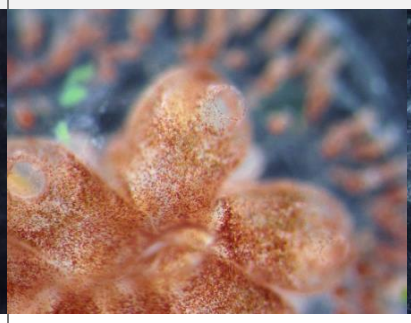
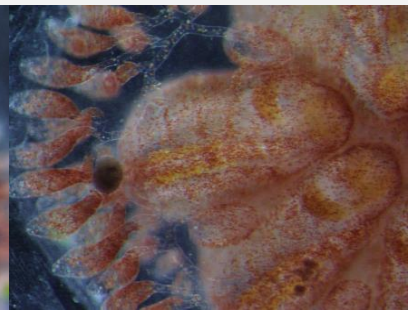
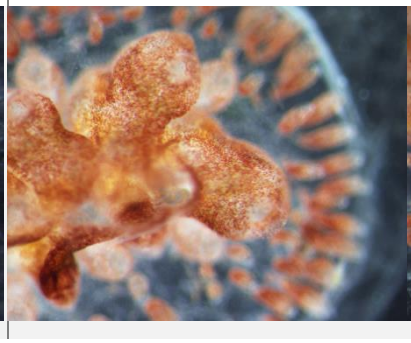


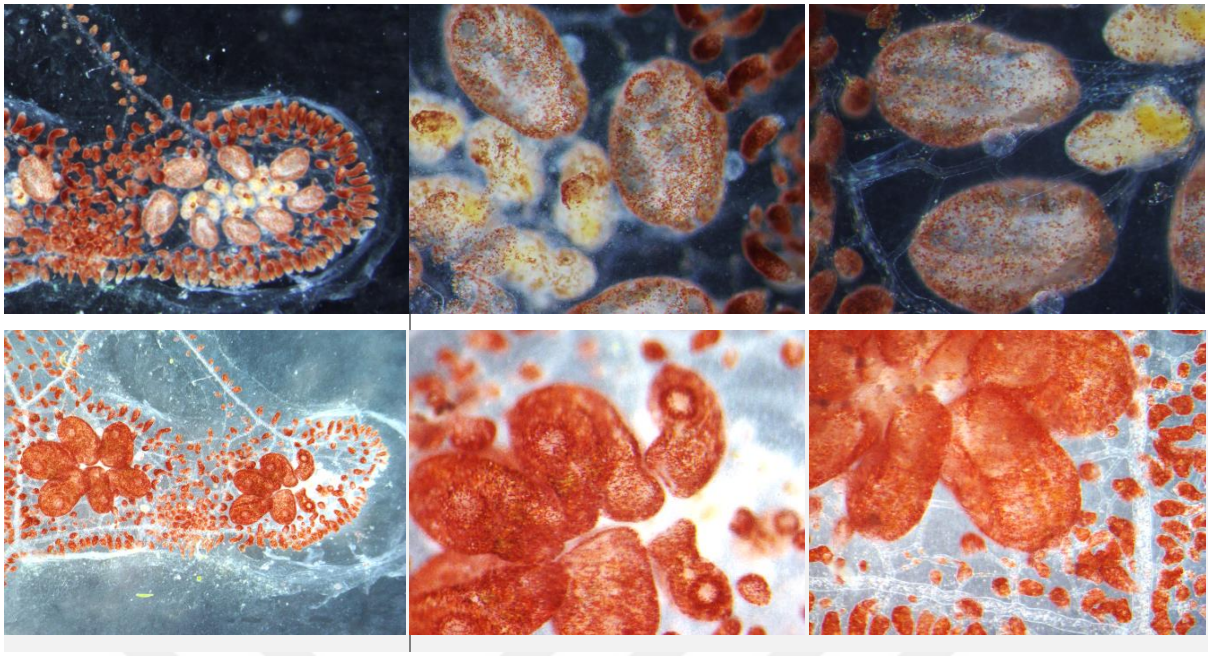
DORSAL - 1 **DORSAL - 2** **VENTRAL**

SAMPLE ID – G15



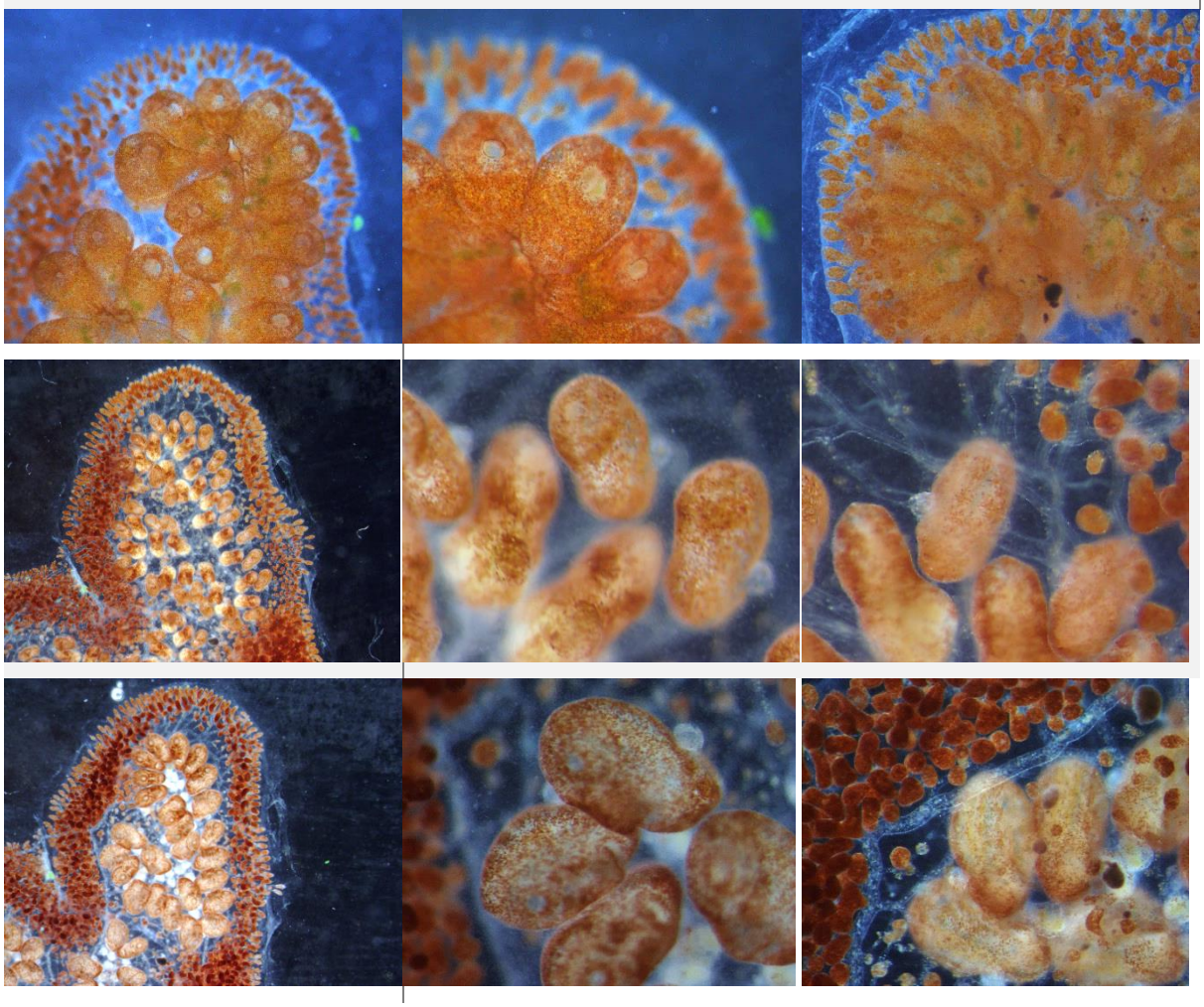


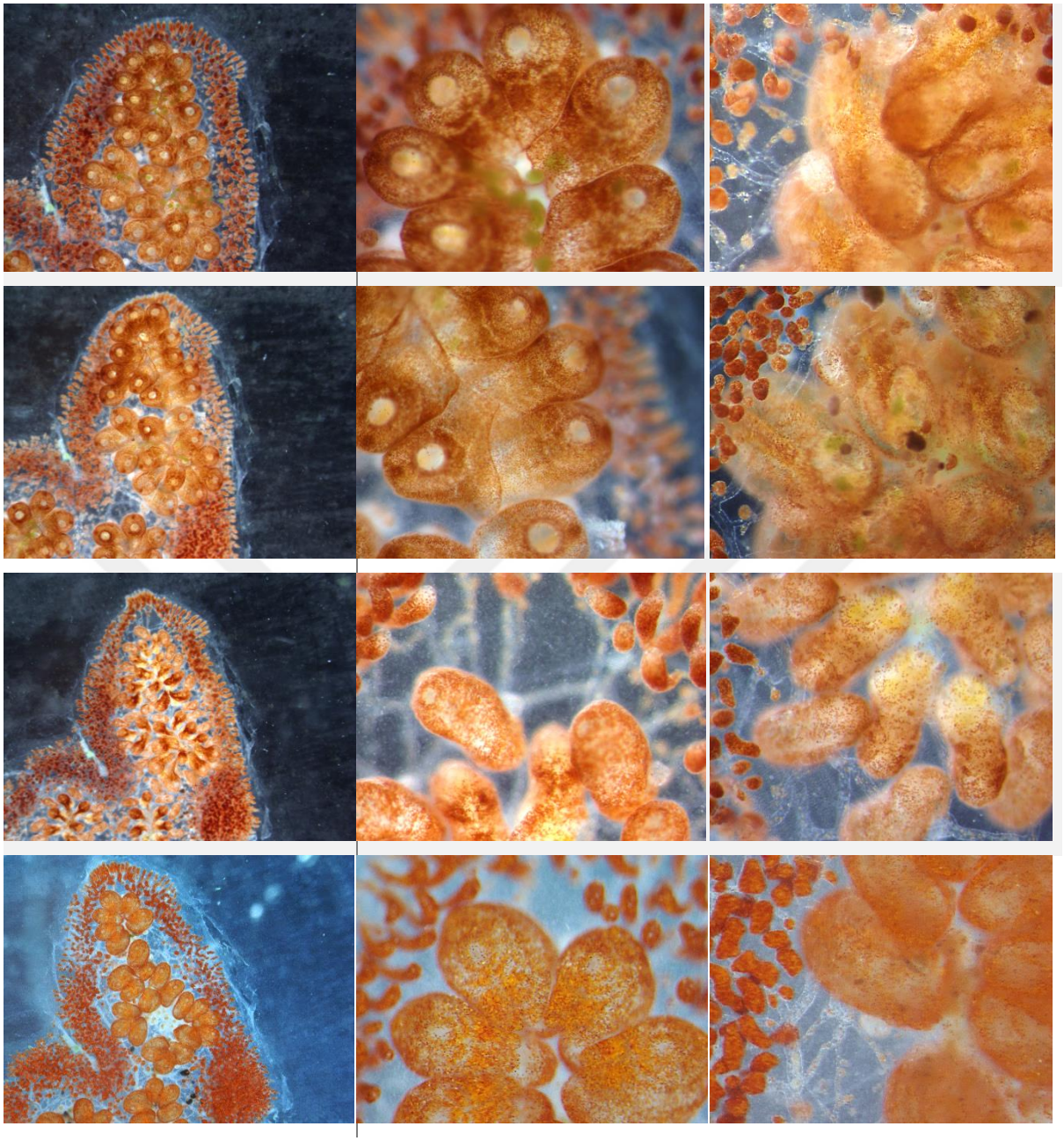
DORSAL - 1	DORSAL - 2	VENTRAL
SAMPLE ID – NN		
		
		
		
		
		



DORSAL - 1 **DORSAL - 2** **VENTRAL**

SAMPLE ID – R1

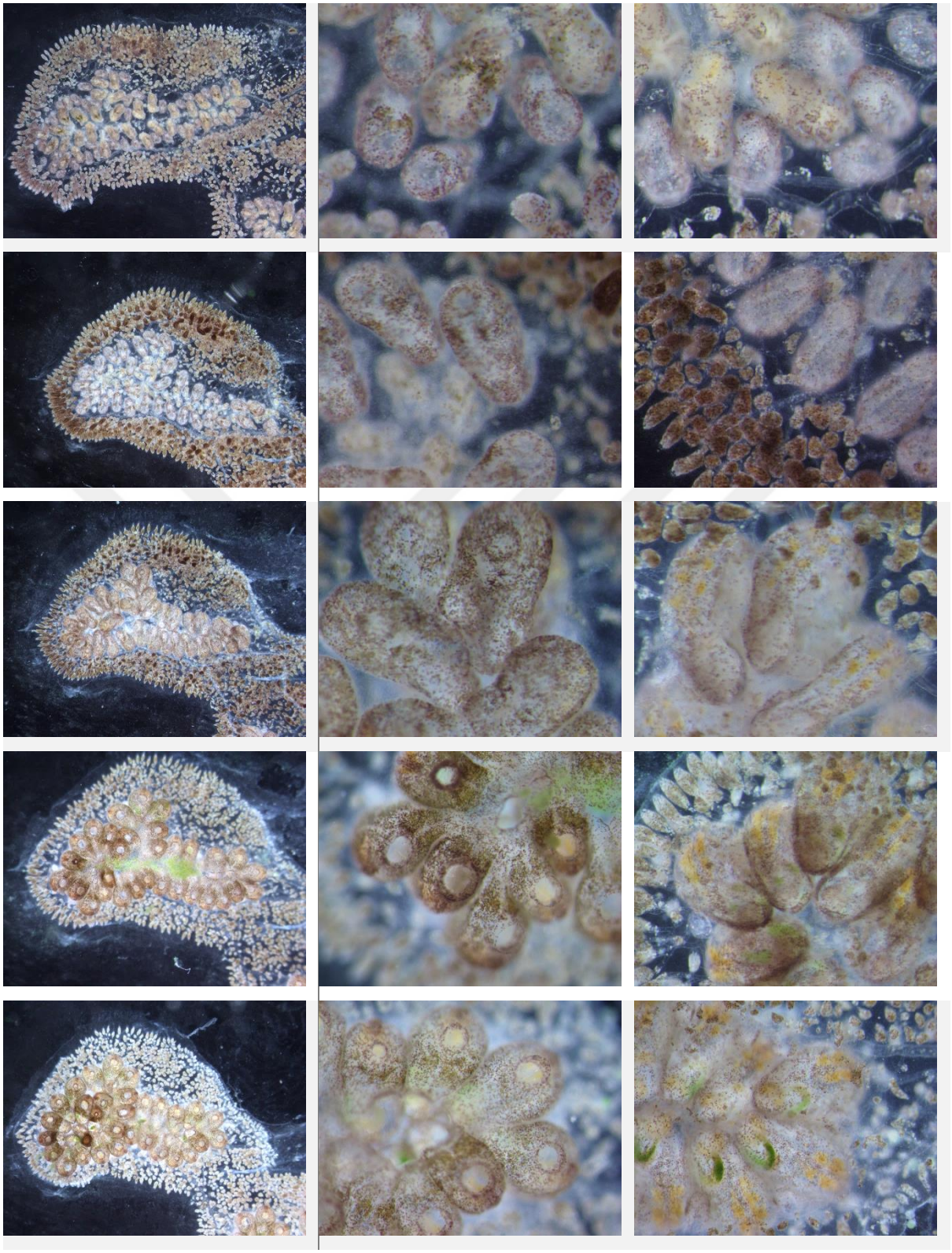


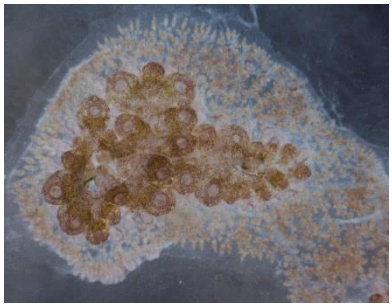
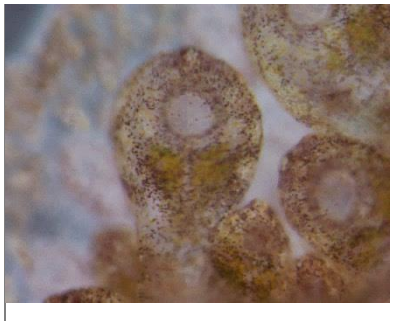


DORSAL - 1 **DORSAL - 2** **VENTRAL**

SAMPLE ID – R4

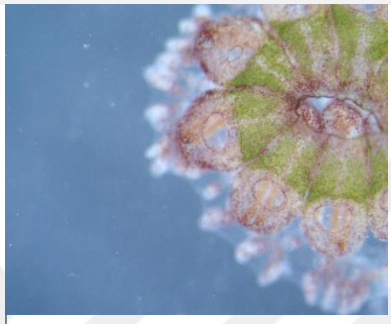
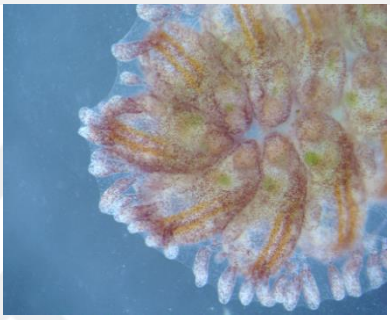


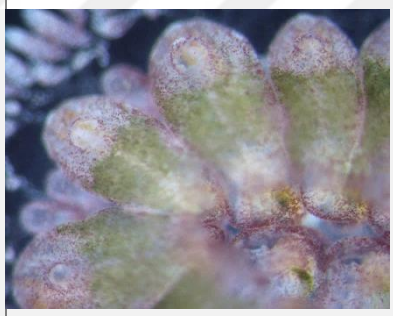
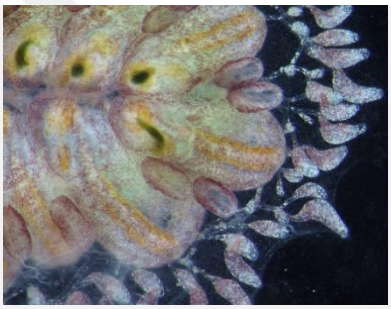


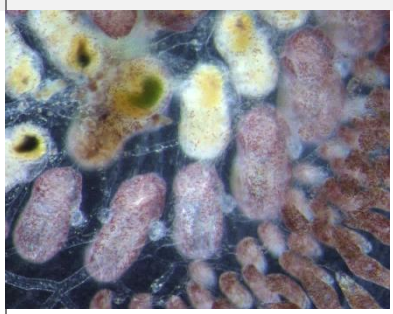
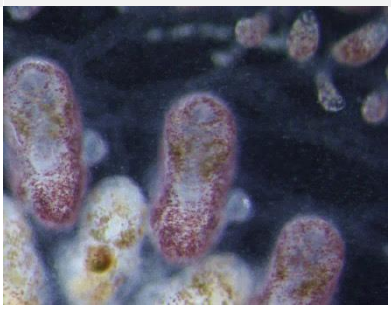
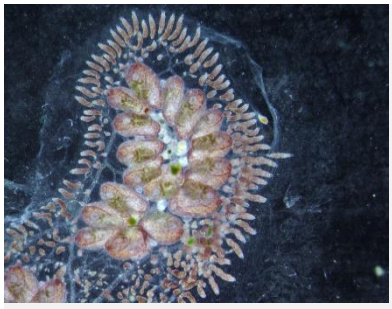
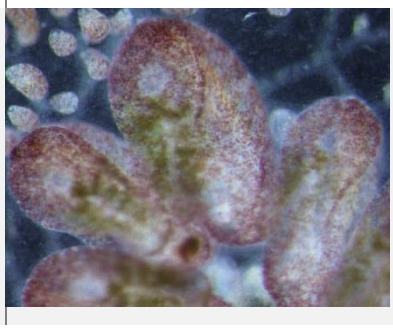
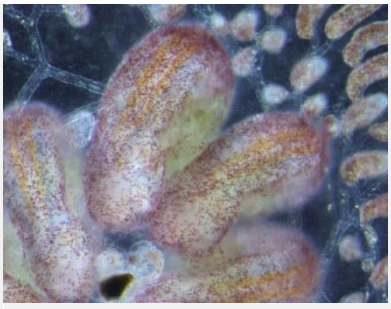



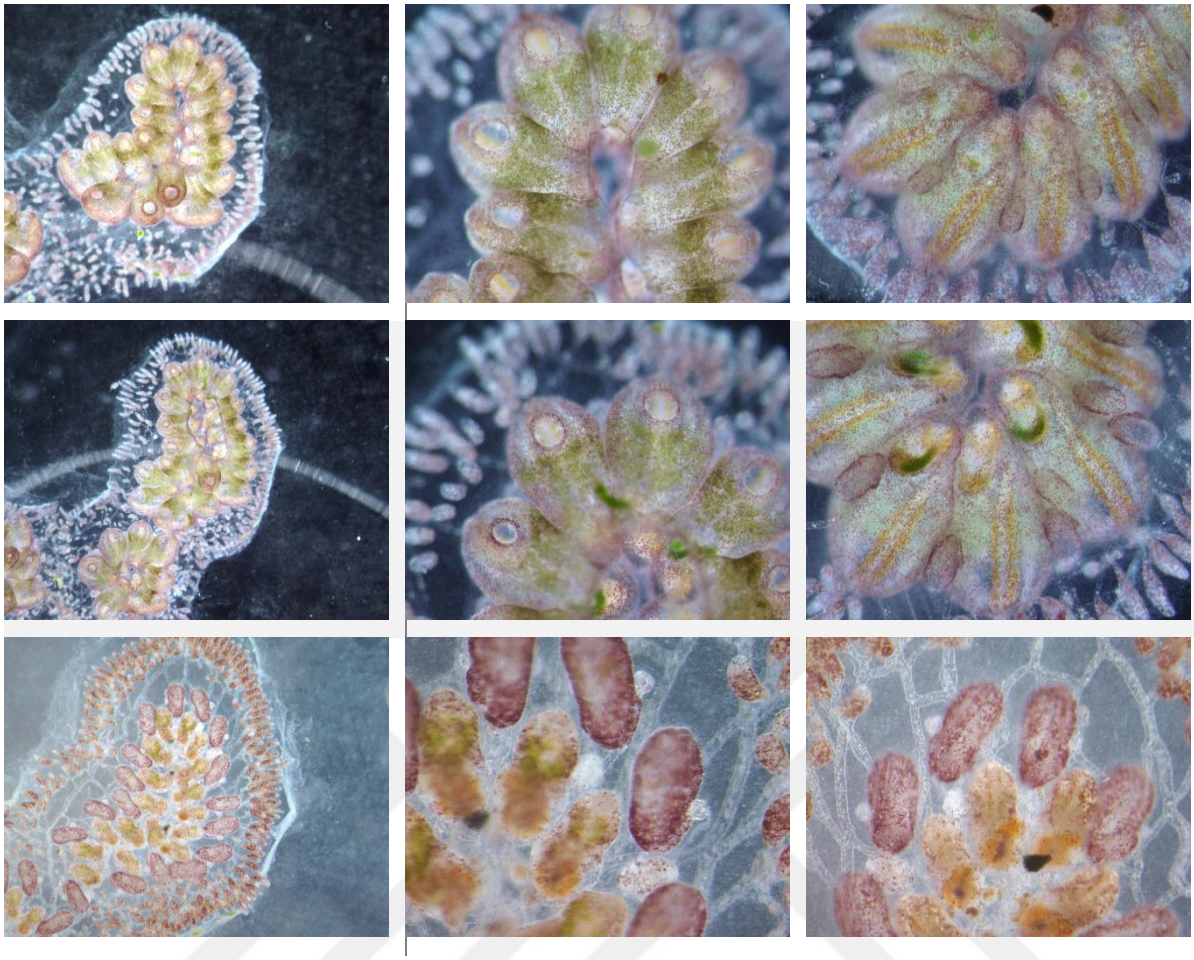

DORSAL - 1 **DORSAL - 2** **VENTRAL**

SAMPLE ID – R6

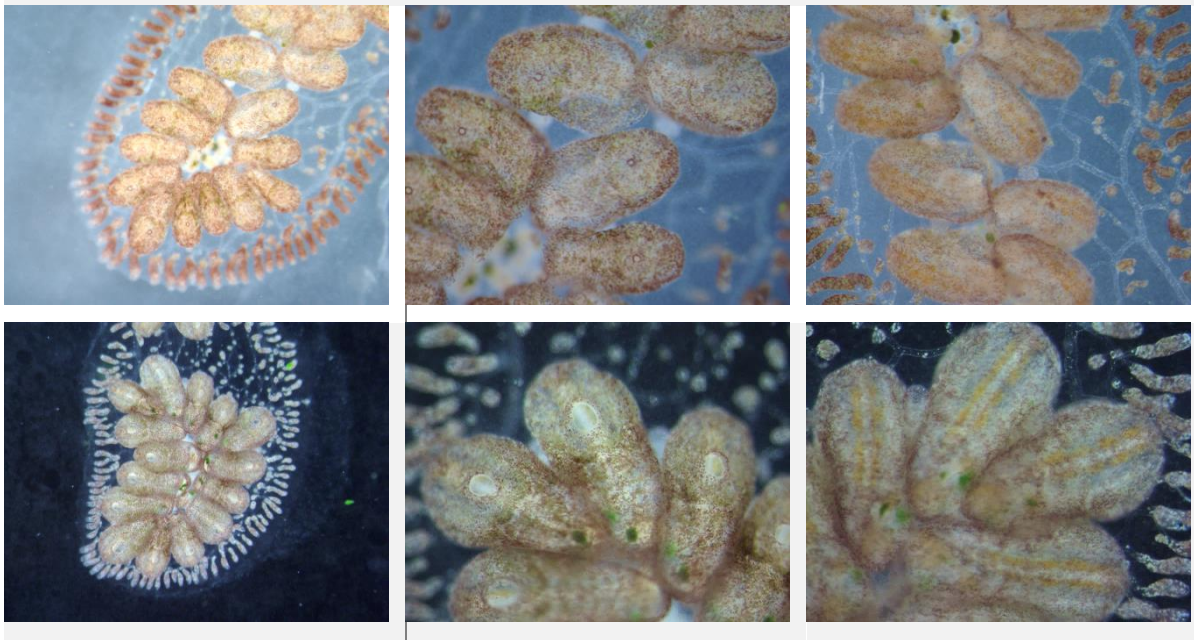





DORSAL - 1 **DORSAL - 2** **VENTRAL**

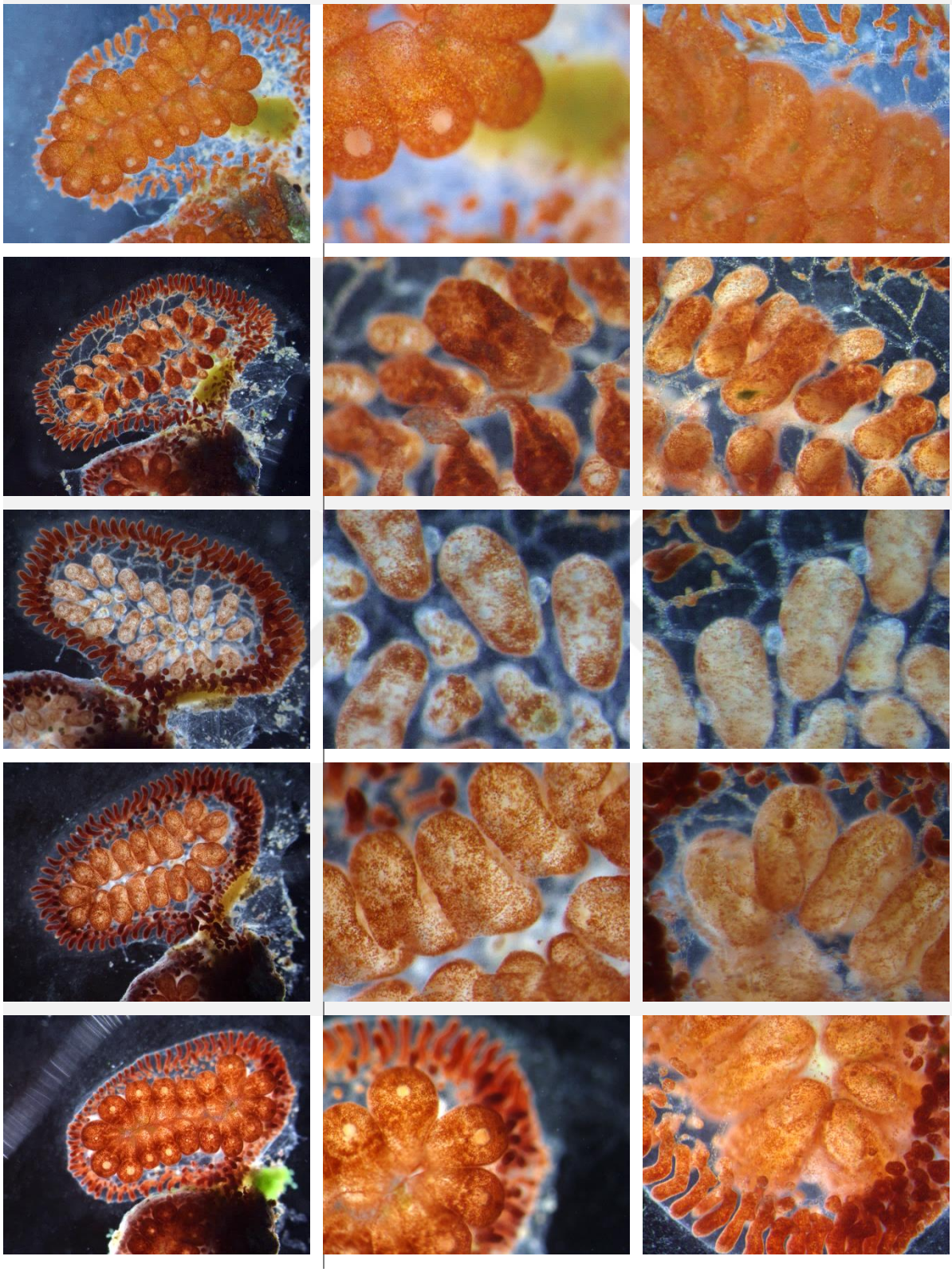
SAMPLE ID – Z1

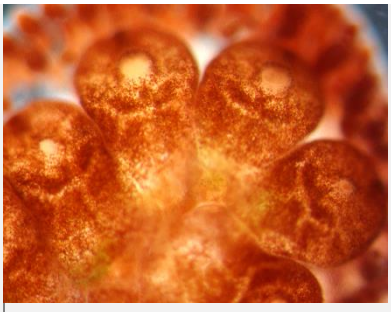


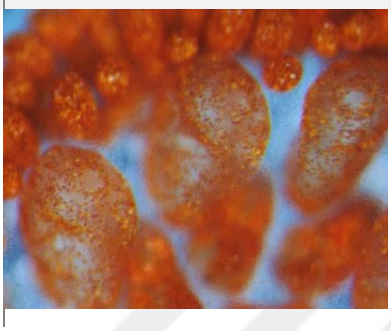
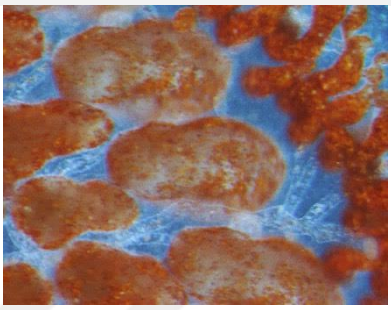


DORSAL - 1	DORSAL - 2	VENTRAL

SAMPLE ID – Z2

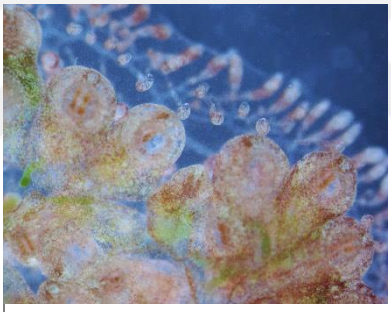
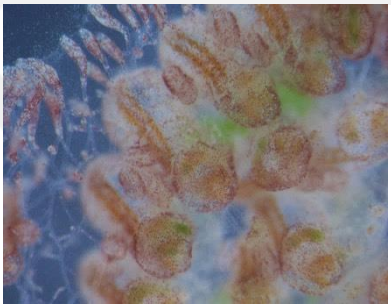


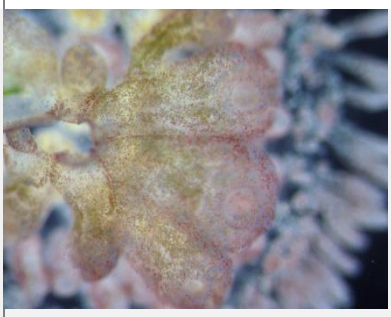
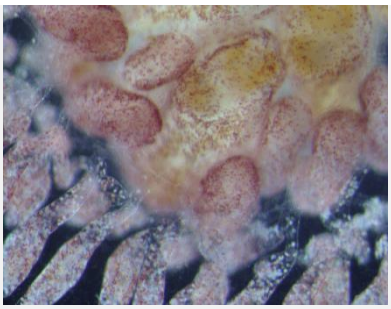



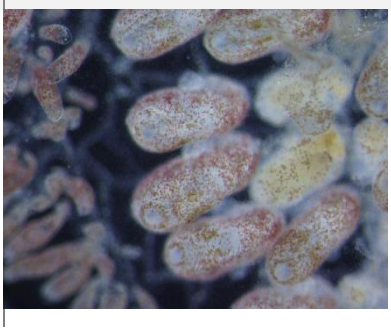
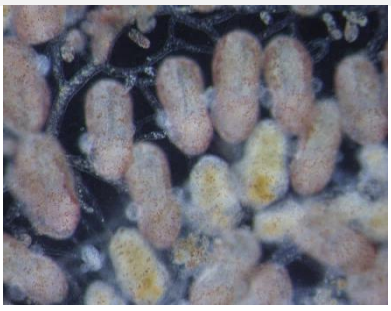




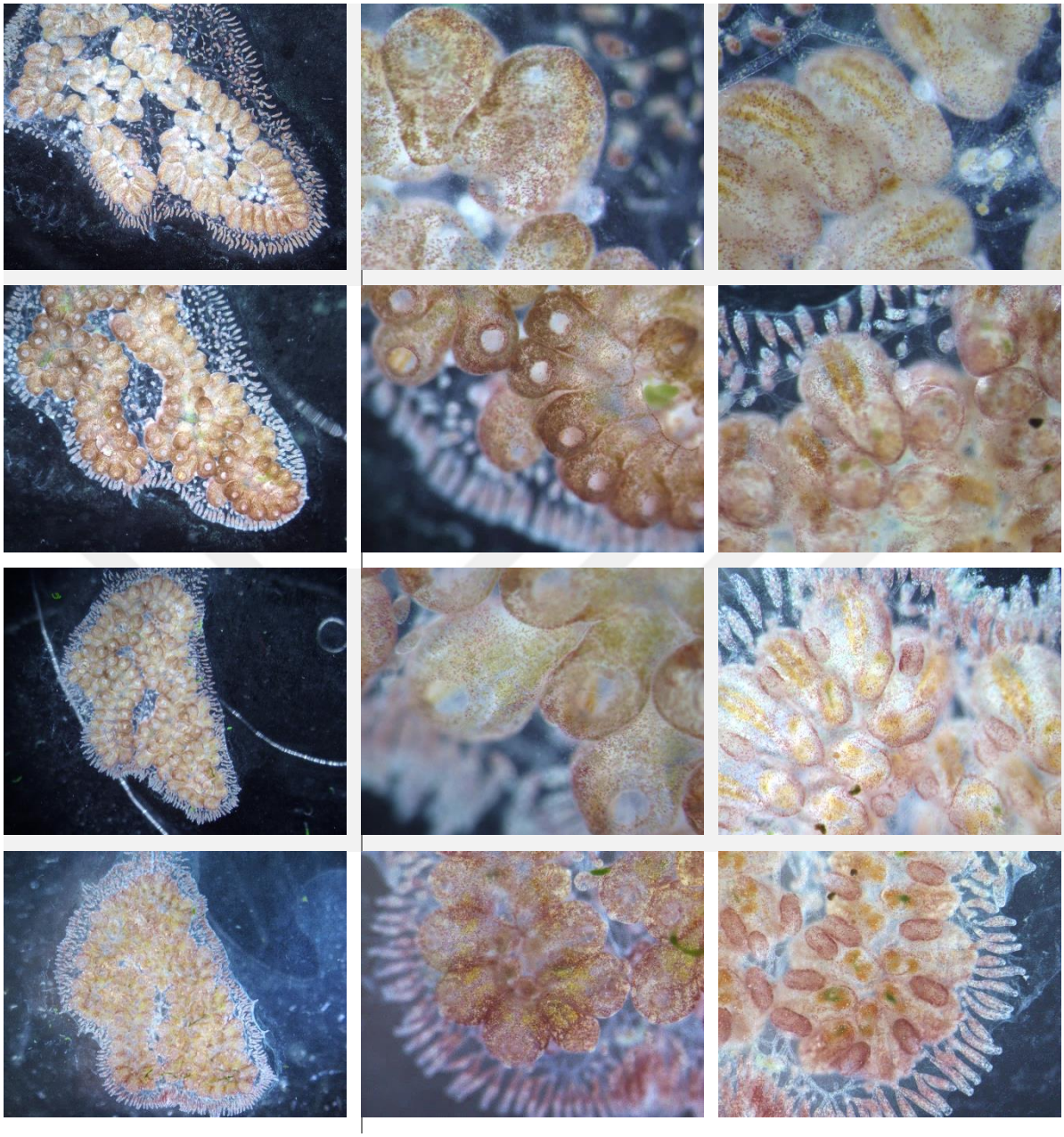
DORSAL - 1 **DORSAL - 2** **VENTRAL**

SAMPLE ID – Z4

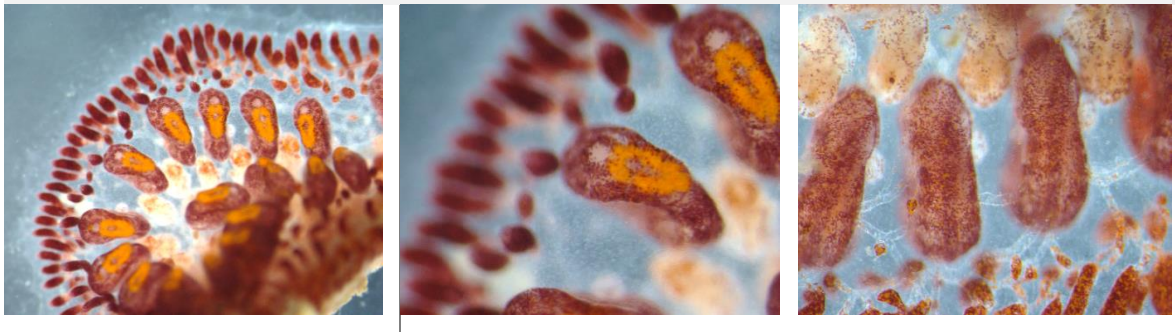



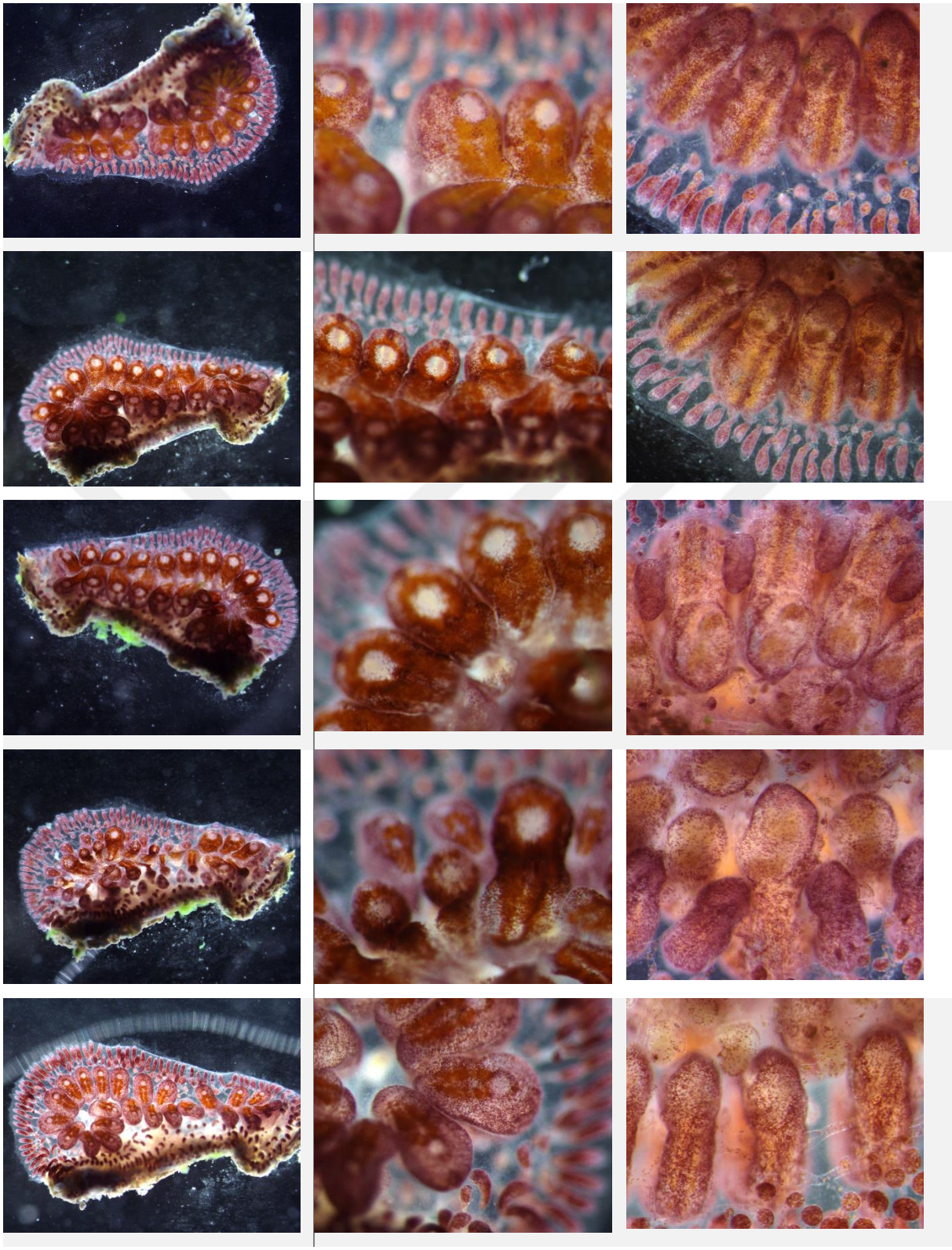





DORSAL - 1 **DORSAL - 2** **VENTRAL**

SAMPLE ID – GK13



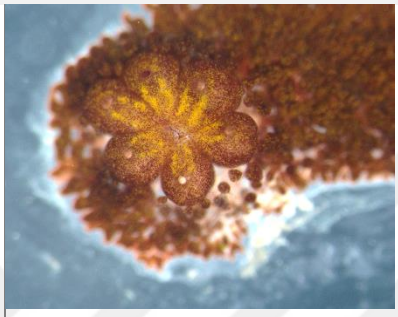
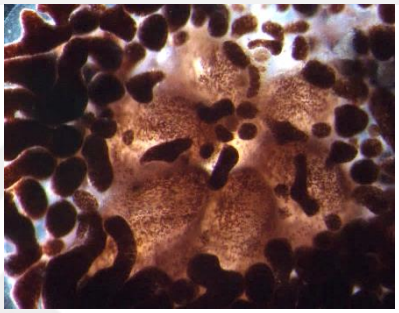


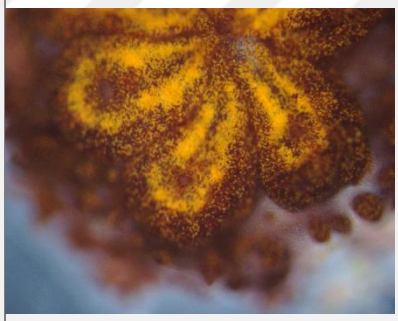
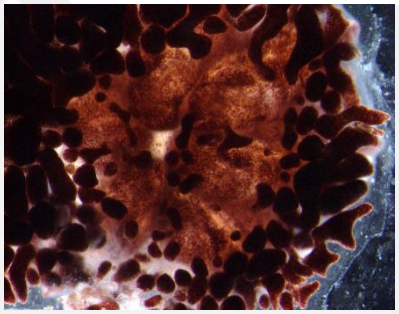
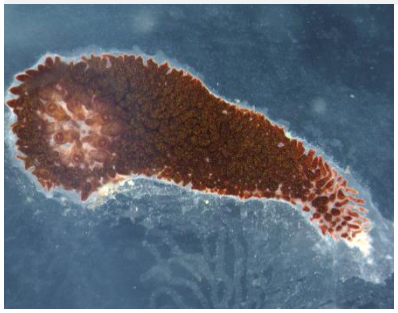
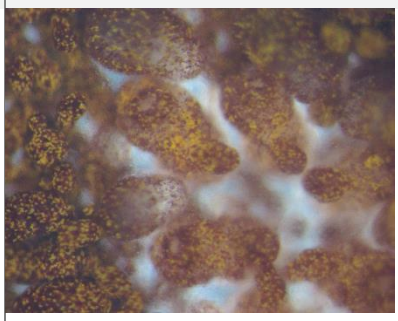
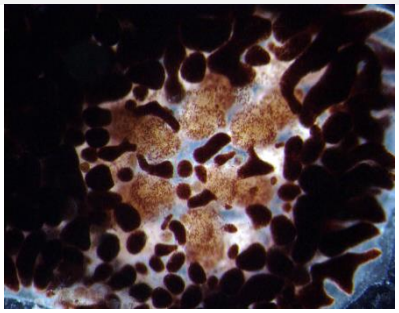
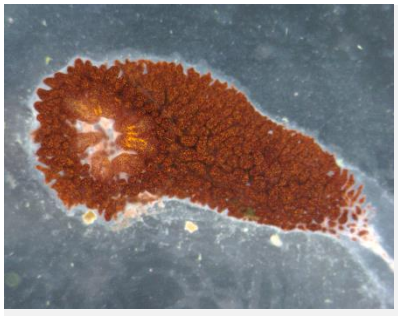
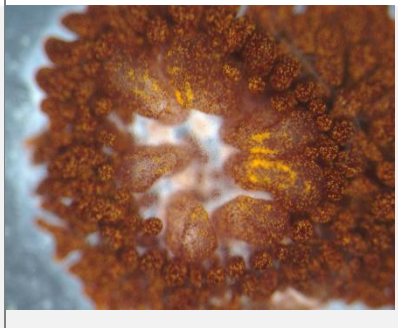
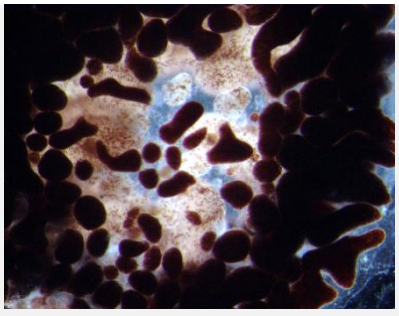


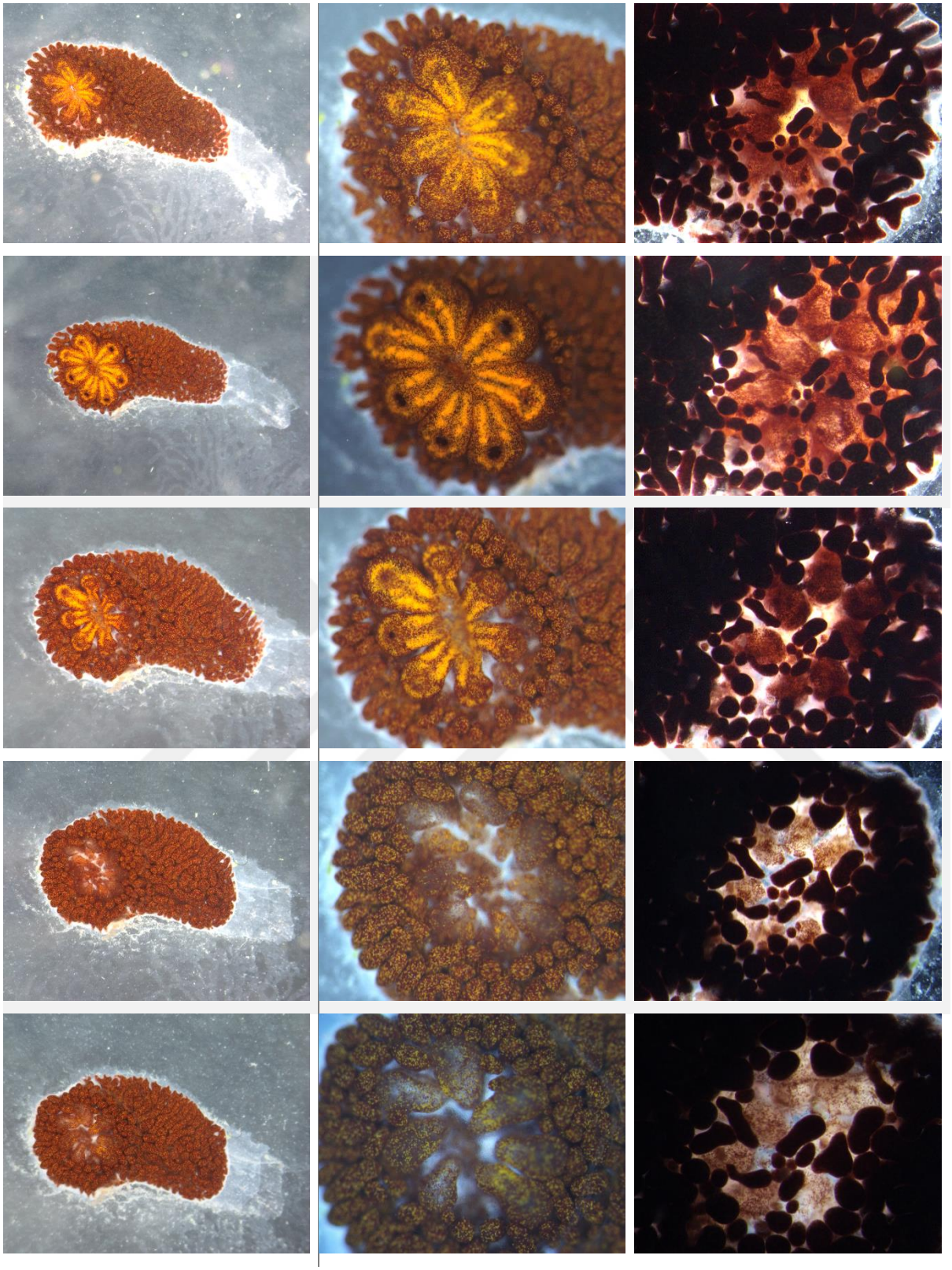


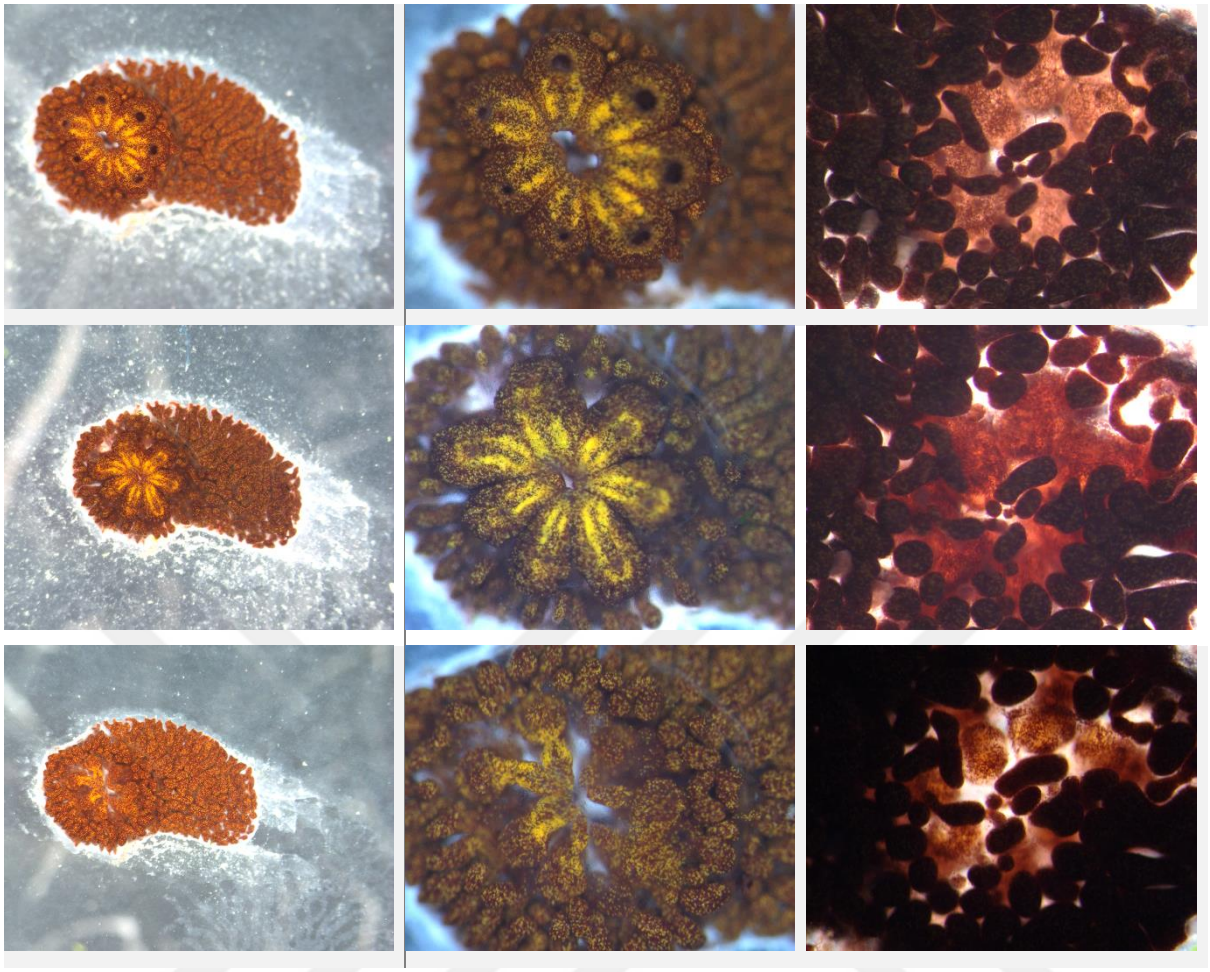
DORSAL - 1 **DORSAL - 2** **VENTRAL**

SAMPLE ID – G8

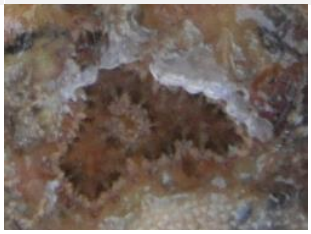









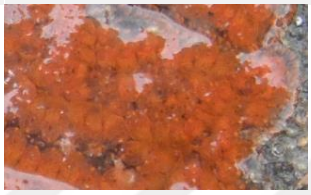


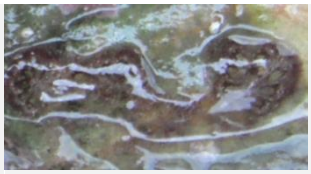
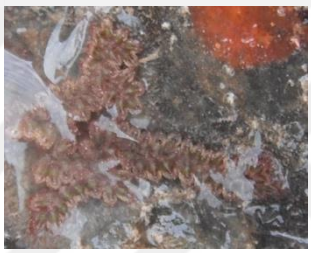
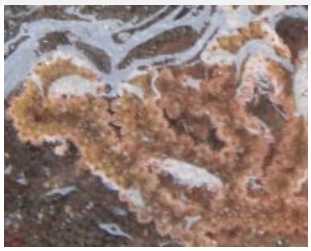
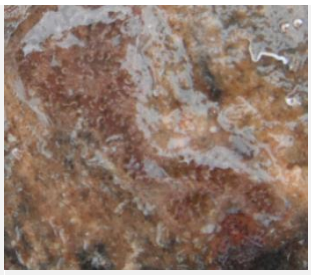


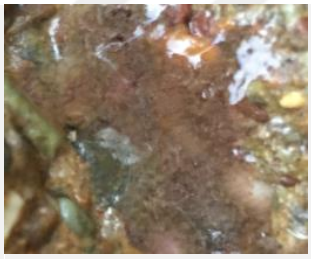
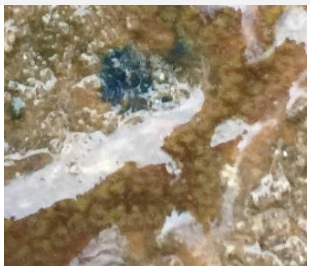
APPENDIX B

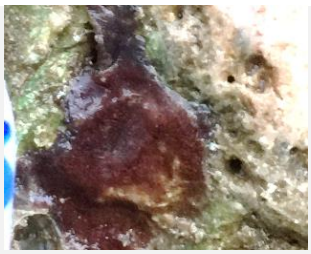
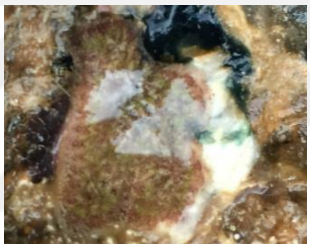
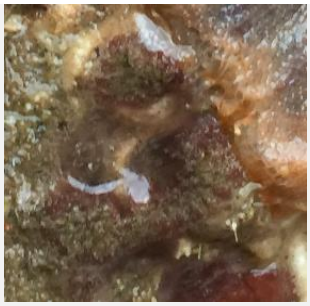
Sampled Specimens

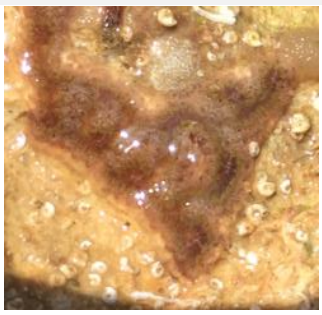
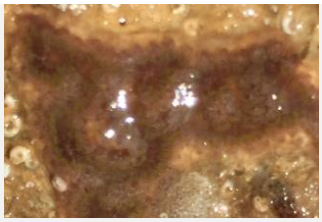
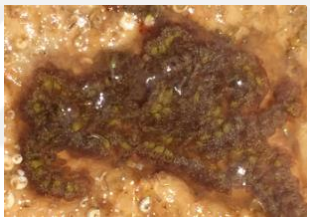
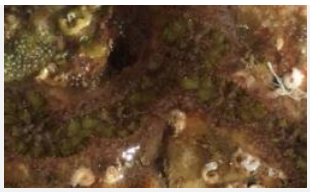
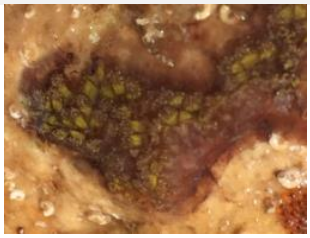
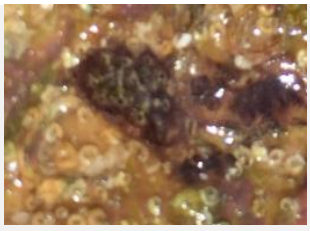
CODE	COLOUR	PHOTO	LOCATION	DATE
A1.İ	Orange-brown		Alanya	27.04.2012
A1	Brown-violet-yellow stripes		Alanya	27.04.2012
A2.İ	Orange-brown		Alanya	27.04.2012
A3.İ	Orange-brown		Alanya	27.04.2012
A4.İ	Orange-brown		Alanya	27.04.2012
A5	Brown-yellow stripes		Alanya	27.04.2012
A6.İ	Orange-brown		Alanya	27.04.2012

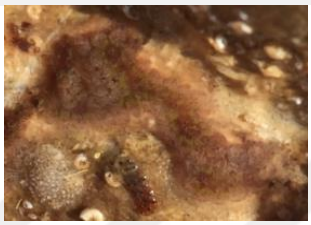
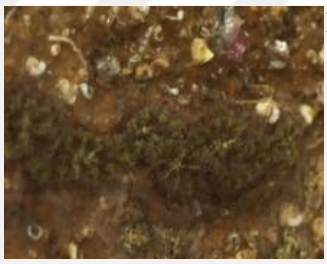
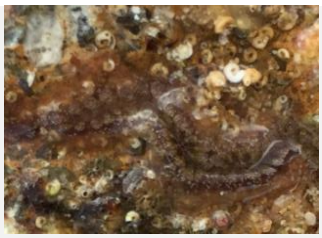
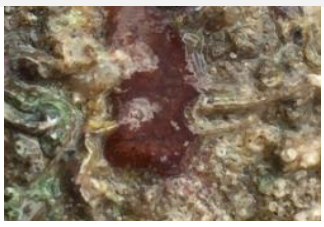
A7.İ	Orange-brown		Alanya	27.04.2012
A8	White-brown		Alanya	27.04.2012
A8.İ	Orange		Alanya	27.04.2012
A9.İ	Orange-brown		Alanya	27.04.2012
A10.İ	Orange-brown		Alanya	27.04.2012
A11	Orange-brown		Alanya	27.04.2012
A12	Violet-green-brown-yellow stripes		Alanya	27.04.2012

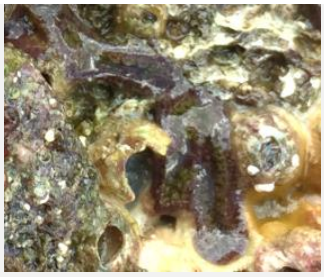
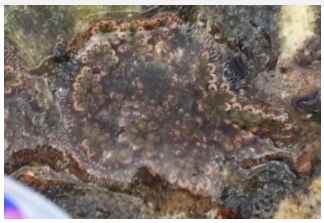
A13	Brown-greenish		Alanya	27.04.2012
A14	Brown-violet		Alanya	27.04.2012
A15	Brown-violet-yellow stripes		Alanya	27.04.2012
A16	Brown-violet-yellow stripes		Alanya	27.04.2012
A17	Brown-violet-yellow stripes		Alanya	27.04.2012
A20	Cream-violet-green		Alanya	27.04.2012
A23	Light Brown-yellow stripes		Alanya	27.04.2012

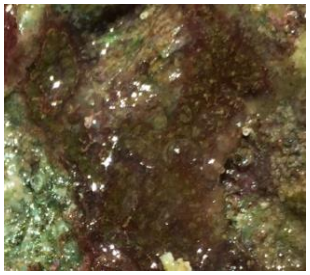
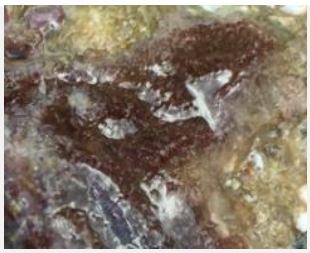
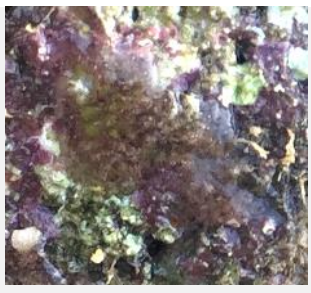
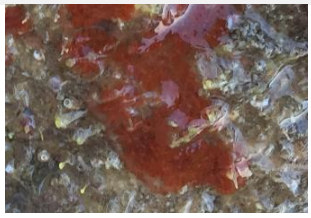
A25	Light Brown-yellow stripes		Alanya	27.04.2012
C10	Brown-violet-green		Alanya	24.10.2018
C16	Orange-brown		Alanya	24.10.2018
C17	Brown-yellow stripes		Alanya	24.10.2018
C18	Light brown-dark brown edges		Side	24.10.2018
C20	Orange-brown		Side	24.10.2018
C21	White-brown		Side	24.10.2018

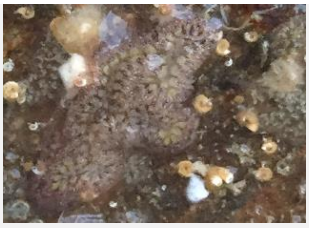
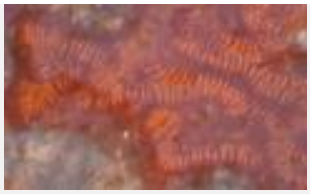
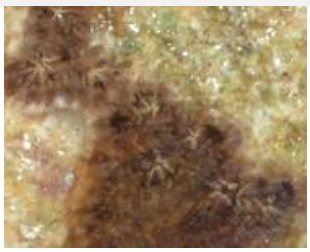
C22	White-light orange-brown		Side	24.10.2018
C24	Orange-brown		Side	24.10.2018
C25	Dark brown-violet		Side	24.10.2018
C26	Violet-green-yellow stripes		Side	24.10.2018
C27	Violet-green-yellow stripes		Side	24.10.2018
C28	Orange-brown		Side	24.10.2018

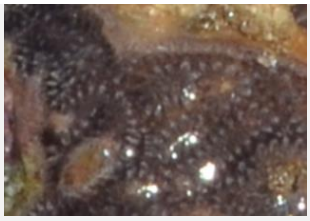
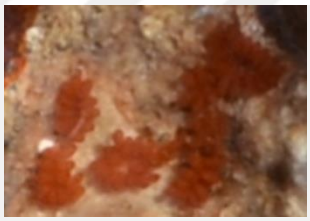
C30	Orange-brown		Kemer	24.10.2018
C31	Violet-green-brown		Kemer	24.10.2018
C32	Violet-green-brown		Kemer	24.10.2018
C33	Violet-green-brown		Kemer	24.10.2018
C35	Violet-green-brown		Kemer	24.10.2018
C38	Violet-green-brown		Kemer	24.10.2018
C39	Brown-yellow stripes		Kemer	24.10.2018

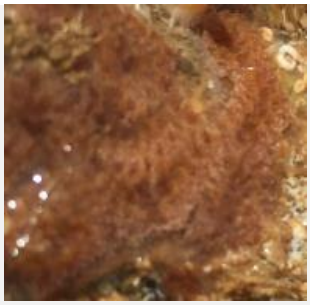
C40	Orange-brown		Kemer	24.10.2018
C41	Orange-brown		Kemer	24.10.2018
C42	Violet-green-brown		Kemer	24.10.2018
C43	Violet-green-brown-yellow stripes		Kemer	24.10.2018
C44	Black-dark brown- yellow stripes end		Kemer	24.10.2018
C46	Violet-yellow-brown		Kemer	24.10.2018
C47	Red		Kemer	24.10.2018

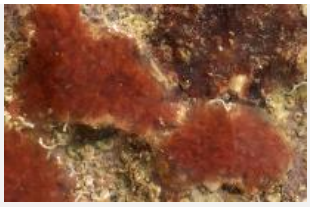
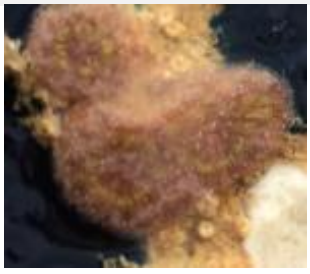
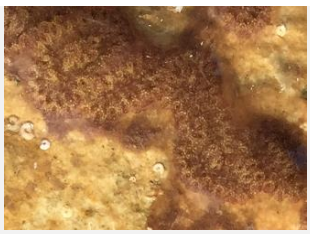
C48	Violet-green-brown		Kemer	24.10.2018
C49	Green-light violet edges		Kemer	24.10.2018
C50	Dark green-brown- violet edges		Kemer	24.10.2018
C51	Blackish-white edges		Kemer	24.10.2018
C52	Orange		Kemer	24.10.2018
C55	Orange		Kemer	24.10.2018
C56	Green-brown		Kemer	24.10.2018

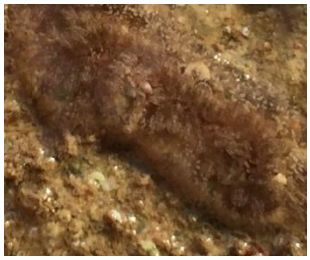
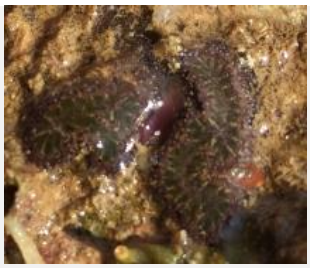
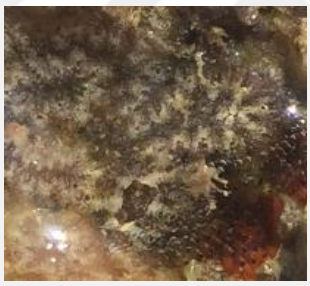
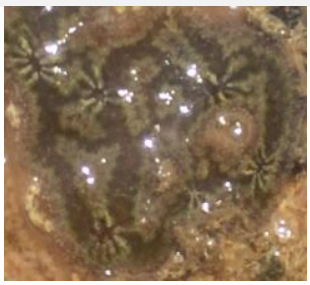
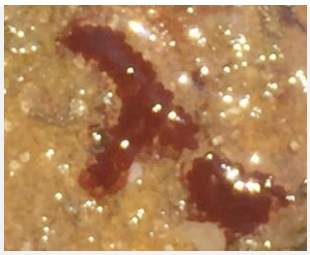
C58	Green-brown		Kemer	24.10.2018
C60	Dark brown-lighter stripes		Kemer	24.10.2018
C61	Dark brown-lighter stripes		Kemer	24.10.2018
C62	Orange-brown		Kemer	24.10.2018
C63	Light brown-lighter stripes		Kemer	24.10.2018
K1	Violet-green		Tershane	29.10.2019
K2	Orange		Tershane	29.10.2019

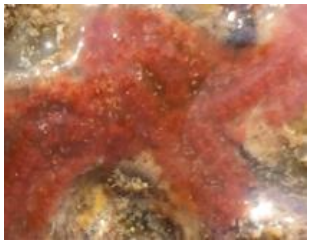
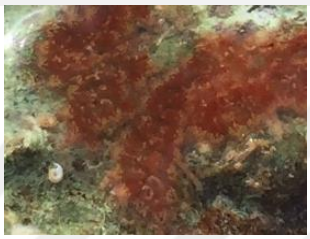
K3	Violet-green-yellow stripes		Tershane	29.10.2019
4BİDES	Orange-Dark Brown		Kızkalesi	20.04.2012
5BİDES	Orange		Kızkalesi	20.04.2012
BİDES 1	Brownish		Kızkalesi	10.07.2014
BİDES 2	Orange-brown		Kızkalesi	10.07.2014
B.LUS 1	Brownish-yellow pigments		Kızkalesi	30.09.2014
(O)4	Orange-brown		Kızkalesi	30.09.2014

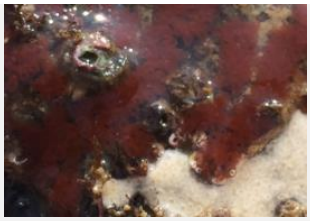
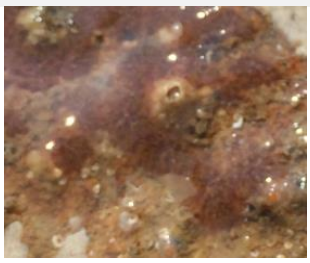
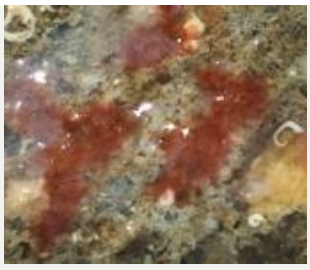
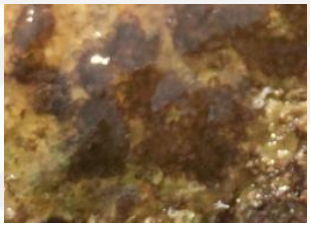
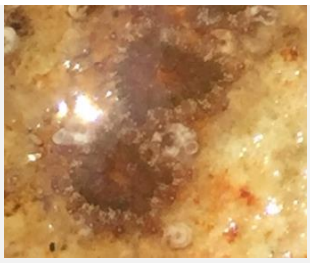
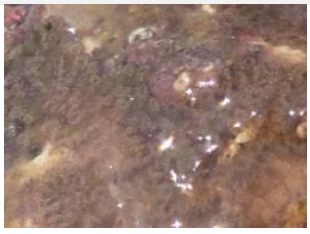
(O)8	Orange-brown		Kızkalesi	30.09.2014
(O)12	Brown- white stripes		Kızkalesi	30.09.2014
B1	Orange-yellow stripes		Kızkalesi	30.09.2014
B2	Orange-red		Kızkalesi	30.09.2014
BS2	Purple-yellow stripes		Kızkalesi	01.11.2017
BV1	Orange		Kızkalesi	01.11.2017
BV2	Orange-brown		Kızkalesi	01.11.2017

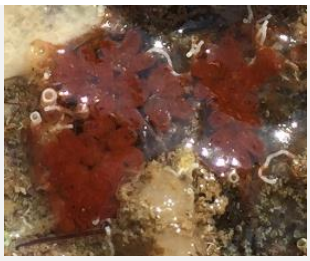
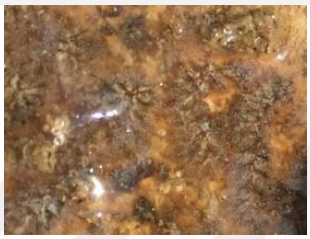
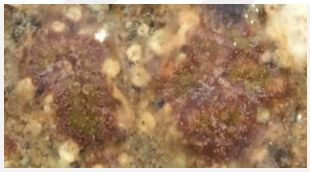
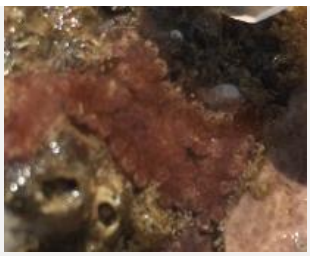
BN1	Violet-light stripes		Kızkalesi	01.11.2017
BV3	Orange-brown		Kızkalesi	01.11.2017
BV4	Orange		Kızkalesi	01.11.2017
BV5	Orange-brown		Kızkalesi	01.11.2017
BN3	Light brown		Kızkalesi	01.11.2017
BS3	Green-yellow stripes		Kızkalesi	01.11.2017

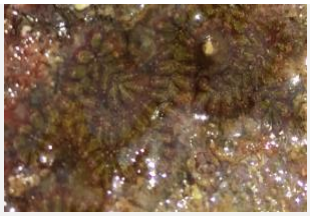
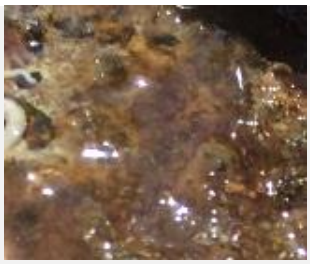
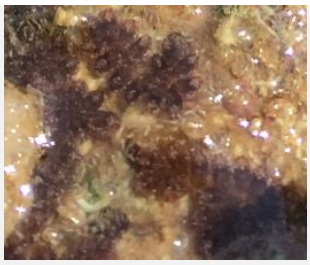
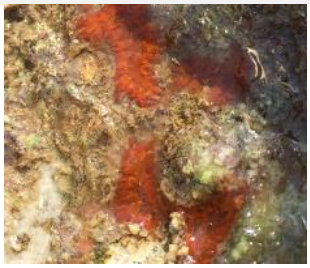
BV6	Orange		Kızkalesi	01.11.2017
BS4	Green		Kızkalesi	01.11.2017
BV7	Orange-red		Kızkalesi	01.11.2017
BV8	Orange-red		Kızkalesi	01.11.2017
BS5	Green-violet-yellow stripes		Kızkalesi	01.11.2017
BS6	Green-violet		Kızkalesi	01.11.2017
BN5	Light-brownish		Kızkalesi	01.11.2017

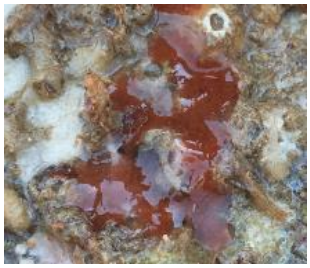
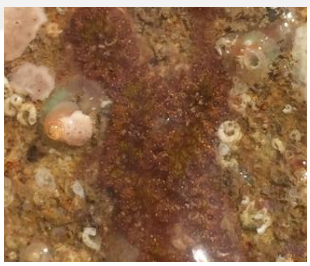
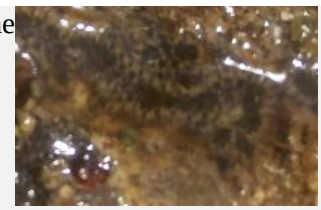
BN6	Light-brownish		Kızkalesi	01.11.2017
BS8	green-violet-yellow stripes		Kızkalesi	01.11.2017
J18-BS1	**GREEN-YELLOW STRİPES**		**KIZKALESİ**	**05.07.2018**
J18-BS2	Green-whiter stripes		Kızkalesi	05.07.2018
J18-BS7	Brownish-yellow-green		Kızkalesi	05.07.2018
J18-BS13	Red		Kızkalesi	05.07.2018

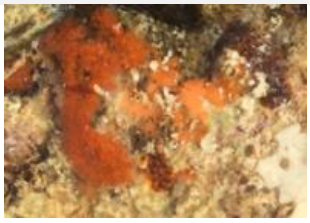
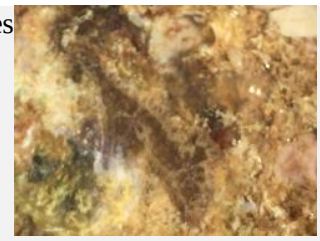
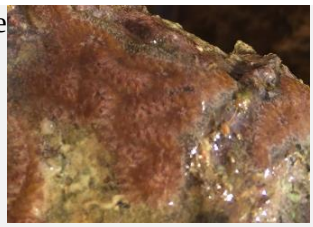
Z1	Orange-red		Kızkalesi	03.08.2018
Z2	red		Kızkalesi	03.08.2018
Z3	Red-yellow stripes		Kızkalesi	03.08.2018
Z4	Brown-violet-green		Kızkalesi	03.08.2018
Z5	Dark brown-green stripes		Kızkalesi	03.08.2018
Z6	Orange-brown		Kızkalesi	03.08.2018
Z8	Orange-brown		Kızkalesi	03.08.2018

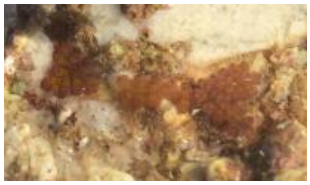
Z9	Red		Kızkalesi	03.08.2018
Z10	Brownish		Kızkalesi	03.08.2018
Z12	Red		Kızkalesi	03.08.2018
Z13	Brownish		Kızkalesi	03.08.2018
Z15	Brown yellow stripes		Kızkalesi	03.08.2018
Z16	Brown-violet-green		Kızkalesi	03.08.2018
Z20	Brown yellow stripes		Kızkalesi	03.08.2018

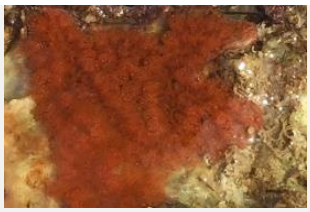
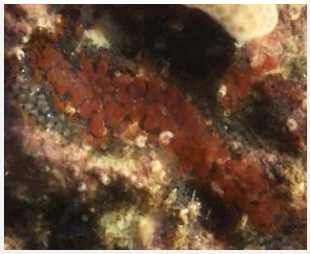
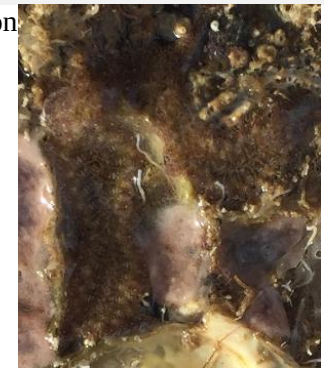
R1	Orange		Kızkalesi	18.09.2018
R2	Red		Kızkalesi	18.09.2018
R4	Brown-yellow stripes		Kızkalesi	18.09.2018
R6	Green-violet		Kızkalesi	18.09.2018
R7	Brownish-lighter stripes		Kızkalesi	18.09.2018
R9	brownish		Kızkalesi	18.09.2018
R10	Black-white stripes		Kızkalesi	18.09.2018

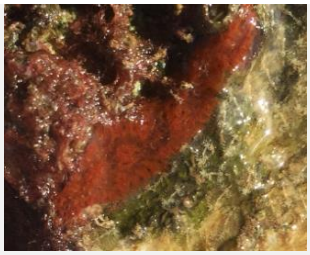
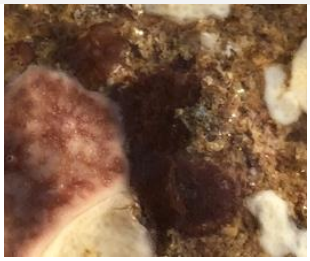
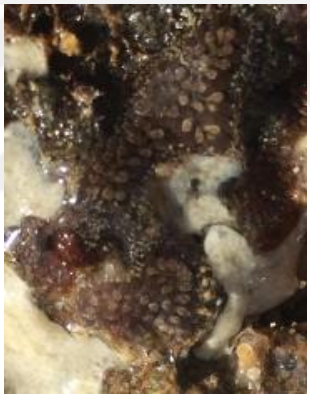
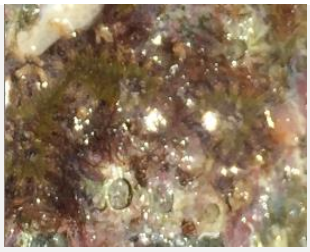
R11	Green-violet-yellow stripes		Kızkalesi	18.09.2018
R14	Orange		Kızkalesi	18.09.2018
R19	Green-violet-yellow stripes		Kızkalesi	18.09.2018
R20	White-brown		Kızkalesi	18.09.2018
R28	Dark brown-white stripes		Kızkalesi	18.09.2018
R32	Orange		Kızkalesi	18.09.2018
R36	Orange-brown		Kızkalesi	18.09.2018

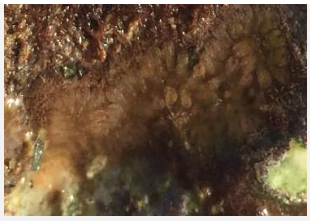
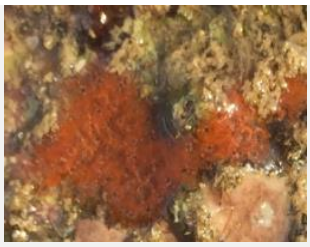
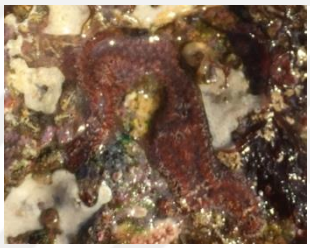
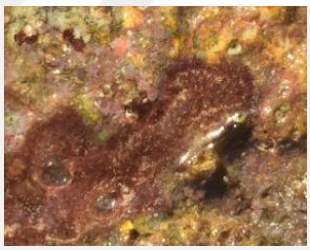
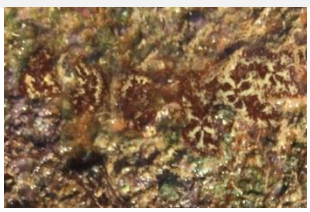
R37	Red		Kızkalesi	18.09.2018
R39	Brownish-yellow stripes-on the end		Kızkalesi	18.09.2018
R40	White-creamish		Kızkalesi	18.09.2018
R41	Orange		Kızkalesi	18.09.2018
R42	Green-violet-yellow stripes		Kızkalesi	18.09.2018
R43	Brownish-yellow stripes-on the end		Kızkalesi	18.09.2018
R44	Brownish-yellow stripes		Kızkalesi	18.09.2018

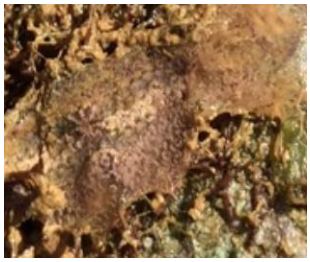
GK1	Orange		Kızkalesi	03.10.2018
GK2	Orange		Kızkalesi	03.10.2018
GK3	Brown-light stripes		Kızkalesi	03.10.2018
GK4	Light brown-violet-yellow stripes on the end		Kızkalesi	03.10.2018
GK5	Brown-greenish-yellow stripes on the end		Kızkalesi	03.10.2018
GK6	Brown-violet-yellow stripes-on the end		Kızkalesi	03.10.2018
GK7	Red-brownish-yellow on the end		Kızkalesi	03.10.2018

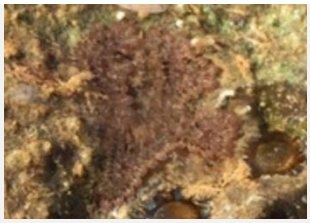
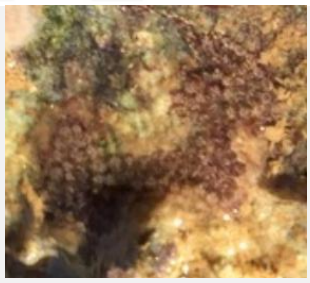
GK8	Brown-green-violetish		Kızkalesi	03.10.2018
GK9	Orange-brown		Kızkalesi	03.10.2018
GK10	Light brown-yellow pigments		Kızkalesi	03.10.2018
GK11	Brown-violet-green		Kızkalesi	03.10.2018
GK12	Orange-brown		Kızkalesi	03.10.2018
GK13	Orange-brown		Kızkalesi	03.10.2018
GK14	Brown-violet-yellow stripes-on the end		Kızkalesi	03.10.2018

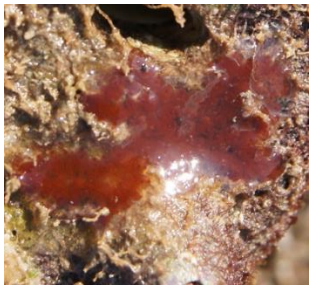
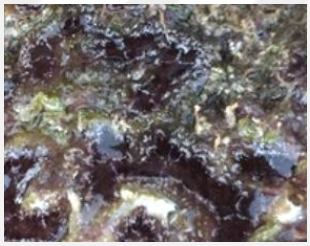
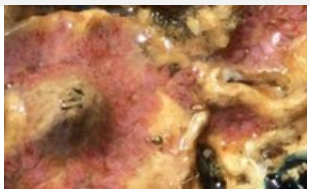
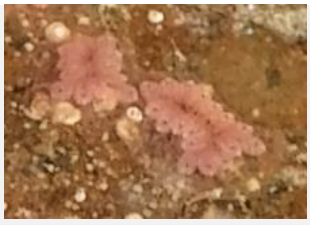
GK15	Dark green-yellow stripes		Kızkalesi	03.10.2018
GK17	Orange-brown		Kızkalesi	03.10.2018
GK18	Orange		Kızkalesi	03.10.2018
GK20	Orange		Kızkalesi	03.10.2018
GK21	Red		Kızkalesi	03.10.2018
GK24	Brown-violet-yellow stripes-on the end		Kızkalesi	03.10.2018

GK25	Red		Kızkalesi	03.10.2018
GK26	Brown		Kızkalesi	03.10.2018
GK27	Orange-brown		Kızkalesi	03.10.2018
GK29	White-brown		Kızkalesi	03.10.2018
GK32	Green-violet		Kızkalesi	03.10.2018
GK33	Orange-brown		Kızkalesi	03.10.2018

GK39	Green-violet-brown		Kızkalesi	03.10.2018
GK40	White-brown		Kızkalesi	03.10.2018
GK41	Orange		Kızkalesi	03.10.2018
GK43	Red-light stripes		Kızkalesi	03.10.2018
GK45	Red-light stripes		Kızkalesi	03.10.2018
GK46	Brown-light stripes		Kızkalesi	03.10.2018
G2	Cream-violet		Tisan	03.10.2018

G4	Cream-violet-light stripes		Tisan	03.10.2018
G5	Brown-yellow stripes		Tisan	03.10.2018
G6	Violet- yellow stripes		Tisan	03.10.2018
G8	Orange-brown		Tisan	03.10.2018
G9	Violet-brown-yellow stripes		Tisan	03.10.2018
G10	Brown-violet-yellow stripes		Tisan	03.10.2018
G11	Brown-white stripes		Tisan	03.10.2018

G12	Violet-brown-yellow stripes		Tisan	03.10.2018
G13	Violet-green-brown- yellow end		Tisan	03.10.2018
G14	Violet-green-yellow end		Tisan	03.10.2018
G15	Brown-violet- yellow end		Tisan	03.10.2018
G16	Violet-green-yellow end		Tisan	03.10.2018
MZ_1	Orange-brown		Mezitli	11.11.2017
MZ_2	Orange-brown		Mezitli	11.11.2017

MZ_3	red		Mezitli	11.11.2017
M2-13	Orange-brown		Mezitli	10.04.2018
M2-14	Brown-violet-green-lighter stripes		Mezitli	10.04.2018
M2-17	Blackish-lighter edges		Mezitli	10.04.2018
M2-19	Violet-pink		Mezitli	10.04.2018
L2	Pink-violet		Konacık	26.09.2018
L15	White-brown-Haplotip		Konacık	26.09.2018

L17	Orange-brown		Konacık	26.09.2018
L18	Brown-white stripes		Konacık	26.09.2018